SCREENING FOR MUTATIONS IN *PAX3* AND *MITF* IN WAARDENBURG SYNDROME AND WAARDENBURG SYNDROME-LIKE INDIVIDUALS

By

Melisa Lynn Carey

A THESIS

Submitted to
Michigan State University
in partial fulfillment of the requirements
for a degree of

MASTER OF SCIENCE

Department of Zoology

1996

ABSTRACT

SCREENING FOR MUTATIONS IN *PAX3* AND *MITF* IN WAARDENBURG SYNDROME AND WAARDENBURG SYNDROME-LIKE INDIVIDUALS

By

Melisa L. Carey

Waardenburg Syndrome (WS) is an autosomal dominant disorder characterized by pigmentary and facial anomalies and congenital deafness. Mutations causing WS have been reported in *PAX3* and *MITF*. The goal of this study was to characterize the molecular defects in 33 unrelated WS individuals. Mutation detection was performed using Single Strand Conformational Polymorphism (SSCP) analysis and sequencing methods. Among the 33 WS individuals, a total of eight mutations were identified, seven in *PAX3* and one in *MITF*. In this study, one of the eight mutations was identified and characterized in *PAX3* exon seven in a WSI family (UoM1). The proband of UoM1 also has Septo-Optic Dysplasia. In a large family (MSU22) with WS-like dysmorphology and additional craniofacial anomalies, linkage was excluded to *PAX3* and no mutations were identified in *MITF*. Herein I review the status of mutation detection in our proband screening set and add to the understanding of the role of *PAX3* and *MITF* in development by exploring new phenotypic characteristics associated with WS.

ACKNOWLEDGMENTS

I would like to thank Drs. Tom Friedman and Jim H. Asher Jr. for their encouragement, support, patience and guidance. A special thanks to Dr. Asher for all of his efforts in collecting families for this study. His dedication and conviction were admirable and he will be missed.

I would also like to thank Tom Barber, Aihui Wang, Yong Liang, Rob Morell, Lori Swenson and Maki Saitoh for their enlightening discussions both scientific and social. A special thanks to Tim Cloutier for his assistance with the project. I would like to thank my committee members, Dr. John Fyfe, Dr. Emanuel Hackel and Dr. Jeff Innis for their helpful suggestions. A thanks to all of our collaborators and the families represented in this project; whose cooperation is greatly appreciated.

I would like to to take a moment to thank my parents, Barbara and Patrick Carey and the rest of my family, Mike, Donna, Courtney, Kyle and Brandon; who gave me both the encouragement and the necessary outlet to get through the trials of graduate school.

This work was supported by Grant DC 01160-04 from the National Institute on Deafness and Communication Disorders, National Institute of Health.

TABLE OF CONTENTS

LIST OF TABLES

LIST OF FIGURES

BACKGROUND and SIGNIFICANCE

Waardenburg Syndrome Phenotype

There are at least four clinical sub-types of Waardenburg Syndrome as defined by McKusick in Mendelian Inheritance of Man (MIM): WSI (MIM 193500), WSII (MIM 193510), WSIII (MIM 148820), and WSIV (MIM 277580). The presence of dystopia canthorum in 98% of WSI individuals distinguish WSI from WSII[1, 6-10] Waardenburg Syndrome (WS) types I, II and III are autosomal dominant disorders. WSI is characterized by congenital deafness, dystopia canthorum, heterochromia irides, poliosis, broad nasal root, synophrys, hypo- and hyperpigmentation of the skin and hair.[1] Other less common clinical anomalies include aganglionic megacolon, cardiac defects, cleft lip and palate and spinal bifida. WSIII has the clinical characteristics of WSI with the addition of limb abnormalities.[11, 12] The classic example of WSIII was described by Klein[11, 13, 14] and hence WSIII is often referred to as Klein-Waardenburg Syndrome. WSIII is rare, with approximately a dozen published cases.[12, 15-23] WSIV (Shah-Waardenburg Syndrome) exhibits WS along with aganglionic megacolon.[24-29] WSIV is also called Hirschprung disease (HSCR) with pigmentary anomaly. Approximately 25% of WS individuals exhibit unilateral or bilateral hearing loss.[1] It is estimated that 2% of all individuals with profound deafness have WS.[1, 4]

Classification of WS is determined by major and minor criteria established by the WS consortium as listed in TABLE 1.[2, 3] The penetrance and expressivity for all WS clinical features vary both within and between families. Thus, WS is both clinically pleiotropic and genetically heterogeneous.[25, 30, 31]

Table 1: Waardenburg Syndrome Diagnostic Criteria

Major Characteristics:

- Sensorineural deafness
- Iris pigmentary abnormalities
  - Heterochromia irides
  - Characteristic brilliant blue iris
  - Hypopigmented iris
- Hair pigmentation
  - White forelock
  - Body hair (eyelashes; eyebrows)
- Dystopia canthorum (only in WSI individuals)
- First-degree relative previously diagnosed with WS

Minor Characteristics:

- Congenital leukoderma (severe areas hypopigmented skin)
- Synophrys
- Broad high nasal root
- Hypoplasia of alae nasi
- Premature graying

Rare Characteristics:

- Hirschprung disease (classified as WSIV)
- Sprengel anomaly
- Spina bifida
- Cleft lip and/or palate
- Limb defects (characteristic of WSIII)
- Congenital heart abnormalities
- Abnormalities of vesitbular function
- Broad square jaw
- Low anterior hair line

Table 1: The clinical diagnostic criteria for Waardenburg Syndrome according to the guidelines established by the Waardenburg Syndrome Consortium.[5] In order to be characterized as having WS, an individual must possess either two major characteristics, one major and a first degree relative diagnosed as affected with WS or 1 major and 2 minor characteristics.

Mouse models for Waardenburg Syndrome

Pigmentary anomalies associated with deafness were documented in domestic animals by Darwin,[32] and others[33, 34] may have been examples of Waardenburg Syndrome. Waardenburg Syndrome was one of the first reported examples of pigmentary anomalies with deafness in humans.[1, 34] The hypothesis of a single gene being responsible for the combined clinical phenotype gained acceptance, after the observations that all of the tissues affected in WS patients were derivatives of neural crest cells.[25, 35-37] Several mouse mutations including the *Splotch* (*Sp*)[38], *microphthalmia* (*Mi*)[39], *piebald-lethal* (S^l)[40] and *Patch* (*Ph*) loci affect neural crest cell development, migration and/or differentiation.[41] The *Splotch* mice when homozygous have severe neural tube defects, pigmentary defects, muscle defects, craniofacial anomalies and usually embryonic or neonatal death[41-52, 321] (TABLE 2). *Mi* mice when homozygous exhibit a white coat, eye abnormalities and ear defects (TABLE 3). *Piebald* homozygotes are completely white, they have megacolon and structural defects of the iris. Likely candidates for Waardenburg Syndrome were predicted on the basis of conserved syntenic relationships between mouse and human,[53] at chromosomal locations, of 2q, 3p, 3q or 4p, near the proto-oncogene KIT.[54]

In 1989, Ishikiriyama et al.[55-57] reported a child with WSI that had a *de novo* inversion of 2q35-q37.3. This was the region predicted for WS on the basis of the *Sp* mutant locus. Genetic linkage of WSI to 2q35 was then demonstrated.[57-60]

Table 2: Pax3/Splotch mutations (modified from Chalepakis et al. 1993)[90]

ALLELE	PHENOTYPE HETEROZYGOTE	PHENOTYPE HOMOZYGOTE
Sp (sd)	white spotting curly tail	embryonic death E14p.c. pigmentation deficiency spina bifida exencephaly meningocele neural overgrowth dorsal root ganglia deficiency schwann cell deficiency truncus arteriosus deficiency thyroid deficiency muscle deficiency
Sp^{d} *(sd)*	similar to *Sp*	anterior structures not affected no exencephaly late embryonic or neonatal death
$Sp^{2H/Sp1H}$	similar to *Sp*	
Sp^{4H}	analogous to *Sp* retarded growth	most severe phenotype postimplantation lethal

Table 3: *Mi* mouse mutations (modified from Steingrimsson et al. 1994)[167]

ALLELE	PHENOTYPE HETEROZYGOTE	PHENOTYPE HOMOZYGOTE
Mi^{or} (oak ridge)	slight dilution coat color pale ears and tail belly streak or heat spot	white coat eyes small/absent incisors fail to erupt osteopetrosis
Mi^{wh} (white)	dilution of coat color reduced eye pigmentation spots on toes, tail and belly inner ear defects melanocytes absent from dermis	white coat eyes small; inner iris pigmented spinal ganglia, adrenal medullae small inner ear defects mast cell deficiency
mi^{ws} (white spot)	white spot on belly toes and tail often white	white coat eyes pink but near normal size
mi^{ew} (eyeless-white)	normal appearance	white coat eyes absent/eyelids never open
mi^{ce} (cloudy-eyed)	normal appearance	white coat eyes pale (cloudy white) and small inner ear defects
mi^{rw} (red-eyed white)	normal appearance	white coat with pigmented spots head/tail eyes small and red
mi^{vit} (vitiligo)	normal appearance	spots on thorax and abdomen gradual depigmentation of pigmented areas old mice are nearly white retinal degeneration
mi^{sp} (spotted)	normal appearance	normal appearance reduced tyrosinase activity in skin
mi^{bw} (black-eyed white)	normal appearance	white coat color inner ear defect

The *PAX* Family of Genes

There are several conserved DNA-binding motifs identified among the genomes of *Drosophila*, mouse, nematode, zebra fish, frog, turtle, chick and human.[61, 62] One evolutionarily conserved DNA-binding domain is encoded by the paired box, first discovered in three Drosophila segmentation genes.[63-65] There are nine known human *PAX* genes that have a paired domain of 128 amino acids[66, 67] (TABLE 4). *PAX* gene members may also contain an octapeptide domain and/or a paired-homeobox.

Table 4: *PAX* Genes

GENE	HUMAN	MOUSE[a]	REFERENCES
PAX1:	20p11.2	2	Stapleton et al. 1993
PAX2:	10q22.1-q24.3	19	Tsukamoto et al. 1992
PAX3:	2q35	1	Stapleton et al. 1993
PAX4:	7q32	6	Stapleton et al. 1993, Tamara et al. 1994
PAX5:	9p13	4	Stapleton et al. 1993
PAX6:	1p13	2	Ton et al. 1991
PAX7:	1p36.2-p36.12	4	Stapleton et al. 1993
PAX8:	2q12-q14	2	Stapleton et al. 1993
PAX9:	14q12-q13	nd	Stapleton et al. 1993

Nine PAX genes with the human and mouse chromosomal locations. (modified from Stapleton et al. 1993)[66] a = Walther et al. 1991, nd = not determined.

The members are grouped according to their DNA-binding motifs (FIGURE 1). *PAX1*[68] and *PAX9*[69] contain a paired domain and an octapeptide domain. *PAX2*[61, 70-72], *PAX5*[73, 74] and *PAX8*[75-77] contain a paired domain, an octapeptide domain and a small portion of the homeodomain. *PAX4*[78] and *PAX6*[79, 80] contain the paired domain and the homeodomain. These two genes do not have an octapeptide domain. *PAX3* is most closely related to *PAX7*[81-84], containing a paired domain, an octapeptide domain and a paired-type homeodomain. The *Sp* phenotype was demonstrated to be due to a mutation in *Pax3*.[42-43, 85] *Pax3* and its human homologue, *PAX3* are members of the paired box (*PAX*) gene family of transcription factors.

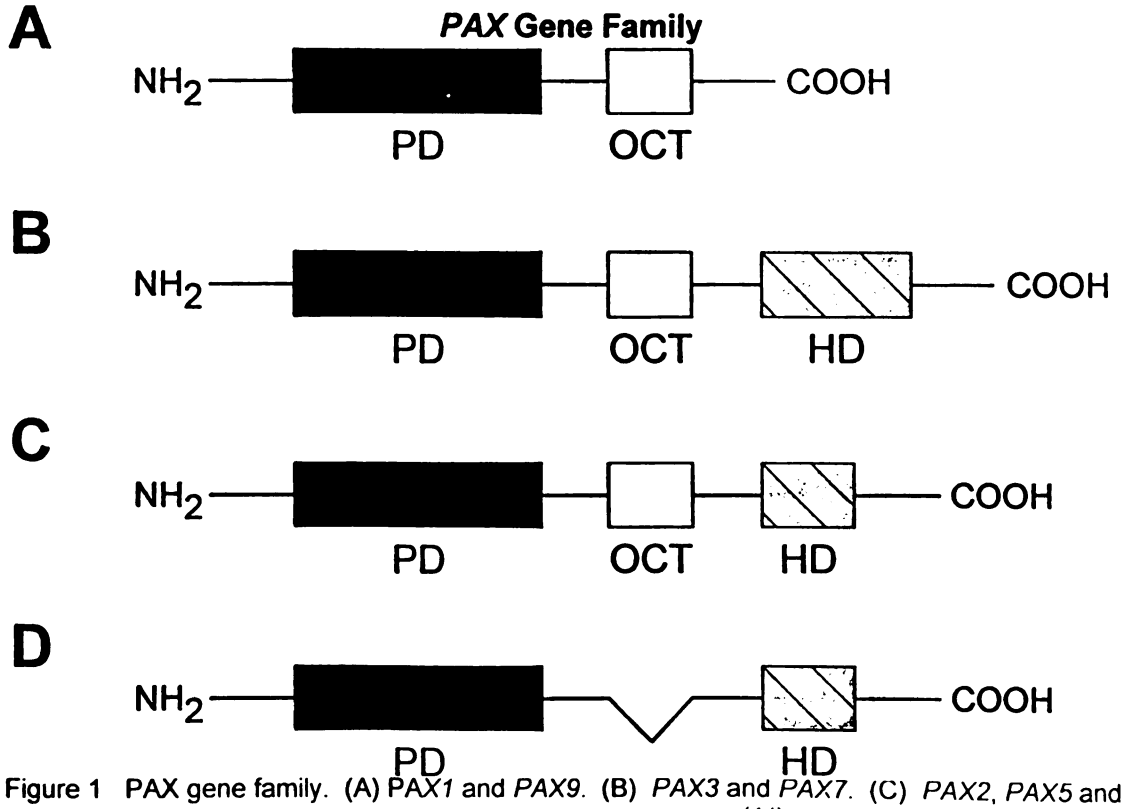

Figure 1 PAX gene family. (A) *PAX1* and *PAX9*. (B) *PAX3* and *PAX7*. (C) *PAX2*, *PAX5* and *PAX8*. (D) *PAX4* and *PAX6*. (modified from Baker et al. 1995)[44]

PAX genes responsible for several disorders

The *PAX* genes have distinct functions throughout development.[62, 86, 89] There are slight overlaps in expression patterns as well as specific organ and tissue development.[86, 87, 90, 91] The *PAX* genes are expressed in the developing nervous system with the exception of *Pax1*[92, 93] and *Pax9*. Many of the *Pax* genes were identified through the use of syntenic relationships between mouse and human (TABLE 4).

Several *PAX* genes have been implicated in human syndromes and disorders. *Pax6* in the mouse is involved in eye development[80, 94] and some *Pax6* mutations are responsible for the small eye phenotype.[79, 95-97] Mutations in human *PAX6* have been identified that cause a number of disorders including: aniridia,[98-102] Peter's anomaly,[103-105] cataracts,[101, 106] WAGR (Wilms' tumor, aniridia, genitourinary abnormalities and mental retardation)[107, 108] and keratitis.[109] A *PAX2* mutation has been implicated in a family with optic nerve colobomas, renal anomalies and vesicoureteral reflux.[110] No human disorder has been identified that is associated with a defect in *PAX1*. Although the *undulated* mouse mutant is caused by *Pax1* and homozygous mice exhibit vertebral malformations along the entire cranio-caudal axis.[111-113]

Several of the *PAX* genes play a role in cancer development.[114-116] *PAX2*[117] and *PAX8*[118, 119] are implicated in the development of Wilms' tumor,[120-122] an embryonic tumor of the kidney. Medulloblastomas express many of the *PAX* genes. *PAX5* expression is upregulated in the tumors compared to slight increase in *PAX2*, *PAX3* and *PAX1*.[123] *PAX5* is a B-cell transcription factor (BSAP) that controls expression of CD19[124] and may also play a role in the development of astrocytoma.[125] Fusion gene products between *PAX3* and *forked head* (*FKHR)* and between *PAX7* and *FKHR* are responsible for alveolar rhabdomyosarcoma.[126-136] *PAX3* and *PAX7* gene translocations result in the 5'-end of either *PAX3*, t(2;13)(q35;14)[126, 127, 131, 132, 136] or *PAX7*, t(1;13)(q35;14)[128] adjacent to the 3'-end of *FKHR*. The 5'-end of both *PAX3* and *PAX7* contains the DNA binding domains and the 3'-end of the *FKHR* gene contains the activation domains.

***PAX3* Expression Pattern**

Pax3 encodes a 479 amino acid, 56 kDa protein that is expressed during embryonic development[90, 91, 137-142] and in the adult.[55, 88] Around embryonic day 8.5 to 9, murine *Pax3* expression is limited to mitotic cells in the ventricular zone of the developing spinal cord and to distinct regions of the hindbrain, midbrain and diencephalon.[137] *Pax3* is expressed in neural crest derivatives, particularly the spinal ganglia and cephalic neural crest cells, including the nasal process and structures derived from the first and second brachial

arches.[143] *Pax3* is expressed in the migrating neural crest cells and the dermomyotome cells.[144] *Pax3* expression during development is observed in the craniofacial mesectoderm and in the limb mesenchyme.[144-148] *Pax3* is also expressed in the Bergmann glia and the basket cells of the Purkinje cell layer of the cerebellar cortex.[88]

Mutations in human *PAX3*

Mutations have been identified in *PAX3* in WS individuals.[59, 60, 149-155] Hundreds of WS families have been identified by the WS consortium; approximately 80% of the mutations in *PAX3* in WSI individuals have been identified.[155] To date more than 50 mutations have been identified in WSI individuals within *PAX3* (TABLE 5). Until recently no common mutations in WSI individuals from unrelated families were identified. However, three identical mutations have since been identified in unrelated families with WSI (TABLE 5).

The majority of *PAX3* mutations that cause WSI are within the DNA-binding domains (FIGURE 2). Many of the codons with mutations are highly conserved among species. On the basis of crystal structure studies, these codons have been identified as important for DNA-binding or phosphate backbone contacts.[156, 157]

arches.[143] *Pax3* is expressed in the migrating neural crest cells and the dermomyotome cells.[144] *Pax3* expression during development is observed in the craniofacial mesectoderm and in the limb mesenchyme.[144-148] *Pax3* is also expressed in the Bergmann glia and the basket cells of the Purkinje cell layer of the cerebellar cortex.[88]

Mutations in human *PAX3*

Mutations have been identified in *PAX3* in WS individuals.[59, 60, 149-155] Hundreds of WS families have been identified by the WS consortium; approximately 80% of the mutations in *PAX3* in WSI individuals have been identified.[155] To date more than 50 mutations have been identified in WSI individuals within *PAX3* (TABLE 5). Until recently no common mutations in WSI individuals from unrelated families were identified. However, three identical mutations have since been identified in unrelated families with WSI (TABLE 5).

The majority of *PAX3* mutations that cause WSI are within the DNA-binding domains (FIGURE 2). Many of the codons with mutations are highly conserved among species. On the basis of crystal structure studies, these codons have been identified as important for DNA-binding or phosphate backbone contacts.[156, 157]

Table 5: *PAX3* mutations. The listing includes the family name, the mutation, and the exon of the mutation. Large deletions and inversions are not included in this table.

Table 5: *PAX3* Mutations

FAMILY	MUTATION	EXON	REFERENCES
WS.055	F45L	2	Tassabehji et al. 1994
BU47	N47H	2	Hoth et al. 1993
MSU17	N47L	2	Sommer et al. 1983; Asher et al. 1995
BU26	P50L	2	da Silva 1991; Hoth et al. 1993, Baldwin et al. 1993
BU35	R56L	2	Carezani-Gavin et al. 1992; Hoth et al. 1993
BU48	V60M	2	Baldwin unpublished
WS.024	V78M	2	Tassabehji et al. 1995
WS.15	G81A	2	Foy et al. 1990; Tassabehji et al. 1993
Zloto 1995	S84F	2	Zlotogora et al. 1995
BU5	K85E	2	Baldwin et al. 1995
WS.009	G99D	2	Tassabehji et al. 1994
MSU3	100ins1	2	Morell et al. 1993
WS.05	185del18	2	Foy et al. 1990; Tassabehji et al. 1992
WS.100	191del17	2	Tassabehji et al. 1995
UGM2	266del14	2	Morell et al. 1992
WS.06	288del1	2	Foy et al. 1990; Tassabehji et al. 1992
BU53	297del28	2	Baldwin et al. 1994
WS.090	364del5	3	Tassabehji et al. 1995
WS.093	358del1	3	Tassabehji et al. 1995
WS.084	451ins1	3	Tassabehji et al. 1994
WS.003	452del2	4	Tassabehji et al. 1994
WS.11	556del2	4	Foy et al. 1990; Tassabehji et al. 1993
WS.138	A196T	4	Tassabehji et al. 1995
Hol, 1995	598del5	5	Hol et al. 1995
BU7	Q200X	5	Baldwin et al. 1995
BU4	S201X	5	Baldwin et al. 1995
BU9	R223X	5	Baldwin et al. 1994
BU8	E235X	5	Baldwin et al. 1995
BU52	F238S	5	Baldwin et al. 1995
WS.030	E251X	5	Tassabehji et al. 1995
WS.001	Q254X	5	Tassabehji et al. 1995
NIH3	V265F	6	Lalwani et al. 1995
WS.028	W266C	6	Tassabehji et al. 1995
WS.016	R270C	6	Tassabehji et al. 1995
WS.10	R271C	6	Foy et al. 1990, Tassabehji et al. 1995
MSU5	R271C	6	Asher et al.1991; Morell et al. in press
NIH8	R271G	6	Lalwani et al.1995
WS.008	R271H	6	Tassabehji et al. 1995
MSU7	W274X	6	Morell et al. in press
WS.123	W274X	6	Tassabehji et al. 1995
BU14	Q313X	6	Baldwin et al. 1995
BU22	874ins1	6	Baldwin et al. 1995
MSU9	874ins1	6	Kapur and Karam 1991; Morell et al. in press
WS.019	874ins1	6	Tassabehji et al. 1995
WS.105	916del1	6	Tassabehji et al. 1995
BU30	954del1	6	Baldwin et al. 1995
UoM1	Q391H	7	Carey et al. 1996 (in preparation)
BU25	1185ins3	8	Baldwin et al. 1995

Figure 2: *PAX3* mutations. A diagram of the mutations characterized in the literature. The top panel displays the paired domain, the octapeptide domain and the homeodomain in relation to the mutations. The lower panel displays the mutations in relation to the eight exons.

PAX3 Mutations

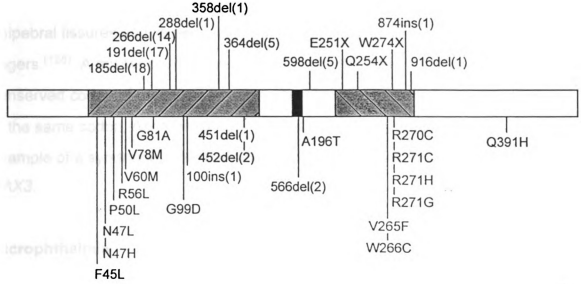

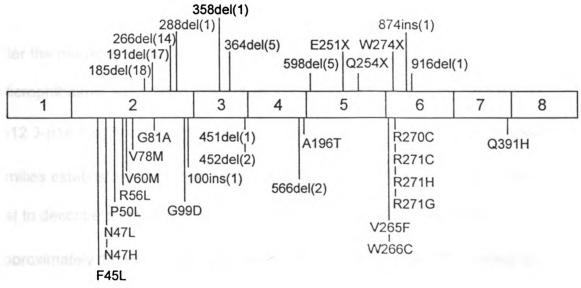

In addition to alveolar rhabdomyosarcoma and WS, a mutation in *PAX3* also causes Craniofacial Deafness Hand Syndrome (CDHS) (MIM 122880). CDHS was first identified in a single small family.[158] CDHS is characterized by the absence or hypoplasia of the nasal bones, profound sensorineural deafness, small and short nose with a slit like nare, hypertelorism, short palpebral fissures and limited movement at the wrist and ulnar deviation of the fingers.[158] A missense mutation, Asn47Lys, in *PAX3* exon two in a highly conserved codon of the paired domain was identified.[159] There is a mutation in the same codon, Asn47His, in a WSIII family.[15] This discovery is an example of a syndrome other than WS being caused by a mutant allele in *PAX3*.

Microphthalmia

Extensive linkage studies suggested that WSII was not linked to *PAX3*.[7,160] At least one additional gene was responsible for WSII mutations. After the mouse *Mi* gene was cloned,[161] its human homologue *MITF* (Microphthalmia-associated Transcription Factor) was cloned and assigned to 3p12.3-p14.1 by fluorescent *in situ* hybridizaiton (FISH).[162] Analyses in WSII families established linkage to 3p12.3-p14.1. Tassabehji et al.[163] were the first to describe mutations in *MITF* responsible for the WSII phenotype. Approximately 10 *MITF* mutations have been reported to date[163] (TABLE 6). The majority of *MITF* mutations fall within the DNA binding domains (FIGURE 3). However, WSII appears to be genetically heterogeneous since the WSII

phenotype in some families is unlinked to *MITF*. Therefore, there must be at least one more gene which when mutant, causes WSII.

***MITF* Mutations**

FAMILY	MUTATION	EXON	REFERENCES
WS.002	G153+1A	IN1	Tassabehji et al. 1994
WS.140	G153+1A	IN1	Tassabehji et al. 1994
WS.026	A562-1C	IN4	Tassabehji et al. 1994
WS.082	del3	7	Tassabehji et al. 1994
WS.115	S250F	8	Tassabehji et al. 1994
WS.078	N278F	8	Tassabehji et al. 1994
WS.022	S298F	9	Tassabehji et al. 1994
MSU11	944del1	8	Morell et al. submitted

Table 6 *MITF* mutations. The listing includes the family name, the mutation, the exon the mutation. Tassabehji et al.[155] discuss non-pathologic mutations which are not included in this table.

MITF/Mi are members of the basic helix-loop-helix-leucine zipper (bHLH-Zip) family of transcription factors (FIGURE 4). In bHLH-Zip proteins, DNA binding is mediated through the basic domain. Dimerization occurs by the helix-loop-helix domain and is stabilized by the zipper.[164, 165] This family of transcription factors bind as dimers and can form stable heterodimers with other members of the bHLH-Zip family.[166] *Mi* is expressed in the murine developing ear, eye, skin and in the adult heart.[167] Melanocytes are not essential for viability, however, *Mi* is essential for melanocyte differentiation, function and survival.[166]

Figure 3: *MITF* mutations. A diagram of the mutations characterized in the literature. The top panel displays the paired domain, the octapeptide domain and the homeodomain in relation to the mutations. The lower panel displays the mutations in relation to the nine exons. S = splice site mutations.

MITF Mutations

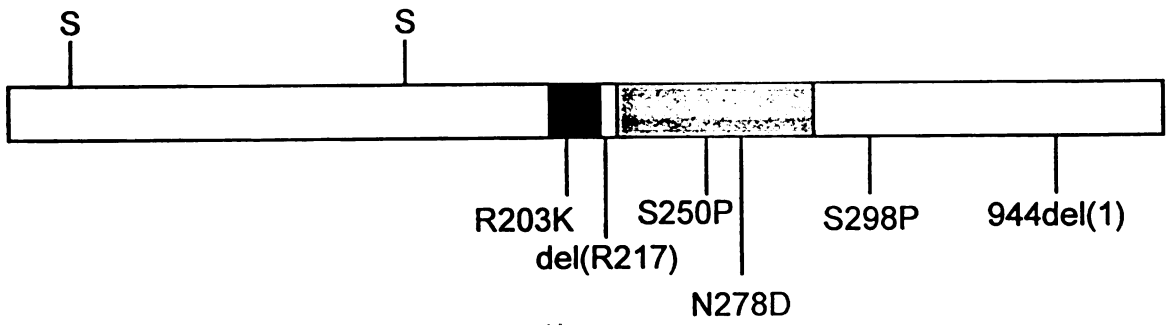

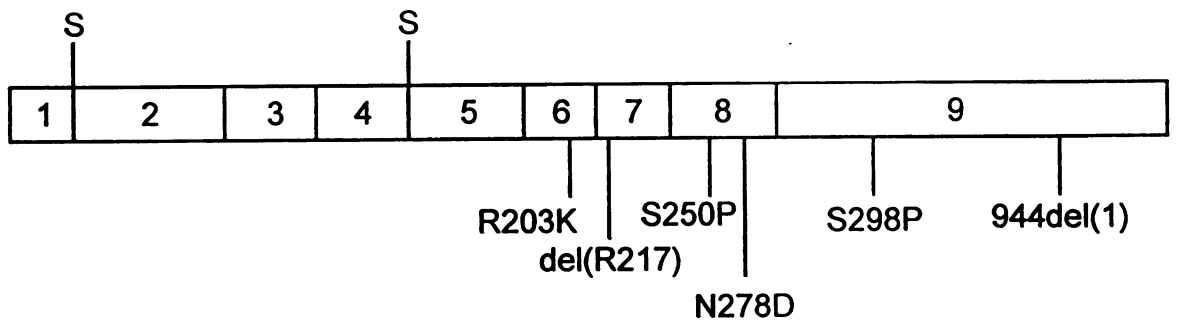

Figure 4: bHLH Protein Family

Class A and B bHLH Proteins

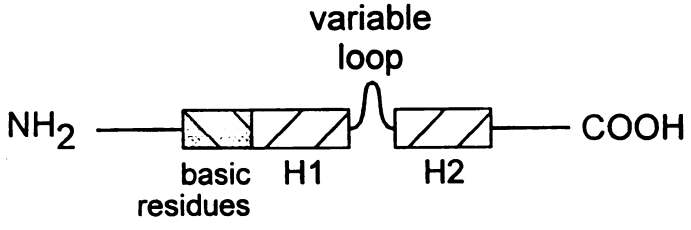

Class C bHLH-zip Proteins

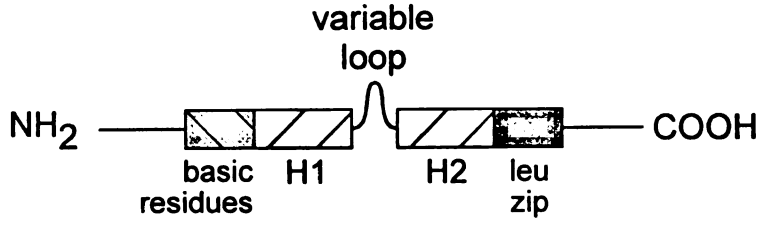

Dominant Negative (Id) HLH Proteins

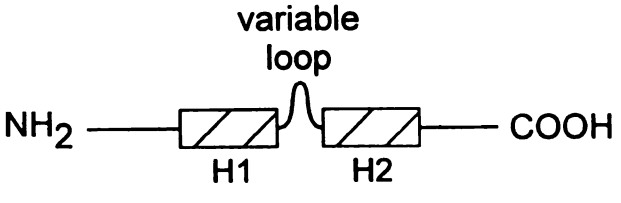

(modified from Baker et al. 1995)[44]

Other genes causing Waardenburg Syndrome

Mutations in several genes have been identified that are associated with WSIV. Mutations have been characterized in Endothelin-3 (*EDN3*),[168] Endothelin Receptor B (*EDNRB*)[169, 170] and the proto-oncogene *RET* (Rearranged during Transfection)[171-179] in individuals with Hirschprung disease and Waardenburg Syndrome. The endothelin family of 21 amino acid peptides act on G protein-coupled heptahelical receptors.[180] *EDNs* are produced from a large prepropolypeptide precursor that is cleaved to the active 21-residue mature form.[180] There are three endothelins (*EDN1*, *EDN2* and *EDN3*) known in mammals. Each *EDN* gene product is encoded by a separate gene and expressed in vascular and nonvascular tissues. There are two subtypes of endothelin receptors (EDNRA and *EDNRB*) that are expressed in various cells. The receptors initiate several intracellular signal transduction events through heterotrimeric G proteins.[180] *EDNRB* plays an essential role in the normal development of epidermal melanocytes and enteric ganglion neurons in mice and humans.[170, 180, 181] *EDNRB* in the mouse is called the piebald locus, which was predicted to be a candidate for WS.[54, 173, 181, 182]

Understanding function

There are now at least five genes, *PAX3* , *MITF*, *EDNRB*, *EDN3* and *RET*, known to be involved in the Waardenburg Syndrome phenotypes. The expression, function, interaction with one another, if any, and the role of these

genes in development are now of great interest. One experimental approach to begin to elucidate the normal function of these genes is to examine the range of mutant phenotypes. Therefore, identifying additional mutations in all of these genes may help in further understand their function.

CHAPTER ONE

Screening for mutations in *PAX3* and *MITF* in families with classical Waardenburg Syndrome and Waardenburg Syndrome-like phenotypes.

INTRODUCTION

The Goals of this study

The main purpose of this study was to determine the molecular defects in WS genes segregating in WS and WS-like probands. The proband screening set consisted of 42 individuals (TABLE 7). The entire set of probands was screened for the eight exons of *PAX3*[151, 183] and the nine exons of *MITF*[163] by SSCP analysis, and sequencing analysis.

The proband screening set included 33 WS individuals representing 33 families (in APPENDIX A TABLES 14-21) of which thirteen were WSI, nine were WSII, three were WSIV and seven were unclassified WS families. In addition, six SOD individuals and two families with WS-like clinical traits not usually considered a part of the WS phenotype were examined. The additional phenotypes of interest in the WS-like families were deafness, other neural tube defects and facial anomalies. The intent of including individuals with WS with other phenotypes and WS-like phenotypes, was to determine if these traits were caused by mutations in *PAX3* or *MITF*. The analysis of two families, designated UoM1 and MSU22, with WS probands exhibiting WS and additional

traits will be discussed in detail in later chapters. There have been many observations of WS associated with various other phenotypes that may or may not be classified as traits of WS.[18, 184-190] The identification of mutations causing related phenotypes or disorders may help in further understanding the role of *PAX3* and *MITF* in normal development.

Table 7: Proband screening set. The table is organized by the WS phenotypic type. The approximate number of individuals in the family are listed A = affected family members and U = unaffected family members. Any other clinical traits associated with the WS phenotype are listed including SOD = Septo-Optic Dysplasia, 18q = 18q Syndrome, CDHS = Craniofacial Deafness Hand Syndrome, AN = Anencephaly, DEAF = Deafness, CA = Craniofacial anomalies and OA = Ocular Albinism. The mutations identified in the set are included.

			PROBAND SCREENING SET				
FAMILY	A	U	TYPE	SSCP ANALYSIS		MUTATION	REFERENCE
MSU1	17	30	WSI	PAX3	MITF		
MSU2	6	9	WSI	PAX3	MITF		
MSU3	10	14	WSI	PAX3	MITF	100Ins1	Morell et al. 1993
MSU5	11	26	WSI	PAX3	MITF	R271C	Morell et al. 1996
MSU7	4	6	WSI	PAX3	MITF	W274X	Morell et al. 1996
MSU9	3	2	WSI	PAX3	MITF	874 Ins1	Morell et al. 1996
MSU29	1	10	WSI	PAX3	MITF		
UGM1-1	15	67	WSI	PAX3	MITF		
UGM1-2	10	20	WSI	PAX3	MITF	266del14	Morell et al. 1992
UGM1-3	4	11	WSI	PAX3	MITF		
UGM1-4	2	28	WSI	PAX3	MITF		
UofM1	7	9	WSI-SOD	PAX3	MITF	Q391H	Carey et al. 1996
MSU25	1	23	WSI-18q	PAX3	MITF		
UoM4	2	5	WSI?	PAX3	MITF		
MSU15	1	7	WSI?	PAX3	MITF		
MSU20	4	14	WSI?	PAX3	MITF		
MSU30	1	?	WSI?	PAX3	MITF		
MSU22	15	39	WS-CA	PAX3	MITF		
MSU11	9	18	WSII-OA	PAX3	MITF	944Del1	Morell submitted
MSU4	6	16	WSII	PAX3	MITF-		
MSU6	7	14	WSII	PAX3	MITF		
MSU10	7	10	WSII	PAX3	MITF		
MSU23	3	16	WSII	PAX3	MITF		
MSU24	2	2	WSII	PAX3	MITF		
MSU27	5	10	WSII	PAX3	MITF		
UGM2-1	1	30	WSII	PAX3	MITF		
UGM2-2	12	26	WSII	PAX3	MITF		
MSU14	1	10	WSII/?	PAX3	MITF		
MSU15	1	10	WSII/?	PAX3	MITF		
MSU12	2	2	WSIV	PAX3	MITF		
MSU13	4	9	WSIV	PAX3	MITF		
MSU28	3	10	WSIV	PAX3	MITF		
MSU26	6	8	DEAF-AN	PAX3	MITF		
MSU17	3	6	CDHS	PAX3	MITF	N47L	Asher et al. 1996
SOD1	1	?	SOD	PAX3	MITF		
SOD2	1	?	SOD	PAX3	MITF		
SOD3	1	?	SOD	PAX3	MITF		
SOD4	1	?	SOD	PAX3	MITF		
SOD5	1	?	SOD	PAX3	MITF		
SOD6	1	?	SOD	PAX3	MITF		

Description of the Proband Screening Set

Among our classic WS families (TABLE 7), four families designated, MSU25, MSU11, UoM1 and MSU22, exhibited clinical traits not commonly associated with Waardenburg Syndrome. The proband of MSU25 has a typical WSI phenotype as well as 18q-syndrome. Both the proband's parents are phenotypically normal. The characteristics of 18q-syndrome are growth deficiency, microcephaly, minor facial anomalies, limb abnormalities, genitourinary malformations, neurological and ocular abnormalities with developmental delay, and mental retardation.[191, 192] Karotype analysis by New York University Medical Center showed a *de novo* 18q deletion.

MSU11 is a WSII family with ocular albinism. A mutation was identified in *MITF* and characterized in this family prior to this study.[319] There are two other families, UoM1 and MSU22 with WS associated with other traits. Both of these families are discussed in detail in chapters two and three, respectively.

There are also families in the data set that would not be classified as having WS although they do have some similarities to the WS phenotype. The characteristics in these families included: Craniofacial Deafness Hand Syndrome[158] (CDHS) , MSU17, hearing loss and anencephaly, MSU26 and six families with Septo-Optic Dysplasia (SOD1-6).

Prior to this study mutations were also characterized in MSU3,[153] UGM2[152] and MSU17[159] in *PAX3* exon two within the paired domain. Mutations were also identified in the homeodomain of *PAX3* in MSU5, MSU7, MSU9 (Morell et al. 1996,[320] see manuscript in APPENDIX B).

RESULTS

The proband screening set included the probands from Waardenburg Syndrome families and Waardenburg Syndrome-like families. These individuals were screened for mutations in *PAX3* and *MITF*. Methods for detecting mutations or sequence variants were SSCP analysis, cycle sequencing and direct sequencing techniques.

A total of 34 primer pairs (TABLES 8 and 9 in Appendix A) were used for SSCP analysis. A diagram of the eight exons of *PAX3* and the nine exons of *MITF*, with the approximate locations of each of the primers, is displayed on FIGURES 5 and 6 in APPENDIX A. Details of PCR and SSCP analysis are described in the Materials and Methods. The PCR fragments labeled with α^{33}P-dCTP or α^{33}P-dATP were electrophoresed on 0.5X hydrolink MDE gels. The length of electrophoresis was sequence dependent and determined empirically. Variant SSCP patterns were identified in several families. Many of the subtle SSCP pattern differences were not reproducible. All DNA fragments that displayed aberrant and reproducible SSCP patterns were subcloned and sequenced. Some of the PCR fragments were cycle sequenced without first sub-cloning.

None of the PCR products was gel purified prior to SSCP analysis which could contribute to the complexity of the SSCP patterns. Only the families with reproducible SSCP variants are discussed below.

SSCP Analysis of *PAX3*

Among the 33 WSI and WSI-like probands in this study several SSCP variants were identified in *PAX3*. However not all of the variants were consistently identified in independent PCR amplification followed by MDE gel electrophoresis. For example, there were two different SSCP variants identified in exon one, in MSU1 and MSU2. Duplicate PCR amplifications were done on the genomic DNA for the probands of both of these families and the variants were not reproduced.

In this WS proband screening set, mutations were identified in exon two in MSU3 and MSU17 prior to this study yet, no other SSCP variants were identified within exon two for the screening set. Prior to this study three SSCP variants were identified in exon six in MSU5, MSU7 and MSU9 , and the mutations have been characterized in these families (see APPENDIX B for reprint). In this study a SSCP variant was identified in UGM4 in exon six, no mutation was identified. The SSCP variant identified in UoM1 was reproducible and will be further discussed in chapter two. There were no SSCP variant patterns identified for any of the WS and WS-like probands for exons three, four or eight.

SSCP analysis of *MITF*

SSCP variants were identified in *MITF*. There were three different SSCP variants identified in exon one in MSU23, MSU26 and UoM1. The variant in

MSU26 in *MITF* exon one was a subtle pattern difference not present in either parent. This variant was also not reproducible in multiple PCR amplifications. The PCR product from MSU26 was included in the sequencing evaluation. The SSCP pattern identified in MSU23 was subtle. The DNA fragments from both the probands from MSU23 and MSU26 were subcloned into the TA-cloning kit pCR™II vector® (Invitrogen) and the clones were analyzed by SSCP analysis. For each proband fifteen clones were screened by SSCP analysis. No SSCP variants were identified in any of the clones for either MSU23 or MSU26.

In MSU26 along with the MITF exon one variant, there were two other possible MITF variants detected, one in exon three and another in exon eight. The parent's genomic DNA was isolated and analyzed for the SSCP variants identified in the proband. The parents were both profoundly deaf. Neither parent had any of the three mentioned SSCP variations. Also after multiple PCR amplification of the proband's genomic DNA, the exon three and exon eight variants were not reproduced.

There were two other SSCP variants identified, one in MSU23 in exon two and one in UoM1 in exon nine. Neither of these subtle pattern variants were identified after consecutive PCR amplifications. No SSCP variants were identified for any of the other probands in the screening set in exons four, five, six or seven of *MITF*.

Cycle Sequencing Analysis of *PAX3* and *MITF*

Cycle sequencing was optimized for *PAX3* exons two through seven and *MITF* exons one, two, six, seven and eight. The primers designed for the remaining exons of *PAX3* and *MITF* were not suitable for cycle sequencing and were therefore omitted from the analysis. All the PCR products were gel purified on low melt agarose gels after PCR amplification. Several of the PCR primers were optimized for cycle sequencing (TABLE 10 in APPENDIX A) and were used to screen a number of the probands from the screening set. However, no sequence variants were identified in the probands screened by cycle sequencing methods. There were a few primers that were optimal for many of the DNA samples including *PAX3* exon two, six and seven and *MITF* exon one, two and eight. However, the sequencing results, even using these primers, did not produce reliable data.

PCR amplified DNA fragments were cycle sequenced from both MSU23 and MSU26. The sequence was of high quality with very little background. There were no sequence changes detected within the coding region of *MITF* exon one. However, not all of the 5'-untranslated region (UTR) sequence was readable by this method. This problem was addressed by subcloning these PCR fragments using the TA cloning kit (Invitrogen). No sequence variants were detected in the region sequenced after cloning the fragments from MSU23 or MSU26.

DISCUSSION

The main goal of this study was to identify and characterize mutations in *PAX3* and *MITF* in WS and WS-like individuals. The proband set included 33 WS individuals and eight WS-like individuals. There have been reports in the literature of various neurocristopathies associated with WS including meningocele,[193] meningomyelocele,[184, 194, 195] spina bifida,[187, 196] cleft lip/palate,[186, 197] neuropathy,[198, 199] piebaldism,[188, 200] vitiligo[201] and albinism.[202] The rationale of including WS-like individuals in this study, and many others,[155, 203] was to determine if mutations in *PAX3* or *MITF* caused a WS-like phenotype.

Several methods were employed to screen the exons of both *PAX3* and *MITF* including SSCP analysis, direct cycle sequencing and sequencing of plasmid clones. The 42 probands (TABLE 7) were screened by SSCP analysis for all known coding exons of *PAX3* and *MITF* (in APPENDIX A TABLES 8 and 9). All probands were included in the screen of both genes to establish controls for the normal SSCP patterns. Mutations were not expected in *MITF* in WSI individuals.[7, 155, 160, 186, 197] *PAX3* mutations were not expected in individuals with WSII. The inclusion of all samples in the screen also increased the number of chromosomes screened which could be used to demonstrate that any given variant was not a polymorphism. Once a variant was identified the genomic DNA was PCR amplified several times to assure the variant was

reproducible, not an artifact of PCR or a concentration dependent variant. Fragments with a persistent SSCP were then subcloned and sequenced.

SSCP Analysis

There were several variants identified by SSCP analysis. All possible variant patterns were documented and the genomic DNA was PCR amplified in duplicate to determine if the variant was real or an artifact. Several variants were not reproducible and excluded from further investigation. Any variant that persisted in multiple reactions was subcloned into the TA-cloning kit pCR™II vector (Invitrogen). Individual clones containing inserts were analyzed by SSCP analysis and clones identified with the variant SSCP patterns were sequenced.

Families with characterized mutations MSU3,[153] UGM2,[152] MSU17,[159] MSU5,[320] MSU7[320] and MSU9[320] identified by SSCP analysis prior to this study were included in the mutational screening in this study. The SSCP variants identified in these families were consistently observed and the mutations characterized (TABLE 7; FIGURES 2 and 3). These DNA samples with characterized *PAX3* and *MITF* mutations served as positive controls for the conditions used in this study for SSCP variant detection.

There were three families that were kept in the screening set even after SSCP patterns were not reproduced. These included MSU23, MSU26 and in UoM1. MSU23 is a classic WSII family, and MSU26 is a family with hearing

loss and multiple anencephalic fetuses. UoM1 is discussed in chapter two. All three of the families had SSCP variants detected in *MITF* exon one. The PCR products generated during the SSCP analysis were subcloned. Two of the families, MSU26 and UoM1, were of considerable interest, because of their phenotypes. MSU23 was included because of the interest in *MITF* exon one. SSCP analysis of the clones determined which clones had the observed variant. In MSU23 and MSU26 no variants were identified in fifteen clones from each of the proband's PCR amplified DNA. Multiple PCR amplification of the genomic DNA from these two families did not consistently identify the SSCP variant. Cycle sequencing was also performed using PCR amplified and gel purified DNA from the probands from each family. No sequence changes were observed in the translated region of exon one of *MITF* for either MSU23 and MSU26. The 5'-UTR was not completely sequenced since the SSCP variants were not consistently observed. There was the possibility that a mutation was missed that fell within the 5'-UTR. The function and relevance of any base change in the 5'-UTR, however, would be difficult to prove. Therefore, further pursuit of this region was not warranted. The variant observed in UoM1 is discussed in chapter two.

Cycle Sequencing

Along with SSCP analyses Direct Cycle Sequencing protocols were used to directly look for mutations in PCR amplified genomic DNA for the exons

of *PAX3* and *MITF*. Direct sequencing has several potential advantages over the traditional cloning and sequencing protocols. Cycle sequencing reactions are cheaper, faster and theoretically more accurate since the cloning step is eliminated. However, cycle sequencing protocols used in this study were difficult to optimize. Several reactions were done for various exons but the sequencing reactions usually did not produce easily interpretable results. High background in the sequencing reactions made single base substitutions difficult to interpret for most of the exons. In addition, over the course of ten years of gathering samples, genomic DNA was isolated by various methods. The differences in the DNA preparations required individual primer optimization for many of the DNA samples.

Cycle sequencing reactions were optimized for each primer of every exon used for the sequencing reaction. Rather than designing new primers, one of the PCR primers was used for the sequencing when possible (TABLE 10 in APPENDIX A). These were the same primers used for the PCR amplification (TABLES 8 and 9) and therefore, were not optimally designed for direct cycle sequencing according to the Amersham protocols. Both ΔTaq Cycle Sequencing Kit and ThermoSequenase (Amersham) were used. The intensities of the bands for the dd-NTPs varied using the ΔTaq method. The enzyme preferentially incorporates certain dd-NTPs causing many artifacts and high background. The ThermoSequenase method was designed by the manufacturer to eliminate the preferential incorporation of dd-NTPs. However,

this method still did not produce optimal sequencing results. Since many of the primers were those designed specifically optimal for PCR, not sequencing, several of the primers did not have optimal lengths or GC-content recommended by Amersham in the protocols. The sequencing extension reaction requires the exclusion of one of the dideoxynucleotides for the primer to be elongated according to the protocols for cycle sequencing. The length and the GC-content of the elongated primers was not consistent between the different primers for each of the exons used in the study (TABLE 10).

Direct sequencing from PCR amplified DNA was suggested to be the most efficient and stringent way to screen for mutations. DNA from several of the WS family members was PCR amplified and cycle sequenced. No new mutations were identified by this method. However, the high background and numerous artifacts made identification of single base substitutions difficult. Further optimization would have added considerable time and material expense to this portion of the study. Therefore considering the technical obstacles this method was abandoned.

Mutation Detection

Prior to screening the entire data set of thirteen WSI, nine WSII, three WSIV and seven WS-like individuals several families MSU3, UGM2, MSU5, MSU7, MSU9 and MSU17 were screened for mutations in exons two, five and six for *PAX3*. Seven new WSI mutations were identified and characterized

(TABLE 7). The mutational searches were dependent upon the availability of the intron flanking sequence to design PCR primers. The entire proband set was analyzed for mutations once primers for all of the exons of *PAX3* and *MITF* became available. A total of 42 individuals were screened in this study, six mutations in WSI individuals were identified and characterized in *PAX3,* one mutation in *PAX3* in a family with CDHS and one mutation in a WSII family in *MITF*. Herein one of the six mutations identified in *PAX3* was characterized in a WSI family. No new *MITF* mutations were found in this study among the nine WSII individuals.

It is estimated that all WSI families map to *PAX3.*[5] In a recent study of one hundred and thirty-four families, *PAX3* mutations were identified in the coding regions in 20/25 WSI and WSIII individuals.[155] In the 42 probands in this screening set, there were thirteen WSI individuals. *PAX3* mutations were detected in six (46%) of the unrelated WSI individuals. Although this estimate is lower than the expected 80%[155], considering the small sample size the maximum number of mutations in WSI individuals in the known regions of *PAX3* may have been identified in this study.

MITF mutations causing WSII have only recently been identified. For WSII individuals approximately 20% of the mutations have been identified in *MITF.* [155] In this screening set, one *MITF* mutation in nine (11%) unrelated

WSII individuals was detected. The results, however, were consistent with the published mutation detection expectation in *MITF* among WSII individuals. There may be at least one other gene responsible for the WSII phenotype that is yet to be identified. The other WSII gene(s) may be important in the regulation of the genes responsible for normal neural crest cell migration and differentiation.

There are six probands in this screening set that were not classified as WSI or WSII. Complete clinical data was lacking for these families, therefore, they could not be characterized. However, they were included in the mutational screening. No mutations were detected in the six unclassified WS individuals. The set also included three WSIV probands that were not included in the WSI or WSII calculations. Also not included in the estimates were the six SOD individuals, MSU17 with CDHS or MSU26.

Evaluation of Clinical Data

Numerous factors may have contributed to the small number of mutations identified in this analysis. However, the most important depends on accurate collection and interpretation of the clinical data for each family. The data on each family was carefully evaluated to be sure families were classified correctly into the WS sub-categories.

My evaluation was based on the data in our files for all the families focusing on the hearing tests, W-index measurements and the mention of any

other clinical traits. The data for each family is described in detail in TABLES 15 through 22 in APPENDIX A. Families in this set were ascertained by different clinicians and/or genetic counselors from all over the United States as well as from out of the country (TABLE 11 in APPENDIX A). The data sheets (see APPENDIX B) supplied to them were completed to various degrees, with emphasis on different portions of the phenotype. Often pedigrees were not included or the detail was limited. This made interpretation of the clinical evaluations difficult. For example, many of the families did not have hearing tests, eye exams, inner-canthal, inner-pupillary and outer-canthal measurements. Other clinical traits not classified as WS may or may not have been included. Pictures were rarely available of affected family members. Most of the descriptions of the clinical data were vague and missing actual reports. Families with questionable phenotype or without W-index ratios were not included in the estimates for the approximate mutation detection.

Another factor that may influence the number of mutations detected is the improper classification of dystopia canthorum with approximately 98% penetrance. *PAX3*, when mutant, is responsible for the occurrence of dystopia canthorum; and is thought to play a direct role in skull and facial development.[204] This gene may also play an indirect role in development by activating other genes that are responsible for skull organization. Variation in the inner canthi, could be mistaken for WSI when in fact the clinical manifestation is something quite different.[205, 206] Families with craniofacial

anomalies should be carefully evaluated before classifying them as WSI or WSII, if they fit the other WS criteria. This does not seem to be the case in our screening set, with the exception of MSU22. There may be skull malformations that are caused by mutations by *PAX3* that do not exhibit the other characteristics of WS. An example of this is Craniofacial Deafness Hand Syndrome (CDHS) described originally in 1983.[158] The clinical manifestation of CDHS is distinct from Waardenburg Syndrome yet a mutation was identified in exon two of *PAX3* within the paired domain.[159]

Mutations Due to Deletions

There are several other explanations for a possible lower than expected efficiency of *PAX3* mutation detection in WS probands. Cytological analyses could have been done to detect very large deletions in the region of *PAX3* or *MITF*. Deletions of *PAX3* have been reported.[207] However, a deletion that was submicroscopic could be overlooked. Such deletions could include the regions homologous to one or both of the primers, the entire gene or a large segment of the gene. None of these types of deletion would be detected by the PCR based methods used in this study. There are several methods that can be used to detect deletions, including: competitive quantitative PCR amplification, southern blotting, cytological testing for submicroscopic deletions using fluorescent probes, and possibly identifying excess homozygosity.

Mutations in Regulatory Regions

Another possible explanation for the low number of mutations detected in this screening set, is that the mutations responsible for the WSI phenotype are within regulatory regions of either *PAX3* and/or *MITF*. These regions may be near the coding sequence or may be hundreds of kilobases away.[208-210] A position effect mutation 85 kilobases away from the 3'-end of the *PAX6* gene causes aniridia.[211] Mutations in regions downstream or upstream of the coding region may be difficult to identify.[212]

Mutations in a regulatory region of either *PAX3* and/or *MITF* may cause the WS phenotype. Regulatory regions may include promoters, enhancers, silencers or even splicing mutants that create cryptic splice sites within introns or alter the branch point site. Mutations within regulatory regions may affect the function of a gene.

Mutations in Alternate Transcripts

The existence of alternative transcripts may also explain why more WSI mutations in *PAX3* and WSII mutations in *MITF* were not identified. Several of the *PAX* genes, including *PAX2*, *PAX8*, *PAX6* have alternative transcripts that, change the 3'-end of the gene altering the carboxy terminus.[76, 213, 214] Two alternative transcripts of *PAX2* are expressed in the human fetal kidney with no observable difference in temporal expression.[214] There are six alternative

transcripts identified in murine *PAX8* that are temporally and spatially regulated during development in the developing central nervous system (CNS), the thyroid gland and the embryonic kidneys.[76] There are two isoforms of *PAX6* mRNA expressed in the developing eye, brain, spinal cord and olfactory epithelium.[213]

There are at least two isoforms of *PAX3* mRNAs expressed in the human adult cerebellum and skeletal muscle as a result of alternative splicing.[55] The 3'-end of these isoforms would not be screened for mutations by the primers used in this study. In addition to these alternate forms there may be other alternative transcripts of *PAX3* that have not been identified. Once these different messages are identified there will be new regions to screen for mutations in classical WS families.

Two different forms of *Mi* have been identified. One expressed in melanocytes [167] and the other in heart and skeletal muscle.[215] The difference in the 5'-ends of these two forms may be generated by different promoters.[167] There is the possibility that other forms of *Mi/MITF* exist.

Technical Obstacles with SSCP

The low number of mutant alleles identified in this screening set may be due to the detection methods that were used in this study. A key component of SSCP analysis is primer design. The primers must be specific for the sequence of interest, and the fragment generated by PCR should be within an

appropriate size range for optimal variant detection. The optimal size range for PCR fragments used in SSCP analysis are 100-200 base pairs for 80% detection, for fragments of 300-400 base pairs the detection frequency is less than 50%.[216] Several of the primers used in this study were designed when little was known about the intron sequences flanking the exons of *PAX3*. Therefore they could not be designed for optimal SSCP analysis. At least one of the primers used with this screening set falls within the 5'-end of the exon (see FIGURE 5 in APPENDIX A). This could account for some of the undetected mutations. The majority of fragments analyzed in this study were between 200 and 400 base pairs, two fragments were greater than 500 base pairs. The fragment sizes detected by the primer pairs utilized in this screen are listed in TABLES 8 and 9 in APPENDIX A. The sub-optimal fragment size could explain why the observed mutations in WSI families were lower than expected. However, it is important to note that the primers used in this study are similar, but not identical to those used in other screens reported in the literature.[151, 155, 203]

Deciphering normal and variant conformational patterns can sometimes be difficult. Often there are background bands that vary in intensity and in pattern. Some of this variation can be eliminated by gel purifying the samples after "cold" PCR prior to the "hot" reaction. Very few of the samples were gel purified prior to PCR. A complex pattern of bands may still exist for a variety of other reasons, including various DNA and primer concentrations, overloading

the sample, differing PCR amplification efficiencies, electrophoresis conditions and overamplification.

Genomic DNA samples not isolated with the PUREGENE kit were often difficult to PCR amplify thus requiring a two step PCR method. Most of the samples were PCR amplified for thirty cycles without isotope and then for twenty-six cycles with isotope. The same primer pairs were used for both the "cold" and "hot" reactions, possibly causing the overamplification.

Important variables for SSCP analysis include: electrophoresis temperature conditions, gel composition and wattage. In this study, gels were run at 4°C and at 23°C. They were prepared with MDE and/or native acrylamide with or without glycerol. The power was set at: 8, 15, 20 or 50 Watts with differing electrophoresis times. The time each fragment should be run for adequate separation is dependent on the sequence as well as the gel and electrophoresis conditions and was determined empirically. Although many combinations of the temperature conditions, gel composition and wattage were used in this study, any one of the combinations may have been under-represented. However, SSCP variants identified by one condition were also observed using others conditions. Also, the SSCP variants observed in families with previously documented mutations were consistently demonstrated using a variety of the above conditions.

Mutations in Other Genes

Mutations in EDNRB, EDN3 and RET have been characterized in individuals with Hischprungs disease (HSCR) and Waardenburg Syndrome. Hirschprung disease or aganglionic megacolon, is associated with the congenital absence of intrinsic ganglion cells in both the myenteric and submucosal plexuses of the distal gastrointestinal tract, leading to the failure of innervation of the colon.[170] HSCR is estimated to occur in 1/5000 live births with a sibling recurrence risk of 4%.[25] Males are more susceptible than females.[25] HSCR is considered to be a developmental defect stemming from a failure of neural crest cell migration, differentiation or colonization during gestation weeks five to twelve.[170] Mapping studies implicated several genes as possible candidates. After the discovery of the genes responsible for the Hirschprung disease phenotype the question of screening our families for mutations needed to be addressed.

We have three families, MSU12, MSU13 and MSU28, in our data set that appear to exhibit Hirschprung disease, along with WS (TABLE 7). All three HSCR families have been screened for mutations in *PAX3* and *MITF* by SSCP analysis but not *EDNRB*, *EDN3* or *RET*. No apparent SSCP variants were identified in these three families.

CONCLUSION

Considering the possible errors in experimental design and the missing clinical data there may be more information to be collected from the 31 Waardenburg Syndrome families discussed in this study. One family designated UGM1, has been shown to be linked to PAX3; however, a mutation within the coding region has not been identified (data not shown).

There are several aspects that could still be considered for exploration. Direct sequencing with optimal primers of each exon of both *PAX3* and *MITF* for each proband is one possibility. The use of automated sequencers could also eliminate differences in reaction conditions.

Several of the families in this study were missing essential clinical data. This made clear classification of WS difficult; thus without accurate and complete clinical data the diagnosis may not be reliable. Prior to undertaking any large scale screening for mutations, a thorough evaluation of the available clinical data is important to ensure that time is not wasted on screening individuals that are unlikely to have mutations in the genes of interest.

The identification of submicroscopic deletions may be possible with the use of competitive quantitative PCR amplification, cytological analysis looking for the deletions or identifying an excess homozygosity. All three of the above techniques are time consuming and technically challenging. The results may not be conclusive. Therefore, without linkage data demonstrating the gene of

interest is responsible for the phenotype, optimizing the techniques may not be cost efficient. In this study markers linked to PAX3 could be used to look for an excess of homozygosity; which may indicate that the alleles are actually hemizygous. The small sample size will not give statistically significant results.

MATERIALS and METHODS

Family Identification and DNA isolation

During the period of this study, WS families were ascertained in various ways and by many different individuals. Several of our families were identified through schools for the deaf, in the United States and in Indonesia. Included in this study were six Indonesian families identified and collected during multiple trips made by Drs. Asher and Friedman to Indonesia (collaborators: SuKarti Moeljopawiro, Sunaryana Winata and I Nyoman Arhya, Udayana University, Denpasar, Bali Indonesia). The more recent families used in this study were identified through collaborations with various physicians and genetic counselors (TABLE 11 in APPENDIX A). Most of the clinical data was collected by different physicians and, as a consequence, is not complete in every respect. The entire proband set is outlined in TABLE 5 in Chapter one. Each family is described in TABLES 14-21 to the extent that our records are complete. All family members contacted were informed of the study and signed consent forms in order to participate (see APPENDIX B for copy of blank forms).

Patient DNA was obtained from either lymphocyte cells from blood or cheek cells isolated by a saline mouthwash method. DNA obtained from blood was isolated using the PUREGENE™ kit (Gentra Systems). The blood sample was incubated with RBC lysis solution, then centrifuged at 2000xg at room temperature. The white cells formed a pellet and the supernatant was

discarded. The white cells were then incubated with WBC lysis solution at 37°C. Protein precipitating solution was added and the supernatant was collected. Two volumes of ethanol were added to the supernatant. The DNA was precipitated and was washed in 70% ethanol for several minutes and then resuspended in $T_{10}E_1$ pH 8.0. In families identified in the early 1990's, the DNA was isolated by various other methods including phenol extraction.

The mouthwash samples were isolated in 10 ml 0.9% sterile saline. The solution was centrifuged and 500 µl 0.05 N NaOH was added to the pellet. Then the solution was incubated at 95°C for five to ten minutes, stored on ice for zero to five minutes before adding 500 µl $T_{10}E_1$ pH 8.0.

Polymerase Chain Reaction

DNA amplification was performed on a MJ Research, Inc., Thermo Controller using the Polymerase Chain Reaction (PCR) for each of the known exons of both *PAX3* and *MITF*. See primer list (TABLES 8 and 9). All of the primer pairs for *PAX3* and *MITF* were amplified using the PCR buffer recipe: 10 mM Tris-HCl, pH 8.3, 1.5 mM $MgCl_2$ and 50 mM KCl (Boehringer Mannheim) except exon seven of *PAX3*. The reaction buffer for exon seven contained: 10 mM Tris-HCl, pH 9.2, 1.5 mM $MgCl_2$ and 75 mM KCl (Stratagene Opti-Prime™ PCR Optimization Kit, buffer 10).

Standard amplifications were performed in a total volume of 25 µl which included: 100 ng genomic DNA, 0.1-0.2 µM of each primer, 0.25 mM dNTP's,

2.5 μl 10x PCR buffer, 0.2 units of Thermal Stable DNA Polymerase (TSP). The cycling parameters were: 94°C for 1 minute, a specified annealing temperature (TABLES 9 and 10), 72°C for 3 minutes for 15-30 cycles and then a 10 minute final extension at 72°C. Labeling reactions also included α^{33}P-dATP or α^{33}P-dCTP (Amersham and/or Andotech).

Markers linked to *PAX3* were used to analyze informative families for linkage. In this study MSU22 was typed for the markers described by Wilcox et al.[183] and Macina et al.[132] See primer list in TABLE 13. The PCR amplification followed the standard protocol outlined above.

Single Strand Conformation Polymorphism

Single Strand Conformation Polymorphism (SSCP) was performed on all known coding exons of *PAX3* and *MITF* for all of the probands. The PCR was performed as above. A 2-3 μl aliquot of each amplification was denatured for 3 minutes at 95°C, chilled on ice, then electrophoresed on a MDE™ 0.5X Hydrolink® gel (AT Biochem). The MDE gels were prepared with 12.5 ml MDE, 3 ml 10X TBE (Tris base, Boric acid and EDTA), 35 ml dH_2O, 540 μl 10% ammonium persulfate (APS) and 30 μl TEMED (Tetramethyl-ethylenediamine). Electrophoresis proceeded in 0.6X TBE buffer in both the upper and lower chambers of a NUGENEration™ Sequencing Systems (OWL Scientific models S1S and S2S). MDE gels were run at 8 Watts both at room temperature and at 4°C. Gels were also run under the above conditions with and without 10%

glycerol. Select gels were run at 15 or 50 Watts at both temperatures. The run time varied from four to 12 hours for each exon due to the size of each fragment and the sequence. Control samples were included for each analysis to distinguish normal patterns from SSCP variants.

For DNA samples with a SSCP variant the genomic DNA was PCR-amplified multiple times and run on several gels to determine if the variant pattern was reproducible. The PCR products from individuals with abnormal and reproducible SSCP patterns were either subcloned and sequenced (Amersham Sequenase™ Version 2.0 Kit, or a modified version) or directly sequenced by cycle sequencing protocols (Amersham ΔTaq Cycle™ Sequencer or ThermoSequenase™ kits).

Allele Specific Amplification (ASA)

Allele-specific primers were designed so that the single base substitution was at the 3'-end of the primer. An allele specific primer (TF195) was synthesized to verify the base change in family UoM1 in *PAX3* exon seven. TF195 was amplified with TF141 for exon seven and in the same reaction tube h a *PAX3* exon four control primer pair set TF35 and TF36. The primers were optimized using the Stratagene Opti-Prime™ Optimization Kit and buffer #2 (10 mM Tris-HCl, pH 8.3, 1.5 mM $MgCl_2$ and 75 mM KCl). The cycling parameters were as above with an annealing temperature of 65°C. The exon four primers (TF35-36) were used for a control fragment, with a product length of 242 base

pairs and the allele-specific fragment amplified with TF141 and TF195 produced a 270 base pairs product. (see the primer list TABLE 8). The fragments were separated by electrophoresis on a 4% 3:1 NuSieve for 3 hours and visualized with ethidium bromide staining.

Cloning fragments

After determining that a SSCP was reproducible, the mutant PCR product containing the SSCP variant was cloned into a pGEM®-T Vector System (Promega) or the TA-Cloning® kit (Invitrogen). The insert:vector molar ratio was either 3:1 or 1:1. The ligation reactions included: T4 DNA ligase 10X buffer (300 mM Tris-HCl, pH 7.5, 100 mM MgCl2, 100 mM DTT and 10 mM ATP), 50 ng pGEM®-T vector, PCR product, T4 DNA ligase (1 Weiss unit/ml) and dH_2O to a final volume of 10 μl. The ligation reaction mix incubated for three to twelve hours at 15°C. The transformation step used a 2 μl aliquot of the ligation reaction mix. After the ligation reactions, the vector was introduced into the Sure Cells by either electroporation or by the cell shock protocol described by Invitrogen®. Cells were grown on LB (Luria-Bertani) plates with ampicillin (50 μg/ml), IPTG (200 mg/ml) and X-Gal (20 mg/ml in dimethylformamide) utilizing the blue-white selection method. LB medium contains 10 grams Bacto®-tryptone, 5 grams Bacto® yeast extract, 5 grams NaCl and 15 grams agar per liter. Inserts cloned into pGEM®-T vector were verified by either restriction digests or PCR. Clones were then propagated in

liquid LB with ampicillin (50 μg/ml) for eight to twelve hours at 37°C and shaking at 225 rpm. Plasmid DNA was isolated using the Wizard™ Minipreps DNA Purification Systems (Promega). SSCP analysis was performed on individual clones and compared to the patterns generated from the genomic DNA in order to identify clones containing the mutation responsible for the SSCP variant.

DNA Sequencing

The DNA sequence of the cloned fragments containing SSCP variants was determined using the forward and reverse primers from the Sequenase 2.0 kit following the manufacturer's protocol. A modified version of the Sequenase protocol called the Quick Double-Strand DNA Sequencing Protocol was used. This method does not require an ethanol precipitation after the denaturation step and thus saves about one hour. Primer concentrations generally ranged from 1-2 mM however, primer concentrations as high as 20 mM were also used. In the denaturation step, the DNA, primer and 1N NaOH was incubated at 68°C for ten minutes. Freshly prepared TDMN (Tes, concentrated HCl, 1M $MgCl_2$, 4M $NaCl_2$ and 1M DTT) was added in the annealing step.

For the cycle sequencing or direct sequencing reactions the PCR products were separated by electrophoresis on 1-2% low melt (FMC) agarose gels and purified using the Wizard™ PCR Purification Systems (Promega). Cycle sequencing reactions were optimized for each primer for each of the exons of *PAX3* and *MITF*. The annealing temperature varied for each primer

(TABLE 10) and either 67°C or 72°C were used for the termination reaction. Cycling was done 50 times at both steps, the overall reaction time was approximately three hours. Cycle sequencing reactions were performed following the manufacturer's protocol using either the ΔTaq Cycle™ Sequencing kit (Amersham) or ThermoSequenase™ Cycle Sequencing kit (Amersham). Sequencing reactions were separated by electrophoresis on 6% acrylamide gels with either flat or wedged spacers. The gel solution was made in 600 ml volumes and stored at 4°C and includes: 90 ml 40% acrylamide (Biorad 19:1 solution), 60 ml 10X TBE, 288 g urea and dH_2O to 600 ml. The standard gels use 75-100 ml from the prepared acrylamide stock, 30-50 μl TEMED and 75-100 μl APS. The gels were pre-warmed for 30-45 minutes in 0.5X TBE buffer prior to denaturing the PCR fragments at 94°C for two to ten minutes. Electrophoresis proceeded at 55 or 95 watts in order to maintain a constant temperature of 55°C. Gels were fixed in 20% methanol and 10% acetic acid for 45 minutes, dried and exposed to Hyperfilm™-MS (Amersham).

CHAPTER 2

A Waardenburg Syndrome type I family with the proband exhibiting WSI and Septo-Optic Dysplasia.

INTRODUCTION

Septo-Optic Dysplasia

Septo-Optic Dysplasia (SOD) also known as Septo-Optic-Pituitary Anomaly (SOPA) has a highly variable phenotype.[217-223] Key characteristics of SOD are optic nerve abnormalities, partial or complete absence of the septum pellucidum[224, 225] and endocrine dysfunction.[226-228] The pituitary dysfunction can be highly variable and change throughout life. Some of the key characteristics of pituitary dysfunction are: short stature, neonatal hypoglycemia, seizures, apnea, cyanosis, jaundice, thermal instability and fever, CNS abnormalities and mental retardation.[226, 227, 229-233] The primary diagnostic characteristic of SOD is visual impairment, including amblyopia and nystagmus.[234, 235]

The cause of SOD is not known. There are some correlations between a young age of the mother and even possible drug use with the occurrence of SOD. There are also examples of various infections during pregnancy including Rubella, viral and urinary tract infections.[228, 236-239] There are two

cases with relatives displaying SOD suggesting the possibility of a genetic component, yet all other reported occurrences of SOD have been sporadic.[240, 241]

SOD arises early in gestation and represents a mild form of holoprosencephaly.[227, 242-246] The approximate time in embryogenesis is at about four to six weeks gestation when the anterior wall of the diencephalon invaginates and the optic nerve ganglion cells develop.[247] Findings of widespread calcification and glial nodules in the septal region and the anterior hypothalamus suggest that a destructive process with necrosis and neuronal loss between eighteen to twenty weeks has occurred.[242, 248] This is approximately the time when the septum pellucidum forms [242, 243] (FIGURE 7).

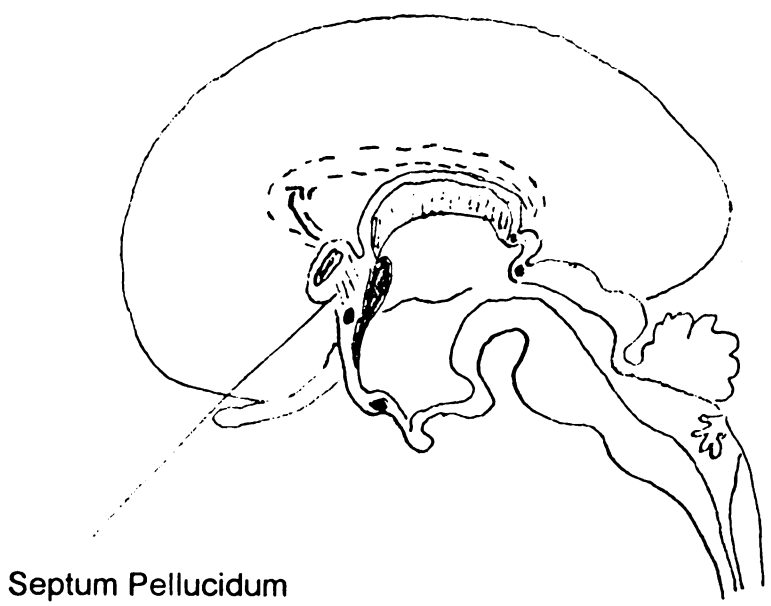

Figure 7 Medial surface of a 4 month human embryo brain. The arrow is pointing to the newly forming septum pellucidum, the broken line indicated the future expansion of the corpus callosum. (modified from Langman's Medical Embryology, Sixth Edition)[322]

The morphological role of the septum pellucidum is to divide the two telencephalic ventricles and to permit the adhesion of the fornix to the corpus callosum[217, 218] (FIGURE 8). When agenesis of the septum pellucidum occurs, the mass of embryonic neuralgia tissue which forms the commissural plaque between the origin of the corpus callosum and the anterior commissure does not form[217, 218] (FIGURE 9). Thus the fornix is not attached to the corpus callosum. If there is a distinct function of the septum pellucidum it is not known.[249]

Figure 8 Normal frontal view of the brain. Arrows pointing to the corpus callosum, septum pellucidum and the fornix. (modified from The Human Brain and Spinal Cord, Lennart Heimer).(323)

Figure 9 Frontal view of a brain with Septo-Optic Dysplasia. Notice the absence of the septum pellucidum which causes an enlargement of the ventricles. The corpus callosum and fornix are not attached and seem malformed. (modified from de Morsier)(242)

Ascertainment of an Individual with WSI and SOD

UoM1 is a four generation family (FIGURE 10) that was ascertained at the University of Michigan Pediatric Genetics clinic by Dr. Jeffrey Innis. Some members of the family exhibited a typical WSI phenotype (TABLE 18 in APPENDIX A). The proband in this family has Septo-Optic Dysplasia (SOD) and WSI, however, the other six individuals with WS do not have SOD. There are no reports in the literature of an individual or family with WS and SOD. There are reports of other clinical associations with SOD including digital anomalies,[250] cleft face,[251, 252] craniofacial anomalies such as Apert Syndrome[253] and other severe brain anomalies not including WS.[254]

Six additional individuals with SOD and/or optic nerve hypoplasia (SOD1-SOD6) but not WS were ascertained by Dr. Innis in collaboration with Dr. Nancy Hopwood. All of these individuals were sporadic cases of SOD, identified at the University of Michigan genetics clinic. A description of the phenotype for each individual is in TABLE 21 in APPENDIX A. Although none of these individuals demonstrated any characteristics of Waardenburg Syndrome they were included to investigate a possible connection between a *PAX3* or a *MITF* mutation and SOD. There are no reports in the literature that individuals with SOD have been examined for mutations in either *PAX3* or *MITF*. Until ascertaining UoM1 there would have been no reason to suspect such a connection.

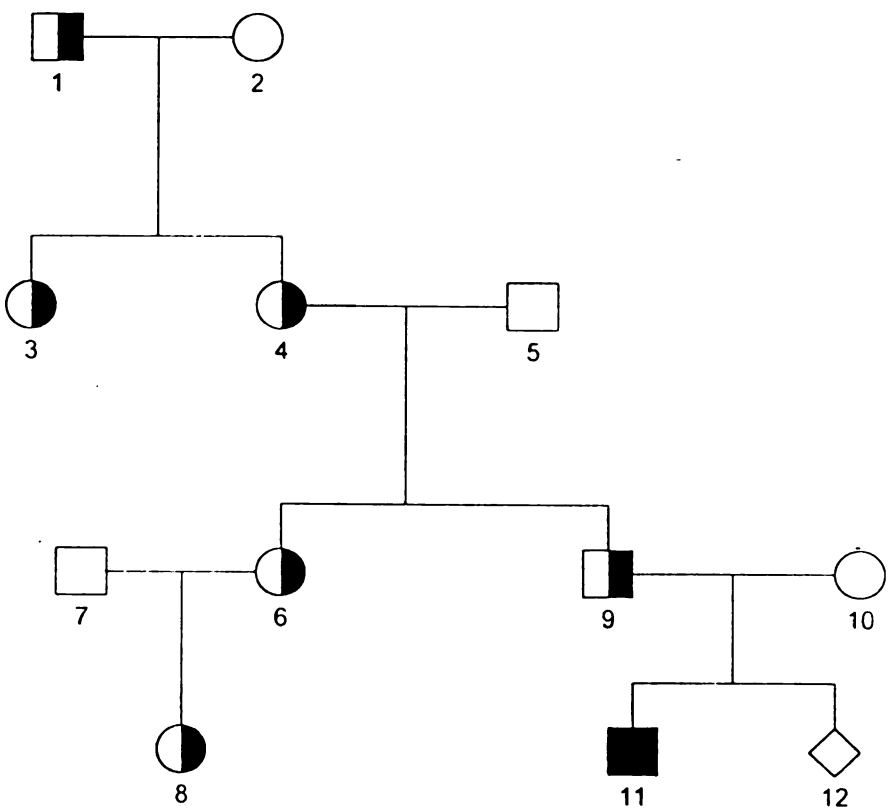

Figure 10 The pedigree of UoM1. The symbols are divided into two halves, the right portion being shaded if the WS phenotype is present and the left portion if SOD is present. The WS phenotypeincluded: dystopia, premature graying and deafness.

RESULTS

UoM1 was screened for all of the exons of *PAX3* and *MITF*. There were three SSCP variants identified in the analysis, one in *PAX3* exon seven, and two in *MITF*, one in exon one and the other in exon nine.

SSCP Analysis of *PAX3*

The SSCP variant found in *PAX3* exon seven was not identified in the any of the other 42 probands (FIGURE 13). The SSCP was reproducible and seen in all WS affected individuals in the family. The *PAX3* exon seven SSCP variant was not seen in the unaffected mother of the proband. The PCR fragment was gel purified and cloned into the p-Gem-T Vector. The materials and methods are described for all experiments in Chapter one.

The clones were analyzed by SSCP analysis and clones with the variant SSCP and the normal pattern were sequenced using the Sequenase version 2.0. A guanine (G) to cytosine (C) transversion was identified in exon seven predicting an amino acid change at codon 391 changing a glutamine (Q) to histidine (H) (FIGURE 11). PCR amplified genomic DNA from several WS individuals from this family were directly sequenced and the same base substitution was identified. An allele-specific primer was designed (TF195) and used to amplify genomic DNA in combination with a normal upstream exon seven primer (TF140). The *PAX3* exon four primers (TF35-36) were included in

the same PCR amplification as a control (see TABLE 8 in APPENDIX A for primer description). All WS individuals in the family amplified the mutant allele-specific fragment while the normal mother only amplified the control band (FIGURE 12). A set of 60 random individuals were screened by PCR amplification with the mutant allele-specific primer set and the control set. None of the random individuals had the allele specific fragment yet all amplified the control fragment.

Figure 11: *PAX3* exon 7 normal and the mutant DNA sequence and the normal and mutant protein sequence. The normal sequence is on top for both the DNA and protein and the mutant is on the bottom. There is a G to C transversion, that is boxed in with an arrow. This change alters the amino acid sequence substituting a glutamine (Gln) with a histidine (His) which occurs at codon 391. This is the 3'-end of exon seven and may alter splicing since the splice consensus is changed from Aggtcagt to Acgtcagt.

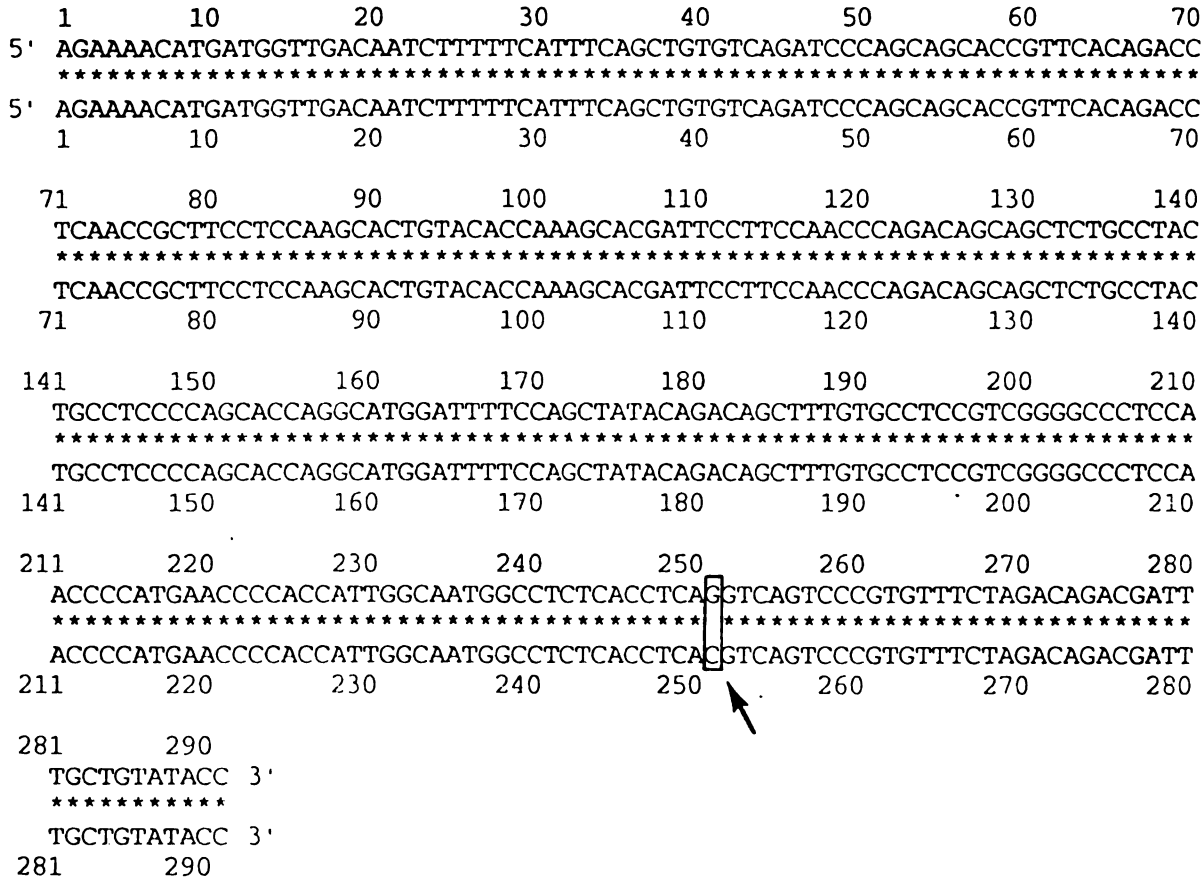

ValSerAspProSerSerThrValHisArgProGlnProLeuProProSerThrValHisGlnSerThrIlePro
ValSerAspProSerSerThrValHisArgProGlnProLeuProProSerThrValHisGlnSerThrIlePro

SerAsnProAspSerSerSerAlaTyrCysLeuProSerThrArgHisGlyPheSerSerTyrThrAspSer
SerAsnProAspSerSerSerAlaTyrCysLeuProSerThrArgHisGlyPheSerSerTyrThrAspSer

PheValProProSerGlyProSerAsnProMetAsnProThrIleGlyAsnGlyLeuSerProGln
PheValProProSerGlyProSerAsnProMetAsnProThrIleGlyAsnGlyLeuSerProHis

Figure 12: ASA of the *PAX3* exon 7. The allele specific amplification of the *PAX3* exon 7 mutation identified in UoM1. Five of the seven WS affected individuals were analyzed by ASA. The WS affected individuals are have the allele-specific fragment which is 270 base pairs. The unaffected mother (#10) does not have the allele-specific band but does have the control fragment which is 242 base pairs. The four random individuals only have the control fragment.

Allele-specific Amplification

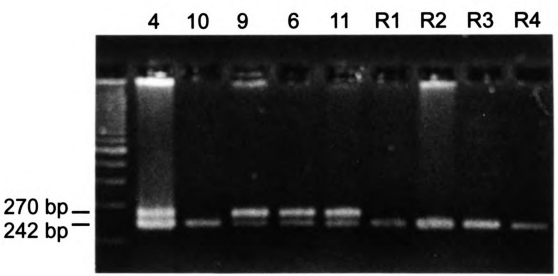

Figure 13: SSCP variants identified in UoM1. The top panel demonstrates a portion of the proband screening set analyzed by SSCP for *PAX3* exon 7, number 27 represents the proband of UoM1. The lower panel demonstrates a sample of probands analyzed by SSCP for *MITF* exon 1, number 27 represents UoM1.

SSCP Analysis

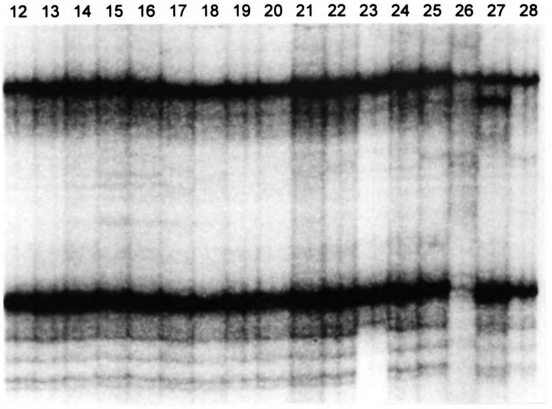

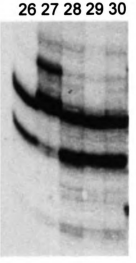

Mutation Identification in *MITF*

The exons of MITF were also analyzed in UoM1 for mutations. Two SSCP variants were identified in *MITF*. In order to determine if the observed SSCP variants identified in *MITF* were reproducible, the genomic DNA from the proband was amplified six times along with both of the proband's parents. The SSCP variant that was identified in exon nine was not consistently observed, therefore it was not further analyzed. An obvious SSCP was identified in exon one (FIGURE 13) however, the variant was difficult to identify in separate PCR amplifications electrophoresed multiple times on different gels made with the same recipe.

In order to determine if there was a sequence change responsible for the SSCP variant in exon one of *MITF* cycle sequencing was performed on the PCR- amplified fragment for the proband and his parents. No sequence variations were observed in the mother, father or proband within the coding region of exon one of *MITF*.

The proband's PCR amplified DNA fragment of 290 base pairs was subcloned and 60 clones were screened by SSCP analysis. None of the clones showed the obvious SSCP variant identified originally in the proband. Two clones with two different SSCP variants, different from the one observed in the genomic DNA from the proband, were sequenced. The only sequence change

was within intron one beyond the splice site junction. No other sequence changes were observed in either clone.

Other Individuals with SOD

Six individuals with SOD were ascertained from the University of Michigan Pediatric Endocrinology clinic. All six individuals were screened for mutations in *PAX3* and *MITF* by SSCP analysis. Two different, subtle SSCP variants in exon seven of *PAX3* were detected in two of the SOD individuals, SOD2 and SOD4, but were not reproducible. The PCR fragments were cloned and 25 clones were analyzed by SSCP. No variant clones were detected.

DISCUSSION

Description of UoM1

UoM1 is a four generation family with Waardenburg Syndrome Type I and one individual with both WSI and Septo-Optic Dysplasia (SOD) or de Morsier Syndrome. Individuals in this family present a typical WSI phenotype with dystopia canthorum, pre-mature graying and deafness. The proband however, also has SOD. The proband has optic nerve hypoplasia and absence of the septum pellucidum. The father was examined by magnetic resonance imaging (MRI)[255, 256] and found to have a normal septum pellucidum and other intracranial structures. He has no vision loss and no apparent endocrine dysfunction. Therefore, there is no indication of SOD in the father of the proband.

Due to the possibility of some connection between the presence of SOD and either a *PAX3* or *MITF* mutation, several additional individuals were ascertained with SOD. This was the first opportunity to explore a possible genetic basis for Septo-optic dysplasia. One hypothesis is that mutations in either *PAX3* or *MITF* were responsible for both the WS phenotype and/or the SOD.

Mutational Analysis of *PAX3* and *MITF*

The UoM1 proband was screened by SSCP analysis for *PAX3*. A SSCP variant was detected in *PAX3* exon seven that was not observed in the 40 other probands (FIGURE 13). There was a glutamine (G) to cytosine (C) transversion identified in the third position of the last codon of exon seven (FIGURE 11). The substitution was verified in three other WS affected individuals in the family by directly sequencing the products from PCR-amplified genomic DNA. This transversion mutation predicts an amino acid change at codon 391 changing a glutamine (Q) to histidine (H) (FIGURE 11). This single base substitution also predicts a splice site mutation that may create a truncated protein due to the premature stop approximately 70 nucleotides downstream, which would possibly eliminate a portion of the *PAX3* transcriptional activation domain. This putative splice site mutant is predicted by the consensus splice sites.[257, 258] Although there are now more than 50 mutations causing WSI, this is the first example of an exon seven mutation of *PAX3* identified in patients with WSI (TABLE 5).

In order to verify the sequence change in the genomic DNA an allele-specific primer was designed (TF195) and used to amplify genomic DNA in combination with a normal upstream exon seven primer (TF140). The *PAX3* exon four primers (TF35-36) were included in the same reaction mix as a control (see TABLE 8 in APPENDIX A). The expected fragment sizes were 270

base pairs for the allele specific fragment and 242 base pairs for the control fragment. The PCR-amplified DNA was separated by electrophoresis on a 4% NuSieve agarose gel and stained with ethidium bromide. All WS individuals in the family had the allele specific band while the normal mother only amplified the control fragment (FIGURE 12). A set of 60 random individuals were screened by PCR amplification with the allele specific primer set and the control set (data not shown). None of the random individuals had the allele specific fragment yet all amplified the control band. This indicates that the mutation identified in UoM1, in *PAX3* exon seven, was most likely the WS associated mutation and not a common polymorphism.

The proband was also screened by SSCP analysis for *MITF*. Two variants were identified in the proband exhibiting both WS and SOD, one in *MITF* exon one and the other in exon nine. Neither parent, the normal mother or the WS affected father, had either of the two SSCP variants seen in the proband. The variant in exon nine was not reproduced in multiple PCR amplifications, and therefore was not further investigated. The MITF exon one variant was an obvious pattern difference (FIGURE 13) compared to the other 40 probands but was not observed in all experiments.

The PCR amplified fragment from exon one was cycle sequenced. No sequence changes were identified in the coding region of exon one (data not shown), however the entire 5'-UTR was not readable by this method. The fragment was subcloned into a plasmid vector and 60 clones were analyzed by

SSCP. There were two clones with SSCP patterns that were different from the original SSCP variant identified in the proband. These clones were sequenced, the only sequence variation was within intron one beyond the splice site. No other variant SSCP patterns were identified in the 58 clones (data not shown).

Other individuals with SOD

Due to the possibility of a connection between WS and SOD in this family and the SSCP variants identified in both *PAX3* and *MITF*, several individuals with SOD were ascertained. There were two individuals with SOD, designated families SOD2 and SOD4, that had two different SSCP variants identified in *PAX3* exon seven. The genomic DNA was PCR-amplified in multiple sets along with control samples and the SSCP variants were not reproduced in SOD2. The variant pattern in SOD4 was subtle. Considering the importance of these data the genomic DNA from SOD2 and SOD4, was PCR-amplified and the fragments were subcloned. A total of ten clones were screened by SSCP analysis for each proband. No SSCP variants were detected in any of the clones. No other SSCP variants were identified in the remaining exons of *PAX3* or *MITF* for either proband. There were no SSCP variants identified for any of the exons of *PAX3* or *MITF* for SOD1, SOD3, SOD5 and SOD6.

SOD1 through SOD6 did not exhibit any WS characteristics (TABLE 21 in APPENDIX A). However, a diagnosis of a mild or subtle form of SOD may be easily missed in WS individuals due to the high variability of the clinical manifestations.[259-261] It is possible that some individuals with WS may also have very mild SOD that was not diagnosed. This was why the father of the proband in UoM1 was examined by MRI. Individuals with only mild endocrine dysfunction, an absent septum pellucidum and without any nerve hypoplasia may not be identified. Verifying the absence of a septum pellucidum is expensive and would not be done without good reason. Therefore, it is possible that WS patients may have SOD with only mild characteristics and would not be identified.

There is a possibility that the *PAX3* mutation in exon seven is responsible for both the WS and SOD phenotypes. The connection may not have been observed before due to a bias of ascertainment, individuals that did not have dystopia canthorum. Ascertaining other SOD individuals with dystopia canthorum or other WS characteristics may further elucidate a possible connection between the SOD and the WS phenotypes in the presence of a *PAX3* mutation.

CONCLUSION

Considering the involvement of *PAX3* with neural crest cell migration and role of *MITF* in melanocyte differentiation it is reasonable to propose that other neural tube defects or melanocyte-deficient diseases may be related to mutations in either of these genes. Identifying families with WS phenotypes associated with other clinical traits may help further characterize the clinical characteristics of the WS phenotype. Although the connection between WS and SOD could not be established in this study, this observation may alter the guidelines set for ascertaining and characterizing disorders. Whether the occurrence of SOD is sporadic or inherited is yet to be determined.

CHAPTER 3

Waardenburg Syndrome co-segregating with other severe craniofacial anomalies.

INTRODUCTION

Genes Causing Craniofacial Anomalies

Several genes have been associated with syndromes that are characterized by craniofacial and limb anomalies. The molecular control of embryogenesis and differentiation is regulated by a system of coordinated genes expressed both spatially and temporally. Some of these genes encode DNA-binding proteins that in turn regulate other genes. Several families of genes fall into this category including HOX, *PAX*, POU and zinc finger genes. In the initial mapping studies for Crouzon Syndrome a candidate gene approach was taken that included several genes important in early development, including the entire *PAX* gene family.[262]

Fibroblast growth factor receptors (FGFRs) are members of the transmembrane tyrosine kinase receptor family with three extra cellular immuno-globulin like (Ig) loops. The FGFRs bind fibroblast growth factors (FGFs). The FGF family is made up of related polypeptides that function in various aspects of embryogenesis, growth and homeostasis. Three of the four human FGFRs (FGFR1, FGFR2 and FGFR3) have been implicated in several disorders. Mutations in FGFRs have been found associated with three skeletal

dysplasias including: achondroplasia[263, 264] (ACH), thanatophoric dysplasia type II[265, 266] (TDII) and hypochondroplasia[267] (HCH); and four craniosynostotic syndromes[268] including: Apert (MIM 101200), Crouzon (MIM 123500), Jackson-Weiss[269] (MIM 123150) and Pfeiffer (MIM 101600) Syndromes.

Description of MSU22

A five generation family (FIGURE 14), MSU22 was identified with both WS and craniofacial anomalies described in TABLE 23 in APPENDIX A. The craniofacial anomalies in MSU22 are similar to those observed in the other craniosynostotic syndromes including: Apert, Saethre-Chotzen (MIM 101400), Crouzon, Pfeiffer and Jackson-Weiss Syndromes. The craniofacial abnormalities in this family appeared to include the typical WS phenotype including dystopia canthorum and broad nasal root, along with craniosynostosis and dysostosis. Craniofacial anomalies like this have not been observed in WS individuals prior to this study. The goal of this study was to determine if the craniofacial anomalies in MSU22 were due to a *PAX3* or *MITF* mutation.

Craniofacial Syndromes

Pfeiffer Syndrome (acrocephalosyndactyly type V) is inherited as an autosomal dominant disorder. The condition is caused by coronal craniosynostosis creating a tall and narrow skull (clover leaf heads). The

individuals exhibit midface hypoplasia, hypertelorism, proptosis, downslanting fissures, thumb abnormalities (broad), syndactyly, fusion of hands and elbows.[270, 271] Some sporadic cases also display hearing loss.[272-275] Mutations in FGFR1, on chromosome 8[276] and in FGFR2, on chromosome 10q[276, 277] have been identified as at least two of the genes associated with Pfeiffer Syndrome in some individuals.

Crouzon Craniofacial Dysostosis Syndrome (acrocephalosyndactyly type II) segregates as an autosomal dominant disorder. The condition is caused by cranial synostosis or premature fusion of the bone sutures. Crouzon is clinically characterized by an abnormally short skull, protrusion of the anterior fontanel (oxycephaly), hypertelorism, external strabismus, exophthalmos, parrot-beaked nose, short upper lip, hypoplastic maxilla, relative mandibular prognathism, hearing loss and visual loss.[278-280] Mutations have been identified in both FGFR2[268, 277, 281-286] and FGFR3, on chromosome 4p,[287] in individuals with Crouzon Syndrome.

Apert Syndrome (acrocephalosyndactyly type I),[288] is yet another craniosynostosis syndrome. Clinical characterization includes hypopigmentation, CNS malformations,[289-291] cleft palate, cervical vertebral fusion, syndactyly, bone fusion and nail abnormalities of the hands and feet.[292-302] Hearing loss has been observed in individuals with Apert Syndrome.[303, 304] The only gene identified with mutations causing Apert Syndrome patients thus far is FGFR2.[305]

Saethre-Chotzen Syndrome (acrocephalosyndactyly type III) is an autosomal dominant disorder characterized by premature fusion of the cranial sutures in association with mild cutaneous syndactyly, brachydactyly and clinodactyly.[318] Individuals may have short stature, skin abnormalities of the fingers and toes. The clinical characteristics include brachycephaly, microcephaly, skull asymmetry, hypertelorism, ptosis, strabismus and unusually shaped ears.[306-315] The gene responsible for the development of Saethre-Chotzen Syndrome has not been identified; however, deletions and linkage studies have implicated 7p21.2 as the candidate region.[313, 316, 317]

In MSU22, the hypothesis that either a *PAX3* or *MITF* mutations was responsible for both the WS and some or all of the craniofacial phenotypes was tested. However, due to the fact that there were only a few individuals with a clear WS phenotype and with obvious craniofacial anomalies, the possibility that two syndromes were co-segregating in this family was a possibility.

Figure 14: MSU22 WS and Craniofacial anomalies

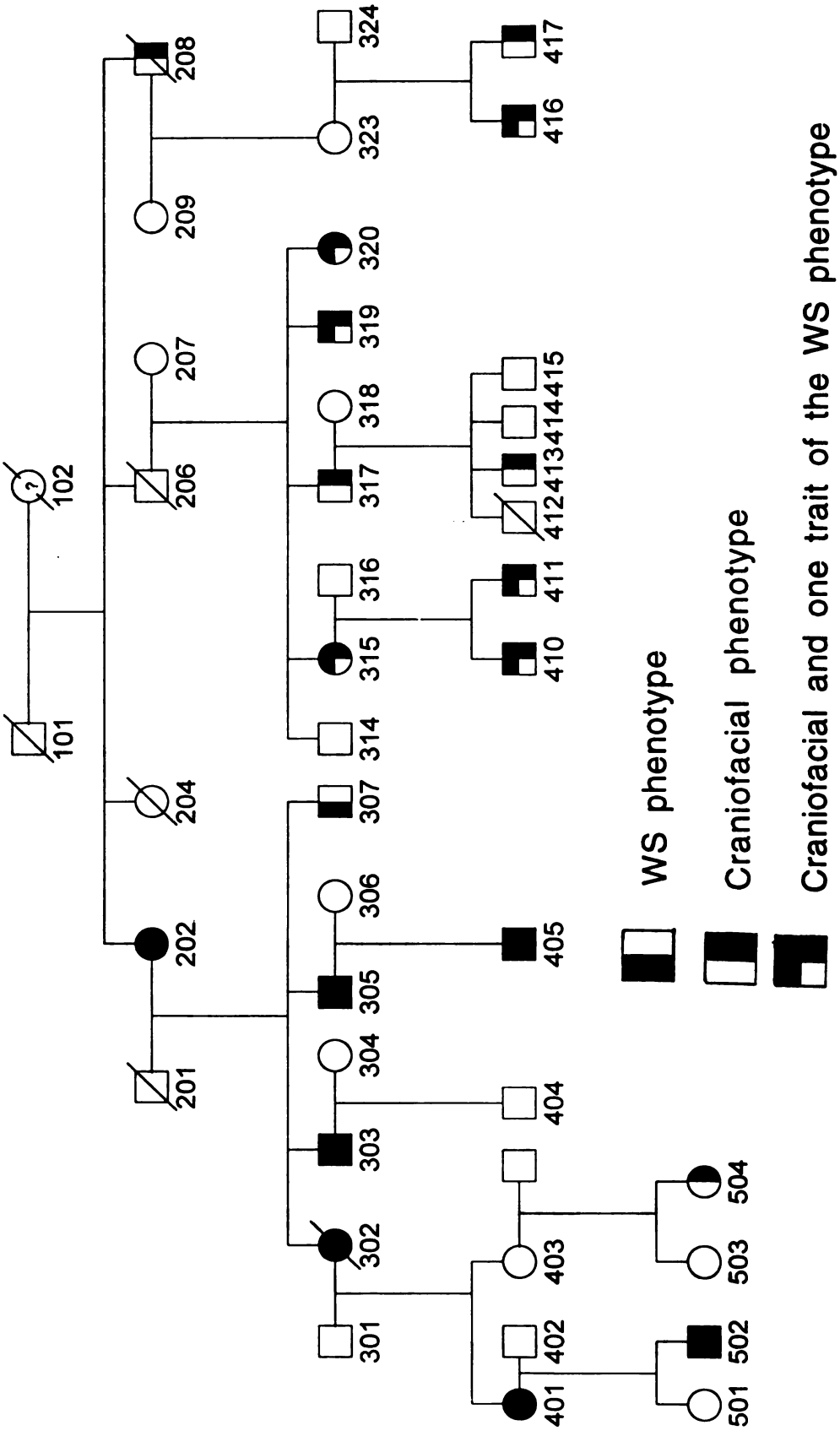

RESULTS

Mutational Analysis

MSU22 was included in the SSCP analysis of *PAX3* and *MITF*. No SSCP variants were identified for any of the exons of *PAX3* or *MITF*. Sequencing was done for *PAX3* exons two and six with no sequence changes identified. These two exons included portions of the paired domain and the homeodomain, respectively, which is why they were examined directly.

Linkage Analysis to *PAX3*

A linkage simulation (SLINK) was performed by Dr. J. H. Asher, Jr. that predicted that it would be possible to determine whether or not this was a single disorder or if either of the two clinical entities were linked to *PAX3*. The simulation indicated the need for additional family members' DNA. DNA samples were obtained for fifteen of the thirty necessary individuals to obtain a LOD score of greater than 3.0. The DNA was typed for two markers linked to *PAX3*: the 5'-marker described by Wilcox et al.[183] and an intron seven marker described by Macina et al.[132] The primers, similar to those described in Wilcox et al.[183] and Macina et al.[132] were designed, and are listed on TABLE 12 in APPENDIX A. The assay used is described in the Materials and Methods in chapter one.

The intron seven marker showed at least two recombinations in individuals that clearly had Waardenburg Syndrome. The data from the 5'-marker also had at least two obligate recombinants. The analysis was done assuming one syndrome including both the WS phenotype and the craniofacial abnormalities, WS alone (FIGURE 15) and the craniofacial anomalies alone (FIGURE 16). The DNA from all the necessary family members' was not available, therefore a formal linkage analysis was not possible.

Figure 15: MSU22 pedigrees: linkage analysis with WS phenotype. This includes individuals with single WS traits that would not be classified as WS by the consortium criteria according to the WS consortium clinical criteria, see TABLE 4. Included is a table with the individuals genotyped for the STRs described by Wilcox et al.[183] and Macina et al.[132] and the genotypes.

Figure 15: MSU22 Waardenburg Syndrome

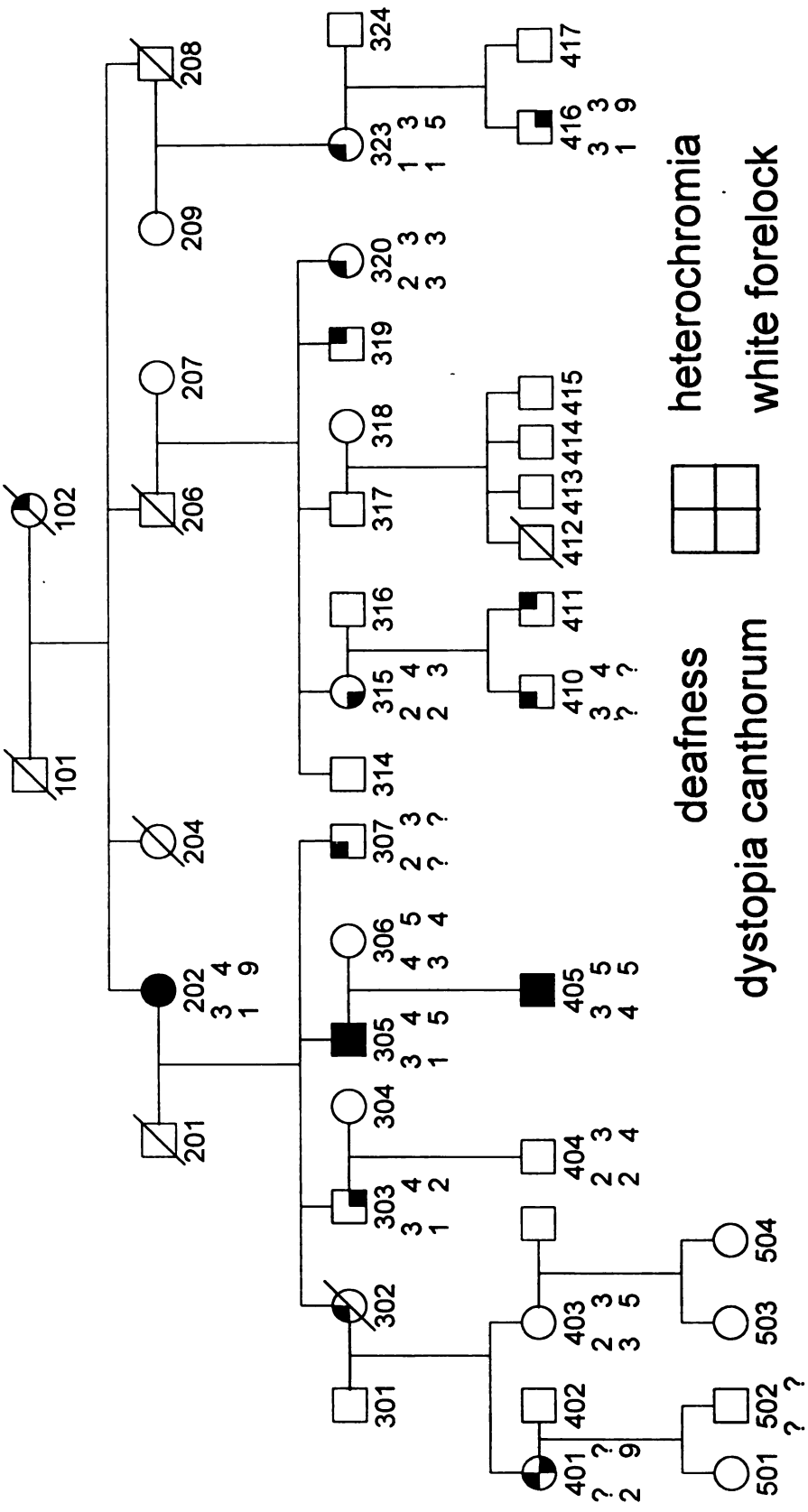

Figure 16: MSU22 pedigree: linkage analysis with the CA phenotype. Those family members that are do not exhibit the phenotype and do not have offspring with the phenotype are not included in this pedigree. All individuals with the craniofacial anomalies have had surgery except 317, this individual has been not been seen by our collaborator. Included is a table with the individuals genotyped for the STRs described by Wilcox et al.[183] and Macina et al.[132] and the genotypes.

Figure 16: MSU22 Craniofacial anomalies

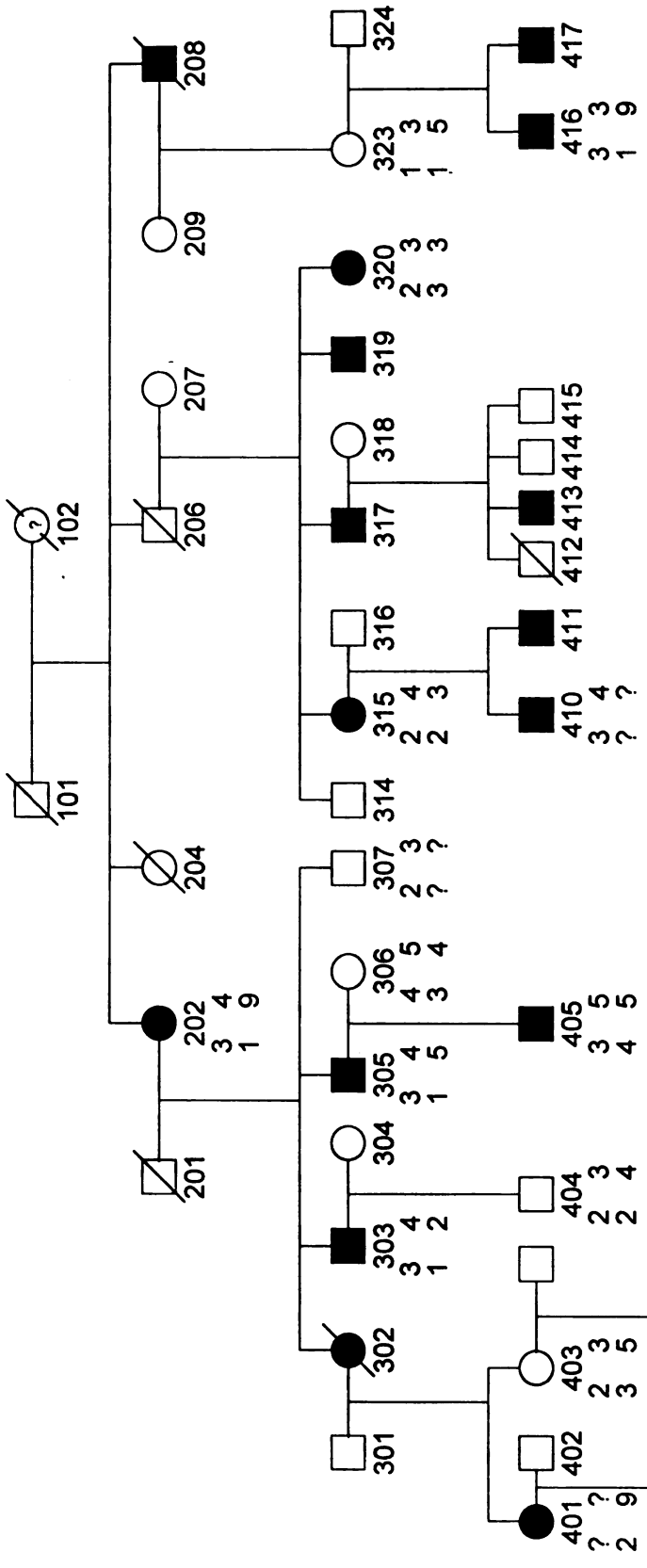

DISCUSSION

Description of MSU22

MSU22 was ascertained due to an inherited form of ulnar neuropathy by Dr. Robert Spinner (Duke University Medical Center). Seven members of the family clearly have a typical Waardenburg Syndrome phenotype including: deafness, heterochromia irides and white forelock. There was a definite correlation between the WS and craniofacial anomalies. Seven family members exhibited only one of the major WS characteristics and would be classified unaffected by WS diagnostic criteria.[5] Seventeen of the family members exhibited severe craniofacial anomalies, with all but one individual needing surgery in infancy. The proband, 405, and his affected grandmother, 202, exhibit the Waardenburg Syndrome and the craniofacial abnormalities. A high resolution chromosomal analysis was done by the Greenwood Genetic Center for both individuals. No obvious chromosomal rearrangements were identified in either individual.

The W-index developed by Arias and Mota in 1978[6] uses inner-canthal (a), outer-canthal (c) and interpupillary (b) eye measurements. The W-index is a quantitative measure of dystopia canthorum. Three individuals, identified as 305, 315 and 405, had both WS and craniofacial anomalies and had a W-index that indicated non-apparent (NAD) dystopia canthorum[6] (TABLE 13). All three of these individuals had multiple extensive facial surgeries throughout early

childhood. One other family member, identified as 202, with extensive craniofacial surgeries clearly had dystopia canthorum (TABLE 13). No other members of this family had any suggestion of dystopia canthorum. The pre-surgery photographs are not available.

Due to the severe craniofacial anomalies in this family a reliable diagnosis of dystopia canthorum could not be made, therefore, both *PAX3* and *MITF* were analyzed for mutations. However, we could not ignore the possibility that two distinct clinical disorders were segregating in this family with mutant alleles in both gene(s).

Table 13: W-index for members of MSU22

			MSU22					
Id	Age	a	b	c	X	Y	W	comments:
303	39	33	60	96	0.4349	0.7852	1.77003	
404	11	30	55	95	0.3785	0.7701	1.69412	
307	40	40	70	120	0.4222	0.8373	1.83093	
409	2	28	48	85	0.4009	0.8355	1.8198	
501	3	28	40	76	0.4735	1.0526	2.22608	note age
323	40	36	68	110	0.4071	0.7516	1.68816	
416	18	37	68	100	0.489	0.7811	1.81418	
417	16	38	75	110	0.4435	0.7115	1.66165	
315	39	40	65	115	0.4498	0.9209	1.98608	NAD-craniofacial surgery
410	8	30	55	90	0.4113	0.7701	1.72692	
411	3	30	55	80	0.4892	0.7701	1.80483	
305	43	43	72	116	0.4958	0.8905	1.98346	NAD-craniofacial surgery
405	teens	43	72	116	0.4958	0.8905	1.98346	NAD-craniofacial surgery
202	60's	41	67	100	0.569	0.9158	2.09679	Dystopia-craniofacial surgery
306	40's	32	62	93	0.4342	0.7195	1.66988	
403	30's	32	63	93	0.4342	0.7041	1.6463	

Table 13 The table includes the a, b and c measurements along with the values for X, Y and W. The individual identification number and approximate ages are also included. The individuals with dystopia canthorum and NAD all have had craniofacial surgery prior to the measurements.
NAD = non apparent dystopia canthorum.

$$W = X + Y + a/b$$

$$X = [2a - (0.2119\,c + 3/909)]/c \quad Y = [2a - (0.2497b + 3/909)]/b$$

$W \geq 2.07$ = dystopia canthorum

$1.87 \leq W \geq 2.07$ = non apparent dystopia canthorum (NAD)

$W < 1.87$ = normal

SSCP and Sequence Analysis

SSCP analysis was performed for the eight exons of *PAX3* and the nine exons of *MITF*. No SSCP variants were detected in the proband for any of the exons of *PAX3* or *MITF*. The sequence analysis for exons two and six of *PAX3* did not demonstrate any sequence variations. Mutations in either *PAX3* or *MITF* cannot be ruled out by SSCP analysis or by sequencing the coding regions alone.

Linkage Analysis

Due to the size of the family and the availability of the two closely linked loci within or adjacent to *PAX3*, a simulation linkage analysis identified individuals that needed to be typed for a LOD score ≥ 3.0. A maximum LOD score of 5.97 at $\theta = 0.0$ could be obtained with thirty family members. DNA samples were received from fifteen of the thirty individuals necessary; thus a formal linkage analysis could not be performed. However, the data indicated that there were at least two different obligate recombinants for both loci, for affected WS individuals (FIGURES 15 and 16). This data strongly suggested an exclusion of linkage to the *PAX3* locus.

Linkage to the *MITF* locus was not possible due to a lack of informative markers closely linked to the gene. The SSCP analysis did not indicate any possible mutations in *MITF*. However, without the availability of informative

linked loci, linkage to *MITF* cannot be ruled out. Once other genes are identified that cause Waardenburg Syndrome at least a portion of this family should be reconsidered for mutation screening or linkage analysis.

CONCLUSION

The linkage data for the two loci linked to *PAX3* demonstrate at least two obligate recombinants therefore, linkage to *PAX3* was excluded. Linkage analysis could not be performed for *MITF* since polymorphic markers linked to *MITF* have not been identified. The WS phenotype and the craniofacial abnormalities in MSU22 are a likely to be two distinct disorders. Therefore, screening the members of this family with the craniofacial anomalies for mutations in FGFR1, FGFR2 or FGFR3 may identify the gene associated with this anomaly. These genes are implicated in Crouzon, Apert, Jackson-Weiss and Pfeiffer Syndromes. The region of chromosome 7p linked to Saethre-Chotzen is another candidate region that could be screened in this family.

APPENDICIES

APPENDIX A

Table 8: *PAX3* PCR Primers

EXON	PRIMER	SEQUENCE	SIZE	TEMP	COMMENT
1	TF167	CCGTTTCGCCTTCACCTGGA	153	60	PCR, SSCP
	TF59	GCGCTGAGGCCCTCCCTTAC			
2	TF30	ATTTTGCCCCATTTGCTGTC	535	61	PCR, SSCP
	TF32	CCGGTCTTCCCCAACACAGG			
3	TF33	CCTGCCCGCCTGTTCTCT	197	60	PCR, SSCP
	TF34	CGACTGACTGTCGCGCCT			
4	TF35	AGCCCTGCTTGTCTCAACCATGT	242	66	PCR, SSCP
	TF36	TGCCCTCCAAGTCACCCAGCAAGT			
5	TF100	TCACTGTAATGGTGTCTTGC	355	55	PCR, SSCP
	TF101	TCCTGTCTGGACTGAAGTAG			
6	TF98	AGAAGCCTCTAATCTGTTTT	390	55	PCR, SSCP
	TF99	GTTCGGACAACCTGATGTAT			
7	TF140	GGATATCAGCAAATCGTCTGTCT	290	49	PCR, SSCP
	TF141	AGAAAACATGATGGTTGACAATC			
8	TF156	CCGGCATGTGTGGCTTAATC	365	50	PCR, SSCP
	TF157	GCTCTTTTTTTAGGTAATGGG			
7	TF195	CTAGAAACACGGGACTGACG		64	ASA UoM1

Table 8 The primers used for PCR amplification, SSCP analysis and Allele-specific amplification (ASA) are listed. The size of the expected fragment, the annealing temperature for each primer set, the exon number and the primer identification number are included.

Table 9: *MITF* PCR Primers

EXON	PRIMER	SEQUENCE	SIZE	TEMP	COMMENT
1	TF120	GGATACCTTGTTTATAGTACCTTC	270	55	PCR, SSCP
	TF121	AAAAGAGCAGATTTATACTTATTG			
2	TF122	TATGAAACTCACAAATAACAGCGC	343	55	PCR, SSCP
	TF123	TATTCAACAGACAAGTTATTTAGC			
3	TF124	CCATCAGCTTTGTGTGAACAGGTC	245	55	PCR, SSCP
	TF125	TTTCAGGAAGGTGTGATCCACCAC			
4	TF126	AACTAAAGACCATTATTGCTTTGG	264	55	PCR, SSCP
	TF127	AGAAAAGAACCCTGGAAACACCTC			
5	TF128	ATAAATCCTAGAGTAGGATATAGG	270	55	PCR, SSCP
	TF129	ACTTTGTCTTATCAGGAAATGGAC			
6	TF130	TCAAGTCAAATAAGCTTCTGTATG	280	55	PCR, SSCP
	TF131	GTAGGAATCAACTCTCCTCTACAG			
7	TF132	GTGCTAAATGCATACATGGCACTG	264	55	PCR, SSCP
	TF133	TTAGGAATAGAACCAAAGGGAGAG			
8	TF134	TTCATTGAGCCTCAAATCCTAAAG	264	55	PCR, SSCP
	TF135	CTGTTTCTACTGTCTTGAAGTCGG			
9	TF136	AGTCCTCTGTGCTCGTCCTATTTC	715	55	PCR, SSCP
	TF137	AAGCTAAAGTCTGTGGTGAATTC			

Table 9 The primers used for PCR amplification and SSCP analysis. The size of the expected fragment, the annealing temperature for each primer set, the exon number and the primer identification number are included.

Figure 5: *PAX3* gene structure with primers

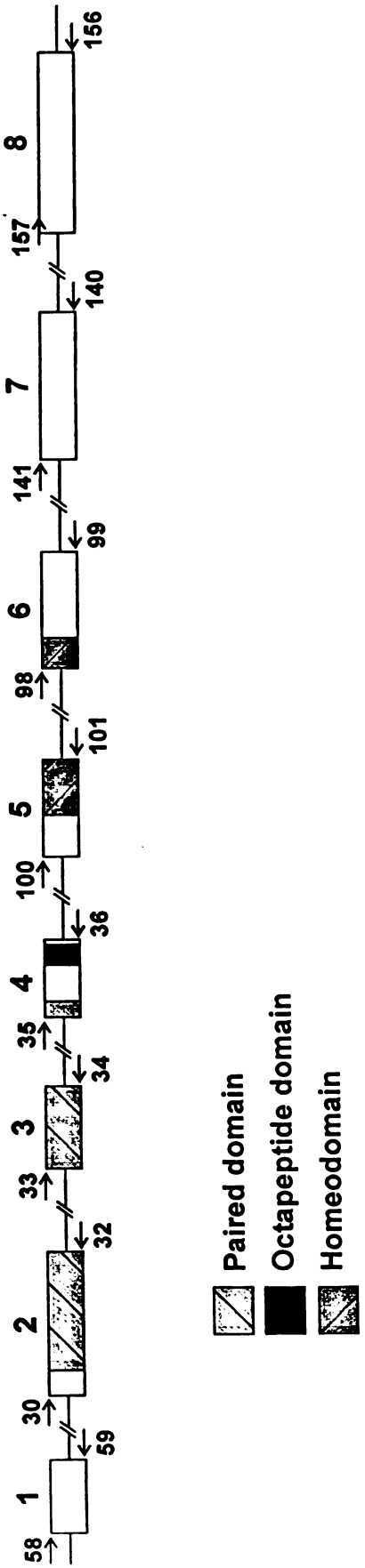

Figure 6: *MITF* gene structure with primers

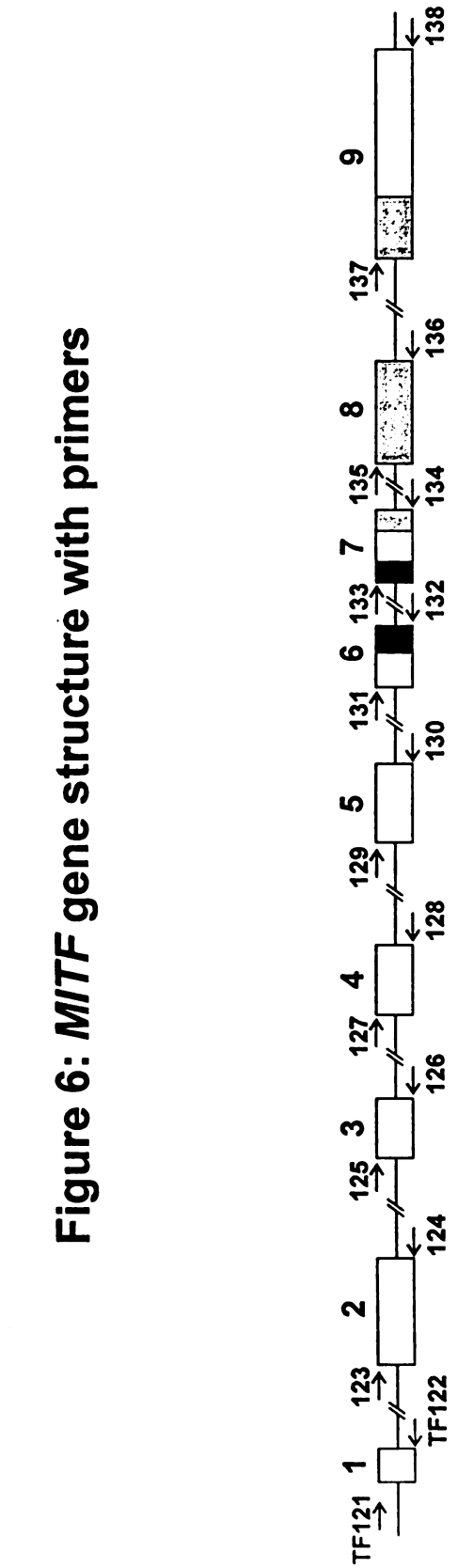

Table 10: Cycle Sequencing Primers

			LABELING REACTION			EXTENSION REACTION			
Gene	exon	primer	bps.	temp	% G+C	bps.	temp	% G+C	omit
PAX3	2	JA5	20	48	50	40	67	35	dATP
PAX3	3	TF34	18	60	67	28	72	71	dTTP
PAX3	4	TF35	22	60	55	55	72	65	dATP
PAX3	5	TF101	20	48	50	30	67	57	dTTP
PAX3	6	TF103	20	48	45	31	67	42	dGTP
PAX3	7	TF141	23	52	35	65	72	30	dGTP
MITF	1	TF120	24	50	38	31	72	42	dATP
MITF	2	TF122	24	50	42	36	72	36	dATP
MITF	6	TF131	24	50	46	31	72	39	dGTP
MITF	7	TF132	24	50	46	33	72	36	dGTP
MITF	8	TF134	24	50	38	30	72	33	dGTP

Table 10 The gene, exon and primer identification number are included along with the length of the primer before and after the extension reaction, the annealing and extension temperatures used, the % G+C before and after the extension reaction and the dideoxynucleotide omitted in the annealing step.

FAMILY	Physician/examiner	Location
MSU 1	James H. Asher Jr., PhD	Michigan
MSU 2	James H. Asher Jr., PhD	Michigan State Speech and Hearing Clinic
MSU 4	James H. Asher Jr., PhD	Michigan
MSU 5	James H. Asher Jr., PhD	Michigan
MSU 6	James H. Asher Jr., PhD	Michigan
MSU 7	Jessica Davis, MD	Division of Human Genetics New York Hospital
MSU 8	James Higgins, PhD	Michigan State University Clinical Center
MSU 9	Saroj Kapur	Michigan State University Genetics Clinic
MSU 10	Paula Czarnecki, GC	Henry Ford Hospital, Michigan
MSU 11	????	Arizona
UGM 1	Arhya/Winata/SuKarti	Indonesia
MSU 3	Karol Christenson, GC	Michigan State University Clinical Center
MSU 12	William B. Dobyns, MD	Division Pediatric Neurology, University of Minnesota
MSU 13	Ephrat Levy-Lahad, MD	Children's Hospital & Medical Center, Washington
MSU 14	Paula Czarnecki, GC	Henry Ford Hospital, Michigan
MSU 15	Paula Czarnecki, GC	Henry Ford Hospita, Michigan
MSU 16	Susan Kirkpatrick, GC	Waisman Center, University of Wisconsin-Madison
MSU 17	Annemarie Sommer, MD	Children's Hospital, Ohio
MSU 18	John Pierpont	Arizona Health Sciences Center
MSU 19	Personal contact by family	Indiana
MSU 20	Uta Francke, MD	Children's Hospital at Stanford California
MSU 21	Erawati Bawle, MD	Children's Hospital, Detroit Michigan
MSU 22	Robert Spinner, MD	Genetic Clinic Veteran's Hospital, N. Carolina
UGM 3	Arhya/Winata/SuKarti	Indonesia
UGM 4	Arhya/Winata/SuKarti	Indonesia
UGM 5	Arhya/Winata/SuKarti	Indonesia
UGM 6	Arhya/Winata/SuKarti	Indonesia
MSU 23	Lester Weiss, MD	Henry Ford Hospital, Michigan
UofM 1	Jeff Innis, MD, PhD	University of Michigan Genetics Clinical Center
MSU 25	Harry Ostrer, MD	New York University Human Genetis Program
MSU 24	David Wargowski, MD	Clinical Genetics Center, University of Wisconsin
MSU 26	Tanya Dien, GC	Michigan State University Clinic
SOD 1	Nancy Hopwood, MD	University of Michigan Clinic
UofM 4	Jeff Innis, MD, PhD	University of Michigan Genetics Clinic
UofM 3	Jeff Innis, MD, PhD	University of Michigan Genetics Clinic
SOD 2	Nancy Hopwood, MD	University of Michigan Clinic
SOD 3	Nancy Hopwood, MD	University of Michigan Clinic
SOD 4	Jeff Innis, MD, PhD	University of Michigan Clinic
MSU 27	Kambouris, PhD	Henry Ford Hospital, Michigan
SOD 5	Nancy Hopwood, MD	University of Michigan Clinic
MSU 28	Lynne Bird, GC	Children's Hospital, San Diego California
SOD 6	Nancy Hopwood, MD	University of Michigan Clinic
MSU 29	Erawati Bawle, MD	Children's Hospital, Detroit Michigan
MSU 30	Jeff Innis, MD, PhD	University of Michigan Clinic

Table 11 Collaborators for each WS and WS-like family. A listing of the clinicians and genetic counselors that identified the families as well as the approximate location of the families in the proband set. One individual from each collaboration is listed. GC = genetic counselor. If the clinic was not indicated the state was mentioned.

Table 12: *PAX3* Linked Markers

GENE	PRIMER	SEQUENCE	SIZE	TEMP	COMMENT
PAX3	TF161	TTTATATGTGGGTGGAATGCGAT	255	50	Macina et al.
	TF162	CCTCTGATGAAACCCAGACTG			
PAX3	TF175	AGTTGCTGAGGGCGGAGAAG	208	50	Chatkupt et al.
	TF176	GAAATCACAAGAGGATAGAGGCT			
PAX3	JA32	GGGAGATGGCAGTTGCTGAG	183	58	Wilcox et al.
	JA33	CACACAGAGGCACAGAAAGA			
PAX3	TF26	CAGGGAGATGGCAGTT	227	50	Wilcox et al.
	TF38	CAGAGGCACAGAAAGA			

Table 12 The list of primers for PCR amplification of the markers linked to *PAX3*. These markers include the marker described by Wilcox et al.[183] at the 5'-end and the marker described by Macina et al.[132] at the 3'-end of *PAX3*. The primer identification number, the size of the PCR fragment and the annealing temperature are included. The primer pair described by Chatkupt amplifies the 5'-end marker described by Wilcox et al.[183]

Table 14: Phenotypes for MSU1-MSU7

PHENOTYPE	MSU I	MSU 2	MSU 3	MSU 4	MSU 5	MSU 6	MSU 7
Dystopia canthorum	+	+	+	-	+	-	+
Broad nasal root	-	+	-	-	-	-	+
Deafness	-	+	+	+	+	+	+
Heterochromia	+	+	-	+	+	+	-
Pre-mature graying	+	-	+	+	-	?	?
White forelock	+	-	-	-	+	?	+
Hypopigmentation	-	-	-	+	-	?	-
Synophrys	-	-	-	-	-	-	-
Hirschprung's disease	-	-	-	-	-	-	-
Cleft palate/lip	-	-	+	-	-	-	-
Ocular albinism	-	-	-	-	-	-	-
Vitiligo	+	-	+	-	-	-	-
Blindness	-	-	-	-	-	-	-
GH deficiency	-	-	-	-	-	-	-
Telecanthus	-	-	-	-	-	-	-
Hypertelorism	-	-	-	-	-	-	-
Hypoplastic blue eye	-	-	-	-	-	-	+
Missing nasal bone	-	-	-	-	-	-	-
Syndactyly	-	-	-	-	-	-	-
Craniofacial anomalies	-	-	-	-	-	-	-
Ptosis	-	-	-	-	-	-	-
Heart defects	-	-	-	+	-	-	-
Neuropathies	-	-	-	-	-	-	-
Septo-Optic Dysplasia	-	-	-	-	-	-	-
Endocrine dysfunction	-	-	-	-	-	-	-
Hypoplasia of optic nerve	-	-	-	-	-	-	-
absent septum pellucidu	-	-	-	-	-	-	-
Hypoplasia of nasal bone	-	-	-	-	-	-	-
Developmental delay	-	-	+	-	-	-	-
Anencephaly	-	-	-	-	-	-	-
18q Syndrome	-	-	-	-	-	-	-
Brachycephaly	-	-	-	-	-	-	-
Kidney disfunction	-	-	-	-	-	-	-
Nystagmus	-	-	-	-	-	-	-
Strabismus	-	-	-	-	-	-	-
Vestibular disturbances	-	-	-	-	-	-	-
Ataxia	-	-	-	-	-	-	-
Mental Retardation	-	-	-	-	-	-	-
Otosclerosis	-	-	-	-	-	-	-
Tarsal coalition	-	-	-	-	-	-	-
Tear duct aplasia	-	-	-	-	-	-	-
Craniofacial surgery	-	-	-	-	-	-	-

Table 15: Phenotypes for MSU8-MSU14

PHENOTYPE	MSU 8	MSU 9	MSU 10	MSU 11	MSU 12	MSU 13	MSU14
Dystopia canthorum	?	+	-	-	-	-	?
Broad nasal root	-	+	-	-	-	-	-
Deafness	?	+	+	-	+	+	+
Heterochromia	-	+	+	-	-	-	?
Pre-mature graying	+	-	-	-	-	+	-
White forelock	+	+	+	-	-	+	+
Hypopigmentation	+	-	+	-	-	+	-
Synophrys	-	+	-	-	-	-	-
Hirschprung's disease	-	-	-	-	+	+	-
Cleft palate/lip	-	-	-	-	-	-	-
Ocular albinism	-	-	-	+	-	-	-
Vitiligo	-	-	-	-	-	-	-
Blindness	-	-	-	-	-	-	-
GH deficiency	-	-	-	-	+	-	-
Telecanthus	-	-	-	-	-	-	+
Hypertelorism	-	-	-	-	-	-	+
Hypoplastic blue eye	-	-	-	-	-	-	+
Missing nasal bone	-	-	-	-	-	-	-
Syndactyly	-	-	-	-	-	-	-
Craniofacial anomalies	-	-	-	-	-	-	-
Ptosis	-	-	-	-	-	-	-
Heart defects	+	-	-	-	-	-	-
Neuropathies	-	-	-	-	-	-	-
Septo-Optic Dysplasia	-	-	-	-	-	-	-
Endocrine dysfunction	-	-	-	-	-	-	-
Hypoplasia of optic nerve	-	-	-	-	-	-	-
absent septum pellucidu	-	-	-	-	-	-	-
Hypoplasia of nasal bone	-	-	-	-	-	-	-
Developmental delay	-	-	-	-	-	-	-
Anencephaly	-	-	-	-	-	-	-
18q Syndrome	-	-	-	-	-	-	-
Brachycephaly	-	-	-	-	-	-	-
Kidney disfunction	-	-	-	-	-	-	-
Nystagmus	-	-	-	-	-	-	-
Strabismus	-	-	-	-	-	-	-
Vestibular disturbances	-	-	-	-	-	-	-
Ataxia	-	-	-	-	-	-	-
Mental Retardation	-	-	-	-	-	-	-
Otosclerosis	-	-	-	-	-	-	-
Tarsal coalition	-	-	-	-	-	-	-
Tear duct aplasia	+	-	-	-	-	-	-
Craniofacial surgery	-	-	-	-	-	-	-

Table 16: Phenotypes for MSU15-MSU21

PHENOTYPE	MSU 15	MSU 16	MSU 17	MSU 18	MSU 19	MSU 20	MSU 21
Dystopia canthorum	?	?	-	-	-	-	-
Broad nasal root	-	?	-	-	-	-	-
Deafness	+	?	+	+	+	+	+
Heterochromia	-	?	-	+	+	-	-
Pre-mature graying	-	?	-	-	+	+	-
White forelock	+	?	-	+	-	-	+
Hypopigmentation	+	?	-	-	+	-	+
Synophrys	-	-	-	-	-	-	-
Hirschprung's disease	-	-	-	-	-	-	-
Cleft palate/lip	-	-	-	-	-	-	-
Ocular albinism	-	-	-	-	-	-	-
Vitiligo	-	-	-	-	-	-	-
Blindness	-	-	-	-	-	-	-
GH deficiency	-	-	-	-	-	-	-
Telecanthus	-	-	-	-	-	-	-
Hypertelorism	-	-	-	-	-	-	-
Hypoplastic bue eye	-	-	-	-	-	+	-
Missing nasal bone	-	-	+	-	-	-	-
Syndactyly	-	-	+	-	-	-	-
Craniofacial anomalies	-	-	-	-	-	-	-
Ptosis	-	-	-	-	-	-	-
Heart defects	-	-	-	-	-	-	-
Neuropathies	-	-	-	-	-	-	-
Septo-Optic Dysplasia	-	-	-	-	-	-	-
Endocrine dysfunction	-	-	-	-	-	-	-
Hypoplasia of optic nerve	-	-	-	-	-	-	-
absent septum pellucidu	-	-	-	-	-	-	-
Hypoplasia of nasal bone	-	-	-	-	-	-	-
Developmental delay	-	-	-	-	-	-	-
Anencephaly	-	-	-	-	-	-	-
18q Syndrome	-	-	-	-	-	-	-
Brachycephaly	-	-	-	-	-	-	-
Kidney disfunction	-	-	-	-	-	-	-
Nystagmus	-	-	-	-	-	-	-
Strabismus	-	-	-	-	-	-	-
Vestibular disturbances	-	-	-	-	-	-	-
Ataxia	-	-	-	-	-	-	-
Mental Retardation	-	-	-	-	-	-	-
Otosclerosis	-	-	-	-	-	+	-
Tarsal coalition	-	-	-	-	-	-	-
Tear duct aplasia	-	-	-	-	-	-	-
Craniofacial surgery	-	-	-	-	-	-	-

Table 17: Phenotypes for MSU22-MSU28

PHENOTYPE	MSU 22	MSU 23	MSU 24	MSU 25	MSU 26	MSU27	MSU 28
Dystopia canthorum	?	-	-	-	-	-	-
Broad nasal root	-	-	-	+	-	-	-
Deafness	+	+	+	-	+	+	+
Heterochromia	+	+	+	-	+	-	+
Pre-mature graying	-	+	-	NA	-	+	+
White forelock	+	+	-	+	-	+	+
Hypopigmentation	-	+	+	-	-	+	-
Synophrys	-	+	-	+	-	+	-
Hirschprung's disease	-	-	-	-	-	-	+
Cleft palate/lip	-	-	-	+	-	-	-
Ocular albinism	-	-	-	-	-	-	-
Vitiligo	-	-	-	-	-	-	-
Blindness	-	-	-	-	-	-	-
GH deficiency	-	-	-	-	-	-	-
Telecanthus	-	-	-	-	-	-	-
Hypertelorism	+	-	-	-	-	-	-
Hypoplastic blue eye	-	-	-	-	-	+	+
Missing nasal bone	-	-	-	-	-	-	-
Syndactyly	+	-	-	+	-	-	-
Craniofacial anomalies	+	-	-	-	-	-	-
Ptosis	+	-	-	-	+	-	-
Heart defects	+	-	-	-	-	-	-
Neuropathies	+	-	-	-	-	-	-
Septo-Optic Dysplasia	-	-	-	-	-	-	-
Endocrine dysfunction	-	-	-	-	-	-	-
Hypoplasia of optic nerv	-	-	-	-	-	-	-
absent septum pellucidu	-	-	-	-	-	-	-
Hypoplasia of nasal bon	-	-	-	+	-	-	-
Developmental delay	-	-	-	+	-	-	-
Anencephaly	-	-	-	-	+	-	-
18q Syndrome	-	-	-	+	-	-	-
Brachycephaly	-	-	-	+	-	-	-
Kidney disfunction	-	-	-	-	-	-	+
Nystagmus	-	-	-	-	-	-	+
Strabismus	-	+	-	-	-	-	-
Vestibular disturbances	-	-	-	NA	-	-	-
Ataxia	-	-	-	NA	-	-	+
Mental Retardation	-	-	-	+	-	-	-
Otosclerosis	-	-	-	-	-	-	-
Tarsal coalition	+	-	-	-	-	-	-
Tear duct aplasia	+	-	-	-	-	-	-
Craniofacial surgery	+	-	-	-	-	-	-

Table 18: Phenotypes for MSU29-MSU32; UoM1, UoM3, UoM4

PHENOTYPE	FAMILIES						
	MSU 29	MSU 30	MSU 31	MSU 32	UoM I	UoM 3	UoM 4
Dystopia canthorum	+	+	-	?	+	-	+
Broad nasal root	-	-	-	+	-	-	+
Deafness	+	+	+	-	+	+	+
Heterochromia	+	-	-	-	-	-	-
Pre-mature graying	-	-	+	-	+	-	-
White forelock	-	+	-	-	-	-	-
Hypopigmentation	-	-	-	?	-	-	-
Synophrys	+	-	-	-	-	-	-
Hirschprung's disease	-	-	-	-	-	-	-
Cleft palate/lip	-	-	-	+	-	-	-
Ocular albinism	-	-	-	-	-	-	-
Vitiligo	-	-	-	-	-	-	-
Blindness	-	-	-	-	-	-	-
GH deficiency	-	-	-	-	-	-	-
Telecanthus	-	-	-	-	-	-	-
Hypertelorism	-	-	-	+	-	-	-
Hypoplastic blue eye	-	-	+	-	-	-	-
Missing nasal bone	-	-	-	-	-	-	-
Syndactyly	-	-	-	-	-	-	-
Craniofacial anomalies	-	-	-	-	-	-	-
Ptosis	-	-	-	-	-	-	-
Heart defects	-	-	-	-	-	-	-
Neuropathies	-	-	-	-	-	-	-
Septo-Optic Dysplasia	-	-	-	-	+	-	-
Endocrine dysfunction	-	-	-	-	-	-	-
Hypoplasia of optic nerve	-	-	-	-	+	-	-
absent septum pellucidum	-	-	-	-	+	-	-
Hypoplasia of nasal bone	+	-	-	-	-	-	-
Developmental delay	-	+	-	+	-	-	-
Anencephaly	-	-	-	-	-	-	-
18q Syndrome	-	-	-	-	-	-	-
Brachycephaly	-	-	-	-	-	-	-
Kidney disfunction	-	-	-	-	-	+	-
Nystagmus	-	-	-	-	-	-	-
Strabismus	-	-	-	-	-	-	-
Vestibular disturbances	-	-	-	-	-	-	-
Ataxia	-	-	-	-	-	-	-
Mental Retardation	-	+	-	-	-	-	-
Otosclerosis	-	-	-	-	-	-	-
Tarsal coalition	-	-	-	-	-	-	-
Tear duct aplasia	-	-	-	-	-	-	-
Craniofacial surgery	-	-	-	-	-	-	-

Table 19: Phenotypes for UGM Families

PHENOTYPE	UGM 1-1	UGM 2-1	UGM 2-2	UGM 1-2	UGM 1-3	UGM 1-4
Dystopia canthorum	+	-	-	+	+	?
Broad nasal root	-	-	-	-	-	?
Deafness	+	?	+	+	?	?
Heterochromia	+	+	?	+	?	?
Pre-mature graying	-	-	-	-	+	?
White forelock	+	-	-	-	-	?
Hypopigmentation	+	-	-	+	-	?
Synophrys	-	-	-	-	+	-
Hirschprung's disease	-	-	-	-	-	-
Cleft palate/lip	-	-	-	-	-	-
Ocular albinism	-	-	-	-	-	-
Vitiligo	-	-	-	-	-	-
Blindness	-	-	-	-	-	-
GH deficiency	-	-	-	-	-	-
Telecanthus	-	-	-	-	-	-
Hypertelorism	-	-	-	-	-	-
Hypoplastic blue eye	-	-	-	-	-	-
Missing nasal bone	-	-	-	-	-	-
Syndactyly	-	-	-	-	-	-
Craniofacial anomalies	-	-	-	-	-	-
Ptosis	-	-	-	-	-	-
Heart defects	-	-	-	-	-	-
Neuropathies	-	-	-	-	-	-
Septo-Optic Dysplasia	-	-	-	-	-	-
Endocrine dysfunction	-	-	-	-	-	-
Hypoplasia of optic nerve	-	-	-	-	-	-
absent septum pellucidu	-	-	-	-	-	-
Hypoplasia of nasal bone	-	-	-	-	-	-
Developmental delay	-	-	-	-	-	-
Anencephaly	-	-	-	-	-	-
18q Syndrome	-	-	-	-	-	-
Brachycephaly	-	-	-	-	-	-
Kidney disfunction	-	-	-	-	-	-
Nystagmus	-	-	-	-	-	-
Strabismus	-	-	-	-	-	-
Vestibular disturbances	-	-	-	-	-	-
Ataxia	-	-	-	-	-	-
Mental Retardation	-	-	-	-	-	-
Otosclerosis	-	-	-	-	-	-
Tarsal coalition	-	-	-	-	-	-
Tear duct aplasia	-	-	-	-	-	-
Craniofacial surgery	-	-	-	-	-	-

Table 20: Phenotypes for SOD Individuals

PHENOTYPE	SOD1	SOD2	SOD3	SOD4	SOD5	SOD6
Dystopia canthorum	-	-	-	-	-	-
Broad nasal root	-	-	-	-	-	-
Deafness	?	-	-	-	-	-
Heterochromia	-	-	-	-	-	-
Pre-mature graying	-	-	-	-	-	-
White forelock	-	-	-	-	-	-
Hypopigmentation	-	-	-	-	-	-
Synophrys	-	-	-	-	-	-
Hirschprung's disease	-	-	-	-	-	-
Cleft palate/lip	-	-	-	-	-	-
Ocular albinism	-	-	-	-	-	-
Vitiligo	-	-	-	-	-	-
Blindness	?	+	?	+	?	?
GH deficiency	-	+	-	+	?	?
Telecanthus	-	-	-	-	-	-
Hypertelorism	-	-	-	-	-	-
Hypoplastic blue eye	-	-	-	-	-	-
Missing nasal bone	-	-	-	-	-	-
Syndactyly	-	-	-	-	-	-
Craniofacial anomalies	-	-	-	-	-	-
Ptosis	-	-	-	-	-	-
Heart defects	-	-	-	-	-	-
Neuropathies	-	-	-	-	-	-
Septo-Optic Dysplasia	+	+	+	+	+	+
Endocrine dysfunction	+	+	+	+	?	?
Hypoplasia of optic nerve	+	+	+	+	?	?
absent septum pellucidu	-	-	+	?	-	?
Hypoplasia of nasal bone	-	-	-	-	-	-
Developmental delay	+	-	-	-	-	-
Anencephaly	-	-	-	-	-	-
18q Syndrome	-	-	-	-	-	-
Brachycephaly	-	-	-	-	-	-
Kidney disfunction	-	-	-	-	-	-
Nystagmus	+	+	-	-	-	-
Strabismus	-	-	-	-	-	-
Vestibular disturbances	-	-	-	-	-	-
Ataxia	-	-	-	-	-	-
Mental Retardation	-	-	-	-	-	-
Otosclerosis	-	-	-	-	-	-
Tarsal coalition	-	-	-	-	-	-
Tear duct aplasia	-	-	-	-	-	-
Craniofacial surgery	-	-	-	-	-	-

Table 21: Phenotype Description for Members of MSU22

PHENOTYPE	MSU 22																	
	102	202	204	208	302	303	305	307	315	319	320	323	401	405	410	411	416	417
Dystopia canthorum	-	?	-	-	-	-	?	-	?	-	-	-	-	-	-	-	-	-
Broad nasal root	-	-	-	-	-	-	-	-	-	-	-	-	-	-	-	-	-	-
Deafness	-	+	-	-	+	-	+	+	-	-	+	+	+	+	+	-	-	-
Heterochromia	-	+	-	-	-	-	-	-	-	+	-	-	-	+	-	+	-	-
Pre-mature graying	-	-	-	-	-	-	-	-	-	-	-	-	-	-	-	-	-	-
White forelock	+	+	+	-	-	+	+	-	-	-	-	-	+	+	-	-	+	-
Hypopigmentation	-	-	-	-	-	-	-	-	-	-	-	-	-	-	-	-	-	-
Hirschprung's disease	-	-	-	-	-	-	-	-	-	-	-	-	-	-	-	-	-	-
Cleft palate/lip	-	-	-	-	-	-	-	-	-	-	-	-	-	-	-	-	-	-
Ocular albinism	-	-	-	-	-	-	-	-	-	-	-	-	-	-	-	-	-	-
Vitiligo	-	-	-	-	-	-	-	-	-	-	-	-	-	-	-	-	-	-
Blindness	-	-	-	-	-	-	-	-	-	-	-	-	-	-	-	-	-	-
GH deficiency	-	-	-	-	-	-	-	-	-	-	-	-	-	-	-	-	-	-
Telecanthus	-	-	-	-	-	-	-	-	-	-	-	-	-	-	-	-	-	-
Hypertelorism	-	-	-	-	-	-	-	-	-	-	-	-	-	-	-	-	-	-
Hypoplastic blue eye	-	-	-	-	-	-	-	-	-	-	-	-	-	-	-	-	-	-
Missing nasal bone	-	-	-	-	-	-	-	-	-	-	-	-	-	-	-	-	-	-
Syndactyly	-	-	-	+	-	-	-	-	-	-	-	+	-	-	-	-	+	+
Craniofacial anomalie	+	-	+	+	+	-	+	-	+	+	+	-	-	+	+	+	+	-
Heart defects	-	-	-	-	-	-	-	-	-	-	-	-	-	-	-	+	-	-
Neuropathies	+	-	-	-	-	-	+	-	-	-	-	-	-	+	-	-	-	-
Septo-Optic Dysplasia	-	-	-	-	-	-	-	-	-	-	-	-	-	-	-	-	-	-
Hypoplasic nasal bone	-	-	-	-	-	-	-	-	-	-	-	-	-	-	-	-	-	-
Developmental delay	-	-	-	-	-	-	-	-	-	-	-	-	-	-	-	-	-	-
Anencephaly	-	-	-	-	-	-	-	-	-	-	-	-	-	-	-	-	-	-
Kidney disfunction	-	-	-	-	-	-	-	-	-	-	-	-	-	-	-	-	-	-
Nystagmus	-	-	-	-	-	-	-	-	-	-	-	-	-	-	-	-	-	-
Vestibular disturbance	-	-	-	-	-	-	-	-	-	-	-	-	-	-	-	-	-	-
Mental Retardation	-	-	-	-	-	-	-	-	-	-	-	-	-	-	-	-	-	-
Otosclerosis	-	-	-	-	-	-	-	-	-	-	-	-	-	-	-	-	-	-
Tarsal coalition	-	-	-	-	-	-	-	-	-	-	-	-	-	+	-	-	-	-
Tear duct aplasia	-	-	-	-	-	-	-	-	-	-	-	-	-	+	-	-	-	-
Craniofacial surgery	-	+	-	+	+	-	+	-	+	+	+	-	+	+	+	+	+	-

Tables 14-21 A description of the phenotypes for all of the families represented by the proband screening set. The clinical traits for each table are identical, with the except of table 22 (MSU22) and includes traits that are not typically associated with the WS phenotype. The minus sign may mean the trait was not present in the family or that the data was unavailable. The plus sign means that at least one individual in the family demonstrated the trait.

APPENDIX B

Department of Zoology, S-320 Plant Biology Building
Michigan State University
East Lansing, Michigan 48824 1/96

INFORMED CONSENT FORM

1. I, _____, freely and voluntarily consent to serve as a subject in a scientific study of a Waardenburg-like Syndrome with craniofacial-skeletal abnormalities conducted by Dr. Thomas B. Friedman and Dr. James H. Asher, Jr.

2. I understand that the purpose of the study is to map and clone the genes causing the Waardenburg-like Syndrome. To perform a mapping analysis, I understand that I may be given a physical examination, a complete analysis of my hearing and an ophthalmologic examination which may require that my eyes be dilated to enable photography of my retina. I understand that all of these examinations will be performed by licensed physicians at no cost to me. I may need to either give up to three 10 ml blood samples or, as an alternative to drawing blood for certain individuals, 10 ml of sterile 0.9% saline (salt solution) will be gargled and expelled into a test tube. Cheek cells normally shed into the mouth can be collected from which my genomic DNA can be isolated. My blood samples may be used in performing a banding analysis of the chromosomes and a genetic mapping analysis. I will be given the results of hearing and opthalmological tests if I so desire.

3. I understand that I will not be exposed to any conditions which constitute a threat to my physical or psychological well-being. I understand that bacteremia and hematoma (bruising and swelling) are very unlikely risks from having blood samples drawn provided sterile procedures are followed. I do not have any known blood disorders and I am not taking medications that would prevent or slow blood clotting. I also understand that iridial dilation (dilation of the pupil) may precipitate acute angle-closure glaucoma. I will be given a test to determine whether I am at risk for this condition prior to any eye examination. If I am at risk, I will not have my eyes dilated during the eye examination. I understand that in the unlikely event of injury from having blood drawn or having an eye examination at Michigan State University (MSU), MSU will provide emergency medical care if necessary. I further understand that if the injury is not caused by negligence of MSU, I am personally responsible for expenses of this emergency care and any other medical expenses incurred as a result of this injury. I understand that in the unlikely event of injury resulting from drawing of my blood sample or dilation of my eyes at a location other than at MSU, this other clinic, hospital or care facility will provide emergency medical care if necessary. If injury is not caused by negligence of individuals at facilities other than MSU, I understand that I am personally responsible for expenses of this emergency care and any other medical expenses incurred as a result of this injury. If I have any questions, I am to contact Dr. Thomas B. Friedman or Dr. James H. Asher, Jr. at 517 355-5059 (phone) or 517 432-1025 (FAX).

4. I understand that data gathered from me for this experiment are confidential, that no information uniquely identified with me will be made available to other persons or agencies, and that any publication of the results of this study will maintain confidentiality.

5. I engage in this study of my own free will, without payment to me for my personal time and without implication of personal benefit from the study. I understand that I may cease participation in the study at any time without prejudice to me.

6. I have had the opportunity to ask questions about the nature and purpose of the study, and I have been provided with a copy of this written informed consent form. I understand that upon completion of the study, and at my request, I can obtain an additional explanation about the study.

Date:_____ Signed: _____
Participant

Signed: _____
Witness

Waardenburg Syndrome Consortium
Clinical Data Intake Form

Pedigree ID # _____
Individual ID #_____
Date _____

Birth Date _____
Age at Assesment _____

1) Facial Morphology

inner canthal distance	_____ mm	
outer canthal distance	_____ mm	
inter-pupillary distance	_____ mm	

Does subject exhibit:	ptosis?	Y	N
	confluent eyebrows?	Y	N
	white forelock?	Y	N
	broad nasal root?	Y	N
	hypoplasia of nasal bone?	Y	N
	cleft lip/palate?	Y	N

2) Eyes

Does subject exhibit:	coloboma?	Y	N
	transillumination defect?	Y	N
	hypopigmentation of fundus and/or maculae?	Y	N
	heterochromia irides?	Y	N

Indicate in a drawing regions of unusual coloration of the irides and location of segments in cases of segmental iris bicolor, and/or unusual pupil shape and location.

3) Audio-vestibular assessment

Hearing test results (provide threshold in decibels):

Ear	250 Hz	500 Hz	1 KHz	2 KHz	4 KHz	8 KHz
right	dB	dB	dB	dB	dB	dB
left	dB	dB	dB	dB	dB	dB

	Left	Right
Pure tone avg.:	dB	dB
Speech reception/Awareness threshold:	dB	dB
Discrimination score:	%	%

Use "NR" for no response;
Use AC/BC when mixed hearing loss.

Standard Romberg test: ___stable ___unstable
(If available)

Any indication of vestibular dysfunction? Y N
(Please describe on back of sheet if "Y").

If hearing loss/vestibular dysfunction detected, indicate whether congenital or age of onset, and whether hearing loss is progressive, conductive, sensorineural, etc.

4) Other

Does subject exhibit:

Severe and/or chronic constipation?	Y	N	
Skin hypopigmentation?	Y	N	
Early greying? (Age?)	Y	N	____yrs.
Spina bifida?	Y	N	
Skeletal abnormalities? (Please describe on next page)	Y	N	
Congenital heart defects?	Y	N	

Please use back of this sheet to elaborate or clarify or to draw pedigrees.

Evaluator's name: _____

Signature: _____

Clinical Data Intake Form

Reporting center:_____
Subject identification #_____

WAARDENBURG SYNDROME CONSORTIUM GROUP

Is this individual a proband? _____Yes ____ No Family Identification # _____

Subject's birthdate: _____/_____/_____ If deceased, date of death _____/_____/_____

Data obtained by : __ interview in person
__ phone interview __ from a relative __ other: _____

Photograph of individual:
___obtained/available ____ unavailable

HISTORY

1. Has this individual been diagnosed with Waardenburg syndrome? Yes No Age at time of diagnosis: _____

   If yes,which type was the diagnosis? Type I Type II Not sure

   By whom was the diagnosis made? (check the individual *primarily* responsible for making the diagnsosis)

   _____ geneticist _____ otolaryngologist _____ ophthalmologist _____ audiologist

   _____ family or other physician _____ relative _____ other: _____

2. Does the individual have relatives known to be affected with Waardenburg syndrome? Yes No

   If yes, list below the *affected* relatives using the terms mother, father, sibling and the letter M or P (to indicate maternal or paternal) in front of the terms grandfather, grandmother, half-sibling,first cousin, second cousin, aunt, uncle, etc.

   _____ _____ _____
   _____ _____ _____
   _____ _____ _____
   _____ _____ _____

   Total number of affected relatives: _____

3. Was there at birth a patch of white hair? Yes No

   If yes, has the patch remained? Yes No

   If the hair is *now* predominantly white, then at what age did the hair *begin* to turn gray? _____ years

4. Is there any hearing impairment? (circle correct answers) Yes No

   If yes, then place check mark next to correct answers below:

   Which ears are involved? ___right ___left ___both

   When did it start? ___at birth ___mid-life ___old age

   How bad is the hearing loss? (check correct answer)

   Right ear: ___none (normal) ___mild ___moderate ___severe

   Left ear: ___none (normal) ___mild ___moderate ___severe

   When is the last time that hearing was tested? Date: _____/_____/_____

   What is believed to be the cause of the hearing impairment?

   __ inherited (genetic) __ noise induced __ from an infection

   ___ from old age ___ other cause: (specify) _____

   Is the hearing continuing to get worse? Yes No

PHYSICAL EXAMINATION

Face

Nose

high nasal root (profile view)	Yes	No
broad nasal bridge (full face view)	Yes	No
hypoplasia alae	Yes	No

Hair

confluent eyebrow (synophrys)	Yes	No

Eyes

distance measured between: medial canthi: _____mm.

outer canthi: _____mm.

pupils: _____mm.

Check and circle below method by which measurements were obtained:

__ in person physical examination: calipers ruler

__ from photograph

__ other method; described here:

Color:

__ two *unusually brilliant* blue eyes (sapphire blue)

__ two different color eyes

__ one eye with two different colors in it right left

Eyelids:

___ no ptosis ___ ptosis right left

Skin

Areas of hypopigmentation: Yes No

Scalp hair

White forelock Yes No

Other (circle those that apply)

Neural tube defect: Hirschsprung Dis. spina bifida other: _____

Additional findings

(Continue to page 3)

Audiovestibular assessment:

Assessment made by information from (check *one* only):

_____relative _____ physician _____ objective test

If objective test, then provide information below (check appropriate answer):

Testor: ___ audiologist ___ physician ___ nurse ___ other: _____

Conditions: ___ soundproof booth ___ portable audiometer

Hearing test results (provide thresholds in decibels):

Ear	250 Hz	500 Hz	1 KHz	2 KHz	4 KHz	8 KHz
Right ear:	____dB	_____dB	_____dB	____dB	____dB	____dB
Left ear:	____dB	_____dB	_____dB	____dB	____dB	____dB

Pure tone average: Left _____dB Right _____dB

Speech reception threshold: Left _____dB Right _____dB

Discrimination scores: Left _____ % Right _____ %

Standard Romberg test: ____ stable ____ unstable

Tandem Romberg test: ____ stable ____ unstable

Caloric tests: ____ normal ____ abnormal

Electronystagmography: ____ normal ____ abnormal

Other vestibular function test: _____

****

This reporting center has determined for the purposes of linkage analysis that this individual is:

___ AFFECTED ___ NOT AFFECTED

Confidence level that affectation status is accurate:

___ Absolutely positive ___ Almost positive

Not entirely sure because: _____

_____

This data form submitted by: _____

Date prepared: _____ Phone number: _____

(Provide additional comments and clarifications on reverse side of this page)

GENOMICS 34, 285–298 (1996)
ARTICLE NO. 0289

Effects of *Pax3* Modifier Genes on Craniofacial Morphology, Pigmentation, and Viability: A Murine Model of Waardenburg Syndrome Variation

JAMES H. ASHER, JR.,*·†·‡ RONALD W. HARRISON,* ROBERT MORELL,*
MELISA L. CAREY,* AND THOMAS B. FRIEDMAN*·‡·[1]

*Department of Zoology and ‡Graduate Program in Genetics, Michigan State University, East Lansing, Michigan 48824

Received April 26, 1995; accepted March 26, 1996

Waardenburg syndrome type 1 is caused by mutations in *PAX3*. Over 50 human *PAX3* mutations that lead to hearing, craniofacial, limb, and pigmentation anomalies have been identified. A *PAX3* mutant allele, segregating in a family, can show reduced penetrance and variable expressivity that cannot be explained by the nature of the mutation alone. The *Mus musculus Pax3* mutation *Sp*^{d} (*Splotch-delayed*, *Pax3*$^{Sp^d}$), coisogenic on the C57BL/6J (B_6) genetic background, produces in heterozygotes a white belly spot with 100% penetrance and very few other anomalies. By contrast, many *Sp*^{d}/+ BC_1 progeny [F_1 ♀ *Sp*^{d}/+ (♀ *Sp*^{d}/+ B_6 × ♂ +/+ *Mus spretus*) × ♂ +/+ B_6] exhibit highly variable craniofacial and pigmentary anomalies. Of the BC_1 *Sp*^{d}/+ progeny, 23.9% are estimated to be nonviable, and 32.1% are nonpenetrant for the white belly spot. The penetrance and expressivity of the *Sp*^{d}/+ genotype are controlled in part by the genetic background and the sex of the individual. A minimum of two genes interact with *Sp*^{d} to influence the craniofacial features of these mice. One of these genes may be either X-linked or sex-influenced, while the other is autosomal. The *A*-locus (*Agouti*) or a gene closely linked to *A* also plays a role in determining craniofacial features. At least one additional gene, possibly the *A*-locus or a gene linked to *A*, interacts with *Sp*^{d} and determines the presence and size of the white belly spot. The viability of BC_1 mice is influenced by at least three factors: *Sp*^{d}, *A*-locus alleles or a gene closely linked to the *A*-locus, and the sex of the mouse. These BC_1 mice provide an opportunity to identify genes that interact with and modify the expression of *Pax3* and serve as a model to identify the genes that modify the expression of human *PAX3* mutations.

INTRODUCTION

Mouse mutations have long been used as models for the study of human clinical conditions. Described here is a mouse model that serves to identify the basis of some of the clinical variability associated with Waardenburg syndrome mutations. Waardenburg syndrome (WS) segregates as an autosomal dominant mutation with variable penetrance and expressivity. WS is a major cause of human deafness, being responsible for over 2% of congenitally and profoundly deaf individuals (Waardenburg, 1951; Partington, 1964). In addition to affecting hearing, WS mutations influence the development of over 18 different characteristics, including pigmentation of the hair, skin, and eyes; skeletal features of the limbs, face, and head; heart development; and neurological features such as the absence of intestinal ganglia observed in associated Hirschsprung disease (Divekar, 1957; DiGeorge *et al.*, 1960; Ray, 1961; Aasved, 1962; Stoller, 1962; Calinikos, 1963; Meijer and Walker, 1964; Rugel and Keats, 1965; Goldberg, 1966; Reed *et al.*, 1967; Arias, 1971; Pantke and Cohen, 1971; Nance and McConnell, 1973; Nance and Sweeney, 1975; Delleman and Hageman, 1978; Wang *et al.*, 1981).

This phenotypic variability is reflected in the current classification of WS clinical types. With the exception of limb abnormalities, Waardenburg syndrome type 1 (WS1, MIM No. 193500) mutations may alter all of the phenotypic features described above. Dystopia canthorum, an increased inner canthal distance relative to the inter pupillary and outer canthal distances, is a craniofacial anomaly and is the most consistent diagnostic feature of WS1 with 98% penetrance (Waardenburg, 1951). Individuals with WS2 (MIM No. 193510) do not exhibit dystopia canthorum but may exhibit all other WS1 features (Arias, 1971, 1980; Hageman and Delleman, 1977; Liu *et al.*, 1995). Individuals with WS3 (MIM No. 148820) exhibit typical WS1 features with the addition of skeletal anomalies of the upper limbs (Klein, 1983; Goodman *et al.*, 1982). Finally, individuals with WS4 (MIM No. 277580) do not exhibit dystopia canthorum but exhibit aganglionic megacolon (Hirschsprung disease) along with a variety of other WS features (Omenn and McKusick, 1979; Shah *et al.*, 1981; Ambani, 1983; Meire *et al.*, 1987).

† Deceased.

[1] To whom correspondence should be addressed at S-320 Plant Biology, Department of Zoology, Michigan State University, East Lansing, Michigan 48824. Telephone: (517) 355-5059. Fax: (517) 432-1025.

0888-7543/96 $18.00

On the basis of phenotypic similarities between mouse and human mutants, Asher and Friedman (1990) predicted that there were at least four mouse mutations that were potentially homologous with human mutations causing Waardenburg syndrome (s): *Mi^{mr}*, *Sp*, *Ph*, and *s*. The chromosomal locations of these four mouse mutations were then used to predict the chromosomal locations of Waardenburg syndrome mutations. The validity of three of the four predictions has been demonstrated. *PAX3* mutations, homologous to mouse *Splotch*, *Sp*, are the cause of WS1 (Foy *et al.*, 1990; Asher *et al.*, 1991; Baldwin *et al.*, 1992; Tassabehji *et al.*, 1992; Morell *et al.*, 1992, 1993; Farrer *et al.*, 1992) and WS3 (Hoth *et al.*, 1993; Pasteris *et al.*, 1993). *MITF* mutations, homologous to mouse *Microphthalmia-Oak Ridge*, *Mi^{mr}*, are one cause of some WS2 cases (Tassabehji *et al.*, 1994). Finally, *EDNRB* mutations, homologous to mouse *piebald*, *s*, are one cause of WS2 cases with and without Hirschsprung disease (Puffenberger *et al.*, 1994).

Mice heterozygous for the mutation *Sp^d* (*Splotch-delayed*), a *Pax3* missense mutation Gly42Arg (Vogan *et al.*, 1993) segregating on the highly inbred C57BL/6J (B_6) genetic background on which it arose (Dickie, 1964), have a white belly spot but do not have craniofacial anomalies. However, as described in this paper, when *Sp^d* segregates among interspecific BC_1 mice, there are significant alterations in skull morphology. A morphometric analysis of 306 BC_1 mice demonstrates the existence of at least two genes that interact with *Sp^d* to alter adult mouse craniofacial morphology. At least one other gene interacts with *Sp^d* to determine the presence and size of the white belly spot. The viability of BC_1 mice is influenced by the interaction among *Sp^d*, the *a* (*non-agouti*) allele, and the sex of the mouse. Thus, BC_1 mice segregating *Sp^d* exhibit many of the features found in human families segregating WS1 mutations.

MATERIALS AND METHODS

Mice. *Sp^d*/+;*a*/*a* mice (*Splotch-delayed*, *non-agouti* black, at N_n generations of back crossing stored as a freezer stock) and +/+;*a*/*a* mice (C57BL/6J *Mus musculus* at F_{77} generations of full sibling mating, B_6) were obtained from the Jackson Laboratory (Bar Harbor, ME). *Sp^d* occurred as a spontaneous mutation on chromosome 1 (Dickie, 1964) in the highly inbred strain B_6 and is coisogenic with the wildtype (+) allele. The *non-agouti* allele *a* is a normal component of the genetic background of B_6 mice and is on chromosome 2 (Lyon and Searle, 1989). The inbred strain *Mus spretus* SPAIN (+/+;*A*/*A*, SPR) was also obtained from the Jackson Laboratory at F_{37} generations of full sibling matings. *Mus spretus* mice do not exhibit white belly patches or craniofacial anomalies and are homozygous for the *A* (*Agouti*) allele.

Crosses. On the inbred B_6 genetic background, *Sp^d* is a fully penetrant, dominant mutation causing the production of a variable sized, white belly spot. *Sp^d*/+;*a*/*a* mice appear to have normal viability. *Sp^d*/+;*a*/*a* *Mus musculus* females from B_6 with white belly spots were crossed to +/+;*A*/*A* *Mus spretus* males. All the F_1 progeny exhibited increased vigor and decreased penetrance of *Sp^d* with only about 1/20 of *Sp^d*/+ F_1 progeny having white belly spots. Because of the apparent lack of penetrance of *Sp^d* with respect to a white belly spot and because these crosses were made prior to the discovery of the molecular defect caused by *Sp^d* (Vogan *et al.*, 1993), there was some initial uncertainty of the *Pax3* genotypes of the F_1 females chosen to be backcrossed to +/+ *M. musculus* B_6 males. The most consistent feature of F_1 female mice suspected of being *Sp^d*/+ was foot soles with diminished pigmentation. F_1 [*Sp^d*/+;*A*/*a* females ♀ B_6 *Sp^d*/+;*a*/*a* × ♂ +/+;*A*/*A* *M. spretus*] with diminished foot sole pigmentation were backcrossed to +/+;*a*/*a* B_6 male mice who were the result of a cross between two black mice producing all black progeny. The resulting progeny are called BC_1 mice (Fig. 1). Each BC_1 mouse has a unique combination of *Mus musculus* and *Mus spretus* alleles at all loci. Many of the resulting BC_1 progeny exhibited extensive phenotypic variation, including large white belly spots and dysmorphic facies. The above crosses were expected to produce an equal number of +/+ and *Sp^d*/+ BC_1 progeny and, segregating independently, an equal number of *a*/*a* and *A*/*a* BC_1 progeny. This null hypothesis was tested with a conventional χ^2 test.

The BC_1 mice used in the craniofacial morphometric study were siblings. Most litters contained +/+ and *Sp^d*/+ siblings. The mean age of +/+ BC_1 mice was 155.2 ± 67.0 days (n = 180), while the mean age of the BC_1 *Sp^d*/+ mice was 155.2 ± 68.5 days (n = 137). The 7 youngest mice (2.2%) were 40 days old, while the 4 oldest mice (1.3%) were 300 days old. The 40-day-old mice did not have skulls with unusual measurements. In addition, at 30 days of age, the skulls of +/+ random-bred mice had reached 93.8% of their adult length, while 150-day-old random-bred +/+ mice were fully grown (Leamy, 1974).

DNA isolation. Mice were anesthetized with Metofane, euthanized by cervical dislocation, inspected for dysmorphic features and pigmentation variation, and photographed, and their livers were removed for DNA extraction. Liver nuclei were isolated and DNA extracted (Davis *et al.*, 1986). The mouse carcasses were labeled and stored at −80°C.

Identification of the Sp^d/+ genotype. To identify the presence or absence of the *Sp^d* allele, a PCR primer containing the 3′ terminal G to C substitution specific to the *Sp^d* mutation was used (Table 1). The genotypes of all BC_1 mice were determined to be +/+ or *Sp^d*/+ by the amplification of exon 2 fragments using the primers and conditions listed in Table 1. The wildtype + allele was detected by the synthesis of a single 236-bp PCR fragment (products of primers JA-30 and JA-31). The *Sp^d* allele was detected by the synthesis of a 217-bp fragment (the product of the allele-specific primer JA-40 and primer JA-31) unique to the *Sp^d* allele. These two fragments were resolved on 4% NuSieve 3:1 agarose gels (FMC) and visualized by ethidium bromide staining followed by exposure to ultraviolet light.

The DNA sequences of the 236-bp fragments from +/+ *M. musculus* and +/+ *M. spretus* are identical (data not shown). To distinguish the origin of the + allele (*musculus* or *spretus*), exons 1 and 5 of *Pax3* were also PCR amplified (Table 1). PCR fragments from exons 1 and 5 exhibit species-specific single-strand conformational polymorphisms (SSCP's) (data not shown).

Thus, three *Pax3* alleles were identified: (1) a wildtype B_6 allele that contains *M. musculus* SSCP variants for exon 1 and 5 fragments and a 236-bp PCR fragment for exon 2; (2) a wildtype allele that contains *M. spretus* SSCP variants for exon 1 and 5 fragments and a 236-bp PCR fragment for exon 2; and (3) the *Sp^d* B_6 allele that contains *M. musculus* SSCP variants for exon 1 and 5 fragments, a 236-bp PCR fragment for exon 2, and a 217-bp allele-specific PCR fragment for exon 2.

Preparation of skulls. Mouse carcasses stored at −80°C were decapitated, the skin and tongue were removed from the head, an identification tag was tied to the lower jaw, and the heads were placed individually in the wells of an egg carton attached by the identification tag. The egg cartons were then placed in a very large stainless steel container of dermestid beetles which were processing many other animal remains. Because of beetle activity, a few mouse skulls were dislodged from the carton and were thus lost. After the majority of the tissue was removed by the beetles, the remaining tissue was macerated in a freshly prepared 1:1 dilution of aqueous ammonia. The skulls and identification tags were then desiccated and individually stored in specimen vials.

The analysis of skull characteristics was performed on 6 B_6 mice

(4 +/+ and 2 $Sp^4/+$), 30 SPR mice (all +/+), 25 F_1 mice (17 +/+ and 8 $Sp^4/+$), and 327 BC_1 mice (190 +/+ and 137 $Sp^4/+$). The 327 BC_1 mice were evaluated for all characteristics and genotyped by PCR analysis. Only 306 of the 327 BC_1 mouse skulls (180 +/+ and 126 $Sp^4/+$) were used in the final morphometric analysis. Twenty-one BC_1 skulls were not included in this analysis because they were lost or damaged during dermistid beetle preparation (4 $Sp^4/+$), grossly deformed on visual inspection with profoundly altered craniofacial measurements (4 $Sp^4/+$), exhibited measurements four or more standard deviations from the means of two skull landmark measurements (3 $Sp^4/+$), or were progeny of an F_1 parent that was +/+ and not $Sp^4/+$ (10 +/+).

The seven $Sp^4/+$ skulls (5.3% of the $Sp^4/+$ mice) described above had landmarks that were larger than four standard deviations from the means of both +/+ and $Sp^4/+$ mice. These seven skulls were atypical of all mice examined regardless of genotype, and because of their extreme outlier status they were omitted from the analysis using the protocol of Snedecor and Cochran (1967). These $Sp^4/+$ mice may have unique genotypes that will be analyzed at a future date.

Digitization of skull landmarks. Prior to the collection of morphometric data from individual skulls, all skulls were examined to determine qualitative differences. Eight landmarks were chosen (X_i, Y_i, i = 1, 2, ... 8; Fig. 2B) that outlined the interfrontal bone, best defined the facial abnormalities observed, and were unambiguously identified in every skull. The skulls were examined using a Wild Heerburgg M5 stereo microscope with a Javelin Electronic CCTV video camera. Skull images were acquired by a PCVISION PLUS frame grabber (Image Processing Solutions) installed in an IBM-compatible PC. Digitizing the landmarks was accomplished using the Bioscan software package OPTIMAS4 (Bioscan, Inc.).

To minimize parallax, distortion of the apparent shape of the skull caused by the nonperpendicular placement of the camera and microscope relative to the skull, the microscope and camera were leveled with a bubble level before each data collection session. A bubble level was then attached to one end of a 1 × 6 × 0.2 cm glass strip (half a microscope slide) with double-sided sticky tape. The bubble level, atop one end of the glass strip, was supported by a small block of clay. Skulls were fastened laterally to the free end of the glass strip by the upper molar tooth rows using double-sided sticky tape. Sp^4 did not appear to alter the placement of the tooth rows. In this way, the skull could be leveled, parallax minimized, and consistency maintained during image capturing.

Analysis of shape coordinate data. Student t tests were performed to determine if the coordinates of each landmark differed and if the slopes of the regression lines through each landmark were significantly different from zero or differed between groups (Snedecor and Cochran, 1967). Each landmark (X_i, Y_i) was analyzed independently. Landmarks i = 2, 3, and 4 represent the right side of the skull from anterior to posterior, and landmarks i = 6, 7, and 8 represent the left side of the skull from posterior to anterior. The symmetric landmarks are 2 and 8, 3 and 7, and 4 and 6 (Fig. 2). If no systematic technical errors were made in capturing and digitizing the images and if Sp^4 does not cause facial asymmetries, the pairs of landmarks should be symmetrically placed. As an example, for the landmark pair 4 and 6, the null hypothesis is $X_4 = X_6$ and $|Y_4| = Y_6$. This equality should be true for the other landmark pairs i = 2/8 and 3/7. When the same data set was used multiple times in one group comparison, the Bonferroni inequality was used to determine individual α levels to ensure an overall α = 0.05 (Nater and Wasserman, 1974). When multiple use of a data set occurs, the number of comparisons and the individual α levels are indicated.

RESULTS AND DISCUSSION

Pax3 Genotypes

Sp^4 is caused by a G to C substitution leading to a Gly42Arg mutation in the paired domain of the Pax3 transcription factor (Vogan *et al.*, 1993). Following an evaluation of the published sequences for exons 1, 2, and 5, PCR primer pairs were synthesized, which allowed, by SSCP and fragment length analysis, the unambiguous identification of the genotype and the origin of each *Pax3* allele in an $Sp^4/+$ or +/+ mouse (Table 1). The + (wildtype) exons 1 and 5 from B_6 *M. musculus* and *M. spretus* differ by clearly recognizable SSCPs (data not shown). These SSCPs were identified by silver staining 50% MDE gels (AT Biochemicals) after electrophoresis at 300 V for 24 h (exon 1) or 9 h (exon 5) of heat-denatured PCR products as previously described (Morell *et al.*, 1993). Comparisons of wildtype exon 2 from B_6 *M. musculus* and *M. spretus* mice failed to reveal SSCP or heteroduplex formations (data not shown). *Pax3* exon 2 PCR fragments from +/+ *M. musculus* and *M. spretus* were then cloned and sequenced in both directions. The wildtype *Pax3* exon 2 sequences from the two species are identical (data not shown). Thus, to identify the presence of a wildtype *M. spretus* versus a wildtype B_6 *M. musculus Pax3* allele, exon 1, exon 5, or both were PCR amplified and examined for SSCPs.

Analysis of Cross

A total of 327 BC_1 mice [F_1 ♀ $Sp^4/+;A/a$ (B_6 ♀ $Sp^4/+;a/a$ × ♂ +/+;A/A *Mus spretus*) × B_6 ♂ +/+;a/a] were produced. The genotypes and phenotypes of these mice are summarized in Table 2. There is a significant deficiency of $Sp^4/+$ mice or an excess of +/+ mice among the total progeny (χ^2 = 8.59, df = 1, P = 0.0034). Two possible explanations for these differences are: (1) some F_1 females with light foot soles used in the backcross were actually +/+ for exon 2 and thus their progeny distort the expected 1:1 (+/+:$Sp^4/+$) ratio, and (2) $Sp^4/+$ BC_1 progeny have lowered viability. Examination of the 327 BC_1 mice for exons 1, 2, and 5 indicated that a single F_1 female, thought to be $Sp^4/+$ based on foot sole pigmentation and used in a backcross, was most probably +/+ and not $Sp^4/+$. Half of her progeny were homozygous for the + *Mus musculus* allele. Thus, all her progeny were removed from the analysis, leaving 317 BC_1 mice in the segregating data set (Table 2). A χ^2 analysis of the 317 progeny presented in Table 2 demonstrates a significant deviation from the expected 1:1 ratio of +/+:$Sp^4/+$ with a deficiency of $Sp^4/+$ progeny (χ^2 = 5.83, df = 1, P = 0.0158). There appears to be a 23.9% reduction of viability of $Sp^4/+$ mice on the diverse genetic background segregating among the BC_1 progeny. Frequently, BC_1 mice were observed with severe growth retardation and white spots that covered as much as ½ of their bodies. They also had craniofacial and posterior neural tube anomalies. These mice died prior to or just following weaning, were cannibalized, and were thus not part of the measurement data set.

Crosses between $Sp^4/+$ (with white belly spots) and +/+ (without white belly spots) mice on the highly inbred B_6 strain produced equal numbers of progeny with

TABLE 1

PCR Primer Pairs, Fragment Sizes (bp), PCR Conditions, and the Presence or Absence of SSCPs Used to Identify the *Pax3* Genotype of BC_1 Mice Segregating *M. musculus* and *M. spretus* Alleles

Exon	*Pax3* allele	PCR primers	Product size (bp)	SSCP
Exon 1	(+)[a]	TF-52 F 5'CTTCGCGGTGCAGTGA3' TF-53 R 5'GGAAGCCGCTGCGTGG3' 95°C, 5 min (hot start); 85°C, add *Taq* DNA polymerase; 94°C, 1 min, 52°C, 1 min; 72°C, 1 min; 30 cycles, 72°C, 10 min	373	Yes
Exon 2	(+)	JA-30 F 5'TGTCCACCCCTCTTGGCCAG3' JA-31 R 5'CTTGGGTTTGCTGCCGCCGA3'	236	No
	(Sp^d)	JA-40 F 5'GGGCCGAGTCAACCAGCTCC3' JA-31 R 5'CTTGGGTTTGCTGCCGCCGA3' 95°C 5 min (hot start); 85°C, add *Taq* DNA polymerase; 94°C, 1 min; 72°C, 1 min; 30 cycles, 72°C, 10 min	217	No
Exon 5	(+)[b]	JA-12 F 5'CAGCGCAGGAGCAGAACCACCTTC3' JA-13 R 5'CCTCGGTAAGCTTCGCCCTCTG3' 95°C, 5 min (hot start); 85°C, add *Taq* DNA polymerase; 94°C, 1 min; 60°C, 1 min; 72°C, 1 min; 30 cycles, 72°C, 10 min	126	Yes

[a] (+) The wildtype fragments of exon 1 are 373 bp and exhibit SSCPs for *M. musculus* and *M. spretus*.
[b] Primers JA-13 and JA-12 are equivalent to primers B and C of Epstein *et al.* (1991).

and without white belly spots (Table 3). An independent set of 83 B_6 mice evaluated by DNA analysis indicates that every mouse with even a trace of a white belly spot has the $Sp^d/+$ genotype (37) and every mouse without a white belly spot has the +/+ genotype (46). Thus, on the B_6 genetic background, the Sp^d mutation appears to be fully penetrant with respect to the presence of a white belly spot and does not cause reduced viability. By contrast, on the diverse genetic background segregating among the BC_1 progeny, $Sp^d/+$ mice were only 67.9% penetrant for a white belly spot (Table 2, 93/137), exhibited considerable variability in the size of the white spot, had variable expressivity with respect to craniofacial measurements (Figs. 1 and 3 and Table 4), and had reduced viability, with only 76.1% of the $Sp^d/+$ mice surviving (Table 2).

Further analysis of the 317 BC_1 mice indicated that there was an equal number of male and female progeny regardless of the *Pax3* genotype (Table 2, ♂ = 171 to ♀ = 146; $\chi^2 = 1.97$, $df = 1$, $P = 0.16$). There was also an equal number of male and female $Sp^d/+$ progeny from this cross (Table 2, ♂ = 71 to ♀ = 66; $\chi^2 = 0.18$, $df = 1$, $P = 0.67$). The expected segregation ratios of sex and Sp^d genotype, regardless of penetrance, is 1 +/+♂ to 1 +/+ ♀ to 1 $Sp^d/+$♂ to 1 $Sp^d/+$ ♀. The observed numbers of progeny were, respectively, 100 to 80 to 71 to 66. χ^2 analysis indicated a significant deviation from the expected values ($\chi^2 = 8.51$, $df = 3$,

TABLE 2

The Number of BC_1 Mice [F, ♀ $Sp^d/+$ (♀ $Sp^d/+B_6$ × ♂ +/+ *Mus spretus*) × ♂ +/+ B_6] Generated and Their Phenotypes and Genotypes as Determined by PCR Analysis of the Alleles of *Pax3*, Exons 1, 2, and 5

Phenotype	N	Genotype +/+	Genotype $Sp^d/+$
White belly spot present[a]	104	11	93
White belly spot absent	223	179	44
Total (unselected)	327	190	137
Expected[b]		163.5	163.5
Total (selected)[c]	317	180	137
Expected[d]		158.5	158.5

[a] The belly spots of BC_1 progeny varied from a large white spot to a clear tuft of white or gray hairs. Of the 11 +/+ mice with belly spots, 3 had definite spots, 8 had small tufts of white hair. 10 were males ($\chi^2 = 7.36$, $df = 1$, $P = 0.007$), and all were *a/a non-agouti* black ($\chi^2 = 11.00$, $df = 1$, $P = 0.0009$). Two $Sp^d/+$ mice did not have belly spots but had large cranial or dorsal white spots and were defined as penetrant for a spot.
[b] $\chi^2 = 8.59$, $df = 1$, $P = 0.0034$.
[c] The progeny from female 15 were removed from the analysis as she was probably +/+ rather than $Sp^d/+$. She produced no $Sp^d/+$ progeny and ½ of her progeny were homozygous for normal *Pax3* exons 1 and 5, alleles of *Mus musculus*.
[d] $\chi^2 = 5.83$, $df = 1$, $P = 0.0158$.

TABLE 3

The Phenotypes Segregating among Highly Inbred C57BL/6J Mice from Crosses between Mice with White Spots ($Sp^d/+$) and Mice without White Spots (+/+)

Phenotype	O[a]	E
Males with white belly spots	61	58
Females with white belly spots	53	58
Males without white belly spots	60	58
Females without white belly spots	58	58
Totals	232	232

[a] O, Observed; E, Expected; $\chi^2 = 0.57$, $df = 3$, $P = 0.90$.

FIG. 1. Two BC_1 mice [F_1 ♀ *Sp*^{d}/+ (♀ *Sp*^{d}/+ B_6 *Mus musculus* × ♂ +/+ *Mus spretus*) × ♂ +/+ B_6 *Mus musculus*]. (A) A +/+;*A*/*a* mouse illustrating normal craniofacial features. (B) An *Sp*^{d}/+;*A*/*a* mouse illustrating craniofacial anomalies and hypopigmentation.

$P = 0.037$, $\alpha = 0.05$). Two of the four classes of progeny contributed to this χ^2: there are too many +/+ ♂ and too few *Sp*^{d}/+ ♀ progeny.

There is also a nonrandom association between the sex of these progeny and the presence or absence of a white belly spot in *Sp*^{d}/+ mice (♂ with spots = 55 to ♀ with spots = 38 to ♂ without spots = 16 to ♀ without spots = 28; contingency $\chi^2 = 6.21$, $df = 1$, $P = 0.013$, $\alpha = 0.05/2 = 0.025$). There are too few *Sp*^{d}/+ nonpenetrant males and too many *Sp*^{d}/+ nonpenetrant females. There are also more nonpenetrant *Agouti* mice than *non-agouti* mice (31 NP *A*/*a*: 13 NP *a*/*a*; $\chi^2 = 7.36$, $df = 1$, $P = 0.007$, $\alpha = 0.05/3 = 0.017$), with roughly an equal number of penetrant *Agouti* and *non-agouti* mice (50 P *A*/*a*: 43 P *a*/*a*; $\chi^2 = 0.53$, $df = 1$, $P = 0.47$). In addition, of the 11 +/+ mice exhibiting white belly spots (Table 2), 10 are males ($\chi^2 = 7.36$, $df = 1$, $P = 0.007$, $\alpha = 0.05$) and all are *a*/*a*, *non-agouti* black ($\chi^2 = 11.00$, $df = 1$, $P = 0.0009$, $\alpha = 0.05/2 = 0.025$). Because of this nonrandom association between the presence of a white belly spot, the sex of the mouse, and the *Agouti* locus, we examined segregation data for the *A*-locus among BC_1 mice.

BC_1 mice were expected to be $\frac{1}{2}$ *A*/*a* and $\frac{1}{2}$ *a*/*a* regardless of the *Sp*^{d} genotype. With 185 *A*/*a* and 132 *a*/*a* progeny, there is a 16.5% deficiency of *a*/*a* progeny ($\chi^2 = 8.86$, $df = 1$, $P = 0.003$, $\alpha = 0.05$). BC_1 mice were also expected to be $\frac{1}{4}$ +/+;*A*/*a*, $\frac{1}{4}$ +/+;*a*/*a*, $\frac{1}{4}$ *Sp*^{d}/+;*A*/*a*, and $\frac{1}{4}$ *Sp*^{d}/+;*a*/*a*. The observed numbers were, respectively, 106, 74, 79, and 58. A χ^2 analysis indicates a significant deviation from the expected values ($\chi^2 = 15.07$, $df = 3$, $P = 0.002$, $\alpha = 0.05$). There is a significant deficiency of *Sp*^{d}/+;*a*/*a* mice and a significant excess of all +/+;*A*/*a* mice. Thus, with respect to the viability of BC_1 progeny, *Sp*^{d} and the *a* allele or a gene closely linked to the *A*-locus play a role in the reduction of viability.

Analysis of Skull Shape

Measurement error. The extent of measurement errors following mounting and digitization of a skull image was evaluated. The images of three representative skulls were captured, stored, and evaluated for the eight landmarks (Fig. 2B). The X_i, Y_i coordinates for each of the eight landmarks found on each of three skulls were digitized 10 separate times from the same skull video image. A FORTRAN program (SKULL, available on request) converts absolute X_i, Y_i coordinates into relative shape coordinates using the algorithm described by Bookstein (1991). As defined in this analysis, the program normalizes the shape coordinate measurements relative to the distance between landmarks 1 and 5, which defines the length of the midsagittal suture of the interfrontal bone. In this case, landmarks 1 and 5 (Fig. 2B) were selected as the baseline and, by division of the absolute value of the distance between landmarks 1 and 5, gave the relative shape coordinate designations of X_1, $Y_1 = (1,0)$ and X_5, $Y_5 = (0,0)$, respectively. All shape coordinates were thus normalized to this baseline measurement, which eliminates differences in absolute sizes of the skulls. Absolute landmark coordinates were captured, transferred to a Microsoft Excel file, and then converted to relative shape coordinates by SKULL. For three different skull images digitized 10 times each, the average coefficient of variation with its standard deviation for the six landmarks (2, 3, 4, 6, 7, and 8) each with two coordinates is 0.012 ± 0.006 for ♀ 245, 0.008 ± 0.003 for ♀ 248, and 0.010 ± 0.004 for ♀ 251. The same three skulls were mounted, the images captured, and landmark coordinates digitized 10 separate times. The average coefficient of variation with its standard deviation for the 6 landmarks each with two coordinates was 0.020 ± 0.005 for ♀ 245, 0.013 ± 0.006 for ♀ 248, and 0.009 ± 0.004 for ♀ 251. A comparison of these two sets of coefficients of variation indicated that the error associated with mounting each skull was less than the error associated with digitizing each landmark. The combined errors were between 0.9 and 2.0% of the value of the relative shape coordinate and did not mask the variation observed between skulls.

Evaluation of symmetry. Skulls from seven groups of mice were examined: +/+ B_6 (4), *Sp*^{d}/+ B_6 (2), +/+ SPR (30), +/+ F_1 (17), *Sp*^{d}/+ F_1 (8), +/+ BC_1 (180), and *Sp*^{d}/+ BC_1 (126). Using Student t tests, the coordinates of the left and right sides of the skulls were compared to determine if there were any skull asymmetries within a given group (data not shown). For each group, the null hypothesis was $X_2 = X_8$, $|Y_2| = Y_8$, $X_3 = X_7$, $|Y_3| = Y_7$, $X_4 = X_6$ and $|Y_4| = Y_6$. These initial analyses required 42 different t tests (seven groups × three pairs of landmarks × two coordinate values X_i and Y_i). To maintain an overall probability of $\alpha = 0.05$ for 42 related comparisons, an individual comparison needed to be significant at $P = 0.001$ (Nater and Wasserman, 1974; Anderson and Sclove, 1986). No left/right t tests involving X_i or Y_i were found to be significant at $P \leq 0.001$. No comparisons of symmetry were made between any of the seven groups. There were only six individual comparisons made within each group that could be argued as possibly dependent. Thus, $\alpha = 0.05/6 = 0.008$ was chosen as the significance level for these evaluations of symmetry. At this level of significance,

TABLE 4

Mean Coordinates (X_i, Y_i) for Landmarks (i = 6, 7, and 8) for the Left Side of Mouse Skulls Comparing *Mus musculus* C57BL/6J (B_6), *Mus spretus* (SPR), F_1, and BC_1 with the Slope (b_i) of the Regression Line Passing through the Landmark (X_i, Y_i), the Standard Deviations ($\hat{s}$), and the t Tests Comparing Individual Means and Slopes

n	Comparison	S	X_6	Y_6	b_6	X_7	Y_7	b_7	X_8	Y_8	b_8
4	B_6 +/+	$\bar{x}$	0.473	0.343	0.403	0.740	0.238	−1.138	0.949	0.335	−0.614
		$\hat{s}$	0.011	0.007	0.331	0.008	0.010	0.338	0.011	0.019	0.947
2	B_6 *Sp*^{d}/+	$\bar{x}$	0.447	0.368	0.522	0.748	0.256	−1.066	0.974	0.364	−1.800
		$\hat{s}$	0.071	0.025	NS	0.011	0.011	NS	0.014	0.025	NS
30	SPR +/+	$\bar{x}$	0.437	0.299	−0.046	0.691	0.231	−0.011	1.000	0.380	0.188
		$\hat{s}$	0.029	0.020	0.128	0.036	0.015	0.080	0.032	0.017	0.095
17	F_1 +/+	$\bar{x}$	0.417	0.285	−0.836[a]	0.673	0.212	−0.095	0.940	0.316	0.079
		$\hat{s}$	0.028	0.036	0.246	0.038	0.015	0.097	0.026	0.013	0.123
8	F_1 *Sp*^{d}/+	$\bar{x}$	0.409	0.298	−0.734	0.671	0.218	−0.145	0.955	0.327	0.065
		$\hat{s}$	0.030	0.040	0.451	0.036	0.015	0.152	0.017	0.012	0.292
180	BC_1 +/+	$\bar{x}$	0.426	0.327	−0.205	0.695	0.237	−0.199[b]	0.937	0.332	0.419[c]
		$\hat{s}$	0.049	0.054	0.080	0.061	0.031	0.034	0.058	0.041	0.043
126	BC_1 *Sp*^{d}/+	$\bar{x}$	0.426	0.336	−0.657[d]	0.697	0.243	−0.041	0.967	0.340	0.274[e]
		$\hat{s}$	0.045	0.049	0.077	0.036	0.029	0.073	0.033	0.036	0.095
B_6 (+/+ vs *Sp*^{d}/+)		t_c	0.817	2.078		1.044	2.026		2.442	1.621	
		P_t	0.460	0.106		0.355	0.113		0.071	0.180	
F_1 (+/+ vs *Sp*^{d}/+)		t_c	0.110	0.089		0.024	0.114		0.229	0.227	
		P_{23}	0.913	0.930		0.981	0.910		0.821	0.822	
B_6 vs SPR		t_c	2.065	6.135		3.460	2.034		3.198	4.587	
		P_{34}	0.047	5.8E-7		0.001	0.050		0.003	5.9E-5	
B_6 vs F_1		t_c	3.795	4.161		4.621	4.763		1.283	4.046	
		P_{25}	0.0007	0.0003		7.3E-5	4.9E-5		0.210	0.0004	
F_1 vs SPR		t_c	2.917	0.793		1.897	4.245		7.195	14.785	
		P_{45}	0.005	0.432		0.063	8.8E-5		2.2E-9	1.9E-20	
BC_1 (+/+ vs *Sp*^{d}/+)		t_c	0.000	1.490		0.330	1.711		5.241	1.765	
		P_{26}	1.000	0.137		0.742	0.088		3.0E-7	0.079	
		t_c			4.071			1.962			1.391
		P_{36}			6.0E-5			0.051			0.165

Note. n, sample size. S, statistics, including the mean ($\bar{x}$) and the standard deviation ($\hat{s}$). t_c, calculated t value comparing the means of the indicated group. P_t, probability of observing the t value that large or larger by chance alone with X, degrees of freedom. For X_i or Y_i of a given group comparison to be considered significant, $P \leq 0.008$ (0.05/6). For b_i within a given group or between two groups to be considered significant, $P \leq 0.017$ (0.05/3). b Values and t values meeting this criterion are in boldface. NS, standard deviation of the slope does not exist.

[a] The slope of the regression line through landmark 6 is significantly different from zero with $t_c = 3.390$, $df = 15$, $P = 0.004$.
[b] The slope of the regression line through landmark 7 is significantly different from zero with $t_c = 5.686$, $df = 178$, $P = 5.24 \times 10^{-8}$.
[c] The slope of the regression line through landmark 8 is significantly different from zero with $t_c = 9.744$, $df = 124$, $P = 5.28 \times 10^{-17}$.
[d] The slope of the regression line through landmark 6 is significantly different from zero with $t_c = 8.532$, $df = 124$, $P = 4.25 \times 10^{-14}$.
[e] The slope of the regression line through landmark 8 is significantly different from zero with $t_c = 2.884$, $df = 124$, $P = 0.0046$.

there was a single difference noted. For +/+ *Mus spretus*, $|Y_4| > Y_6$. This was a 5.4% increase in the skull half width. Because 41 of the 42 comparisons indicated that skull landmarks were symmetric, further analyses were restricted to the left side of the skull (Table 4).

Displacements of skull landmarks. The null hypotheses for these comparisons were +/+ X_6 = *Sp*^{d}/+ X_6 and +/+ Y_6 = *Sp*^{d}/+ Y_6 and were similar for landmarks 7 and 8. As six comparisons were made between pairs of groups, $\alpha = 0.008$ was chosen as the level of significance. In B_6 mice, there are no differences in the locations of skull landmarks caused by *Sp*^{d} (Table 4). This is also true on the F_1 genetic background (Table 4). Among BC_1 skulls, *Sp*^{d} causes landmark 8 to be displaced 3.2% anteriorly (Table 4).

Some mouse skull landmarks for B_6, SPR, F_1, and BC_1 differ significantly in their location (Table 4). As a consequence of the displacements of these landmarks, the relative size and shapes of the interfrontal bones differ significantly. From these measurement differences, the size and shape of the interfrontal bone is controlled by genes with a number of different modes of inheritance. The relative lengths of the left interfrontal bones (X_8–X_6) were compared with $\alpha = 0.05/10 = 0.005$. The order of the group means with equivalent means underscored is

$$\underline{B_6\ BC_1\ +/+\ F_1\ BC_1\ Sp^d/+}\ \underline{\text{SPR}}$$

The ranking of the above means indicates that genes that cause the interfrontal bone to be short are dominant ($P < 0.005$). For the F_1–SPR comparison, P =

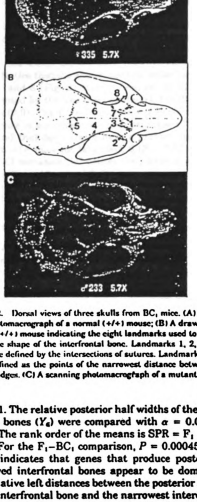

FIG. 2. Dorsal views of three skulls from BC_1 mice. (A) A scanning photomacrograph of a normal (+/+) mouse; (B) A drawing of a normal (+/+) mouse indicating the eight landmarks used to characterize the shape of the interfrontal bone. Landmarks 1, 2, 4, 5, 6, and 8 are defined by the intersections of sutures. Landmarks 3 and 7 are defined as the points of the narrowest distance between the orbital ridges. (C) A scanning photomacrograph of a mutant (Sp^4/+) mouse.

0.00051. The relative posterior half widths of the interfrontal bones (Y_2) were compared with $\alpha = 0.05/6 = 0.008$. The rank order of the means is SPR = F_1 < BC_1 = B_6. For the F_1–BC_1 comparison, $P = 0.00045$. This result indicates that genes that produce posteriorly narrowed interfrontal bones appear to be dominant. The relative left distances between the posterior aspect of the interfrontal bone and the narrowest interorbital distances (X_7–X_8) were compared with $\alpha = 0.05/6 = 0.008$. A single comparison was found to be significantly different: $BC_1 < B_6$ ($P = 0.00021$). The relative interorbital half widths (Y_7) were compared with $\alpha = 0.05/6 = 0.008$. The rank order of means is F_1 < SPR = BC_1 = B_6. For the F_1–SPR comparison, $P = 8.84 \times 10^{-4}$. These results indicate that the interorbital half width exhibits negative heterosis. Finally, the relative anterior half widths of the interfrontal bones (Y_8) were compared with $\alpha = 0.05/6 = 0.008$. The rank order of means is F_1 = BC_1 = B_6 < SPR. For the B_6–SPR comparison, $P = 5.86 \times 10^{-5}$. This result indicates that narrow anterior half width interfrontal bones are inherited as a dominant trait.

Morphometric variability. The above analysis indicates that craniofacial morphology of mouse skulls is influenced by genes that control the location of given landmarks. Craniofacial morphology is also influenced by genes that may independently control the variability of the location of a given landmark without changing the average location of the landmark. To evaluate this aspect of the craniofacial variability, the slope (b_i) of the linear regression line through a given mean landmark location (X_i, Y_i) was determined (Table 4). The null hypothesis was $b_i = 0$ for a given landmark. For each group (B_6, SPR, F_1, BC_1 +/+, and BC_1 Sp^4/+), there were three slopes tested and as a consequence, $\alpha = 0.05/3 = 0.017$. With the exception of a single landmark (F_1 +/+ X_4, Y_4), all slopes for B_6, SPR, and F_1 Sp^4/+ were not significantly different from zero (Table 4). As B_6 and SPR are highly inbred strains and as the Sp^4 mutation occurred spontaneously on the B_6 strain, B_6 mice with a given *Pax3* genotype (Sp^4/+ or +/+) should lack genetic variability. Since Sp^4/+-containing litters were stored as frozen embryos following nine generations of backcrossing to B_6 to minimize the accumulation of newly arising mutations linked or unlinked to Sp^4, Sp^4/+ and +/+ mice should differ at very few other loci. The significant slope of the regression line through landmark 6 of +/+ F_1 mice cannot be explained by segregating genes.

F_1 mice should have identical genotypes at all autosomal loci. F_1 males should be identical genetically and physiologically with a SPR Y chromosome and a B_6 X chromosome. F_1 females should be identical genetically with a SPR X chromosome and a B_6 X chromosome. However, it may be possible that the significant regression slope at landmark 6 of F_1 mice could be related to X chromosome inactivation. If F_1 mice are pooled into males and females regardless of genotype (Table 4), we note that the regression line through landmark 6 has a slope significantly different from zero in females ($b_6 = -0.773 \pm 0.199$, $t_c = 3.884$, $df = 15$, $P = 0.0014$, $\alpha = 0.05/6 = 0.008$) and a slope not significantly different from zero in males ($b_6 = 0.217 \pm 0.461$, $t_c = 0.470$, $df = 6$, $P = 0.655$).

BC_1 mice are segregating *M. musculus* and *M. spretus* alleles at all loci including *Pax3*. The slopes for all three landmarks in BC_1 mice show significant differences from zero (Table 4). Paired comparisons between slopes using t tests indicated that for two of these landmarks (6 and 7) the slopes are significantly different between +/+ and Sp^4/+ (Table 4), again using $\alpha = 0.017$. The slopes at landmark 6 indicate that BC_1 Sp^4/+ mice have both broader and narrower posterior interfrontal bone width compared to their +/+ siblings. The slopes at landmark 7 indicate that BC_1 +/+ mice have both broader and narrower interorbital widths compared to their Sp^4/+ siblings. Finally, the slopes at landmark 8 are roughly equivalent for BC_1 +/+ and Sp^4/+ siblings, indicating that the anterior interfrontal measurements are influenced by the genetic background in the BC_1 mice but are not influenced by Sp^4.

Thus, Sp^4 increases the range of variability observed in craniofacial measurements in a systematic manner. $Sp^4/+$ mice can have very narrow as well as very broad interfrontal bones. The shape of the interfrontal bone depends upon the interaction between Sp^4 and the genetic background.

To illustrate, Figs. 3A and 3B present plots of the relative shape coordinates for all +/+ and $Sp^4/+$ BC_1 mouse skulls, respectively. The shape coordinates are normalized using the distance between landmarks 1 and 5. Notice that the shape coordinates for landmarks 2, 4, 6, and 8 (Fig. 2) diverge from the skull midline represented by the line from landmark 1 (1,0) to landmark 5 (0,0). The t tests in Table 4 indicate that this divergence is significant for each genotype ($P < 0.017 = \alpha$) and that $Sp^4/+$ mice have a greater divergence than do +/+ mice for landmark 6 ($P = 5.57 \times 10^{-5}$). The *Pax3* mutation Sp^4 causes the posterior aspect of the interfrontal bones of $Sp^4/+$ mice to be significantly wider and narrower than that of +/+ mice (Table 4 and Fig. 2C).

Selection of Animals with Skull Shape Extremes

To determine if the genes controlling the average location and variability of a given landmark are the same for all landmarks, a subset of selected skulls were plotted. Using the coordinates of landmark 6 (Fig. 3 and Table 4), 10 animals of each genotype with either the widest or the narrowest skulls were selected (6th and 8th percentiles, respectively, Figs. 3A and 3B). The coordinates of these animals appear in Figs. 3C and 3D. Note that animals selected in this manner produce, as expected, two separate nonoverlapping clusters of points for landmarks 4 and 6 but produce a single cluster of overlapping points for landmarks 2 and 8. On the other hand, when 10 animals are chosen from the extremes of the distributions for landmark 8, two separate nonoverlapping clusters are observed for landmarks 2 and 8 and a single cluster is observed for landmarks 4 and 6 (Figs. 3E and 3F). The animals that exhibited the extreme values for landmarks 4 and 6 were not the same animals that exhibited the extreme values for landmarks 2 and 8. These observations suggest that the location, and variability of the location of these two pairs of landmarks, 2/8 and 4/6, and thus the anterior and posterior width of the head, are under independent genetic controls.

If the sexes of the animals chosen because of their extreme position within the distribution are pooled across genotypes, there is a significant excess of males among mice with the narrowest faces with respect to landmark 6 (the lower 6th and 8th percentiles for +/+ and $Sp^4/+$, respectively). There are 17 males and 3 females ($\chi^2 = 9.80$, $df = 1$, $P = 0.002$). There are equal numbers of males and females among mice with the widest faces with respect to landmark 6 (the upper 6th and 8th percentiles for +/+ and $Sp^4/+$, respectively). There are 12 males and 8 females ($\chi^2 = 0.80$, $df = 1$, $P = 0.371$). On the other hand, if the sexes of animals chosen from the extremes of the distributions for landmark 8 are pooled, the numbers of males and females are not significantly different, with 13 males and 7 females with the narrowest faces and 7 males and 13 females with the widest faces. These observations suggest that one of the genes controlling the posterior shape of the skull is X-linked or sex-influenced, while the genes controlling the anterior shape of the skull are autosomal.

To see if the distortion in sex ratio would persist with an increase in the number of selected skulls, 10 additional skulls were chosen from the extremes of the distributions of each genotype. A summary of the phenotypic characteristics of the selected animals appears in Table 5. With respect to +/+ mice, there are more males than females with narrow skulls regardless of the selected landmark (Table 5). With respect to $Sp^4/+$ mice, there are many more males than females with narrow skulls at landmark 6. Following independent selection at landmarks 7 and 8, there are an equal number of males and females with narrow skulls. Thus, mice with narrow skulls have different sex ratios depending on the landmark selected and the *Pax3* genotype.

Unselected mice have a significant distortion in the transmission ratio with respect to the *A*-locus. A contingency χ^2 analysis indicates that mice with narrow skulls have the same segregation ratios regardless of the landmark selected (Table 5). In addition, the pooled ratio is not significantly different from the distorted transmission ratio seen in unselected mice. Thus, the *A*-locus or a gene closely linked to it does not appear to influence the shape of the skull for the narrowest of these skulls.

Mice with the most narrow skulls do not exhibit the same degree of penetrance of the white belly spot depending upon the landmark selected. Penetrance is high in mice selected for narrow skulls at landmark 6 and lower in mice selected for narrow skulls at landmarks 7 and 8 (Table 5).

Comparisons of the skull landmarks, sex ratio, *A*-locus segregation ratios, and penetrance yields quite different results when considering mice selected for very wide skulls. First, the sex ratios among mice with the widest skulls are not different from each other and are not different from 1:1, contrary to what is observed for mice with very narrow skulls (Table 5). Second, transmission ratio distortions for the *A*-locus among mice with the widest skulls do not differ with respect to the selected landmarks but these distorted ratios are different from the transmission ratio distortion seen in the unselected data set (Table 5). Finally, penetrance of the white belly spot is not different in mice with wide skulls regardless of the landmark selected, contrary to what is observed in mice with very narrow skulls (Table 5). Penetrance among the selected mice is not different from the penetrance in the unselected data set.

In addition to the segregation analysis performed on

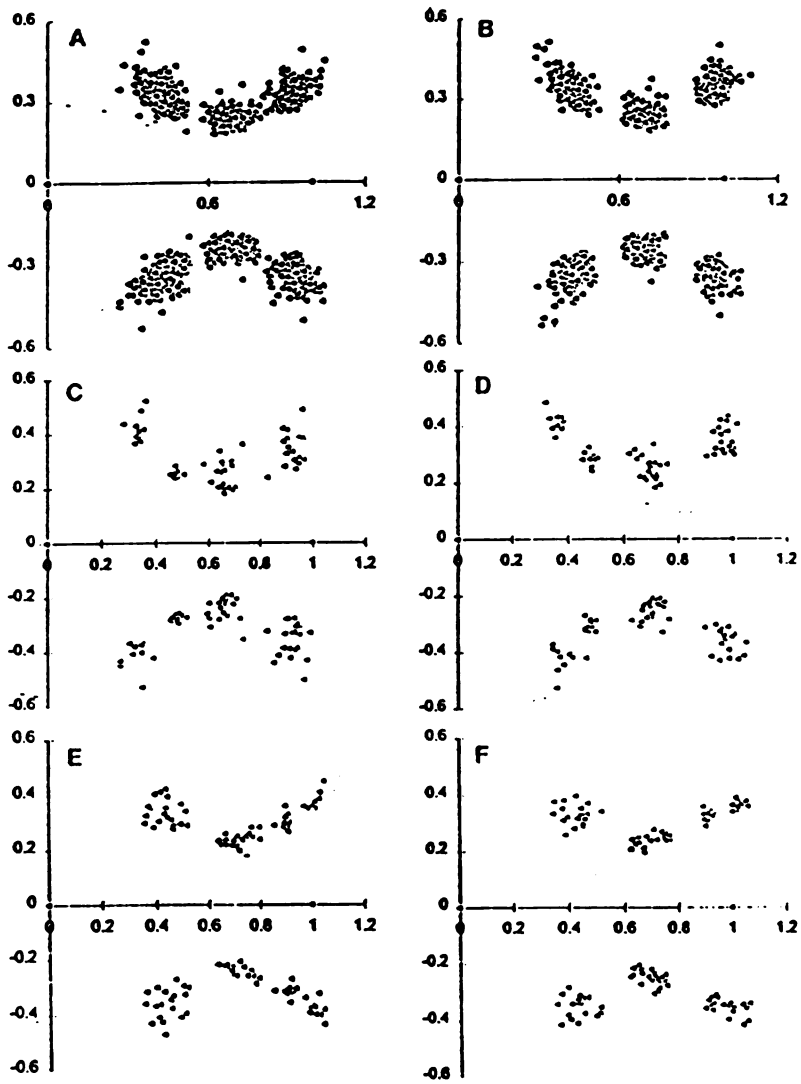

FIG. 3. The distribution of shape coordinates for landmarks 2, 3, 4, 6, 7, and 8 from BC_1 mouse skulls as illustrated in Fig. 2. (A) The distribution of shape coordinate landmarks for 180 +/+ mice. (B) The distribution of shape coordinate landmarks for 126 Sp^4/+ mice. (C) The distribution of shape coordinate landmarks for 20 +/+ mice selected because they are from the two extremes of the distribution in A (upper and lower 6th percentile). Selection was based on landmark 6. (D) The distribution of shape coordinate landmarks for 20 Sp^4/+ mice selected because they are from the two extremes of the distribution in B (upper and lower 8th percentile). Selection was based on landmark 6. (E) The distribution of shape coordinate landmarks for 20 +/+ mice selected because they are from the two extremes of the distribution in A (upper and lower 6th percentile). Selection was based on landmark 8. (F) The distribution of shape coordinate landmarks for 20 Sp^4/+ mice selected because they are from the two extremes of the distribution in B (upper and lower 8th percentile). Selection was based on landmark 8.

these selected mice (Table 5), the analysis of the location and variation of the location for landmarks for each selected group is presented in Table 6. Sp^4/+ mice with narrow skulls, with regards to landmarks 6 and 8, have broader skulls than +/+ mice selected for narrow skulls (Table 6). On the other hand, mice selected for the widest skulls do not differ in landmark location regardless of genotype or landmark of selection (Table 6). Thus, the structure of the mouse face is controlled in part by the interaction of Sp^4 with a number of different

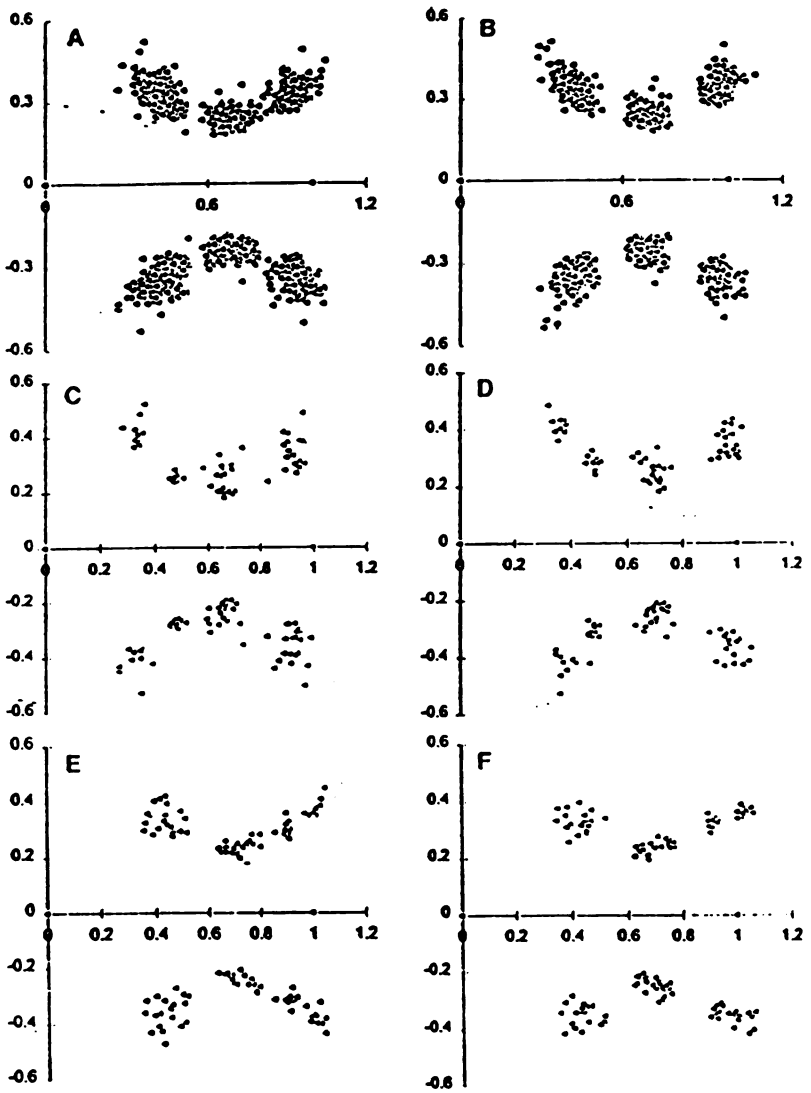

FIG. 3. The distribution of shape coordinates for landmarks 2, 3, 4, 6, 7, and 8 from BC_1 mouse skulls as illustrated in Fig. 2. (A) The distribution of shape coordinate landmarks for 180 +/+ mice. (B) The distribution of shape coordinate landmarks for 126 Sp^4/+ mice. (C) The distribution of shape coordinate landmarks for 20 +/+ mice selected because they are from the two extremes of the distribution in A (upper and lower 6th percentile). Selection was based on landmark 6. (D) The distribution of shape coordinate landmarks for 20 Sp^4/+ mice selected because they are from the two extremes of the distribution in B (upper and lower 8th percentile). Selection was based on landmark 6. (E) The distribution of shape coordinate landmarks for 20 +/+ mice selected because they are from the two extremes of the distribution in A (upper and lower 6th percentile). Selection was based on landmark 8. (F) The distribution of shape coordinate landmarks for 20 Sp^4/+ mice selected because they are from the two extremes of the distribution in B (upper and lower 8th percentile). Selection was based on landmark 8.

these selected mice (Table 5), the analysis of the location and variation of the location for landmarks for each selected group is presented in Table 6. Sp^4/+ mice with narrow skulls, with regards to landmarks 6 and 8, have broader skulls than +/+ mice selected for narrow skulls (Table 6). On the other hand, mice selected for the widest skulls do not differ in landmark location regardless of genotype or landmark of selection (Table 6). Thus, the structure of the mouse face is controlled in part by the interaction of Sp^4 with a number of different

TABLE 5

The Sex, Genotype, and Penetrance of White Belly Spot for 20 Animals Selected from the Extremes (Narrowest or Widest) of the Skull Measurements

		Narrowest						Widest					
L[a]	G	♂	♀	*Aa*	*aa*	P	NP	♂	♀	*Aa*	*aa*	P	NP
6	+/+	15	5	7	13	—	—	8	12	13	7	—	—
	Sp[4]/+	17	3	15	5	16	4	9	11	16	4	14	6
7	+/+	14	6	10	10	—	—	11	9	15	5	—	—
	Sp[4]/+	13	7	10	10	10	10	9	11	15	5	13	7
8	+/+	13	7	14	6	—	—	11	9	15	5	—	—
	Sp[4]/+	9	11	9	11	8	12	12	8	17	3	15	5
χ^2	+/+	0.48[b]		2.04		—		1.20		0.66		—	
χ^2	*Sp*[4]/+	7.03[c]		4.21		7.06[d]		1.20		0.63		0.48[e]	
χ^2	Pooled			9.43[f]				0.00		2.41[g]			

[a] L, landmark; G, *Pax3* genotype; *A/a*, *Agouti*; *a/a*, *non-agouti*; P, penetrant for a white belly spot; NP, not penetrant for a white belly spot; χ^2 for +/+ or *Sp*[4]/+ is a contingency χ^2 with $df = 2$; χ^2 for the pooled samples is a contingency χ^2 with five degrees of freedom.

[b] The sex ratios among the +/+ mice with narrow skulls and landmarks 6, 7, and 8 are not different but are significantly different from the expected 1:1 ratio (♂/♀ = 42/18, $\chi^2 = 9.60$, $df = 1$, $P = 0.002$, $\alpha = 0.05/2$). There are significantly more +/+ males with narrow skulls than there are females with narrow skulls.

[c] The sex ratios among the selected *Sp*[4]/+ mice with narrow skulls are not equivalent ($P = 0.03$, $\alpha = 0.05$). With respect to landmark 6, there are more *Sp*[4]/+ males with narrow skulls (♂/♀ = 17/3, $\chi^2 = 9.8$, $df = 1$, $P = 0.0018$, $\alpha = 0.05/3 = 0.017$). With respect to *Sp*[4]/+ mice with narrow skulls at landmarks 7 and 8, the sex ratios do not differ.

[d] The penetrance of the white belly spot differs between the landmarks of narrow skulls ($P = 0.03$, $\alpha = 0.05$). *Sp*[4]/+ mice with narrow skulls at landmark 6 have greater penetrance than animals with narrow skulls at landmarks 7 and 8.

[e] The penetrance of the white belly spot among mice with wide skulls does not differ with respect to landmarks. This penetrance (P/NP = 42/18) is not different from the penetrance in the unselected data set (P/NP = 93/44, contingency $\chi^2 = 0.09$, $df = 1$, $P = 0.771$).

[f] The transmission ratios of *Aa/aa* among selected samples do not differ ($df = 5$, $P = 0.09$) and the pooled ratio (*Aa/aa* = 65/55) is not significantly different from the distorted transmission ratio seen in the unselected sample (*Aa/aa* = 192/125; contingency $\chi^2 = 1.47$, $df = 1$, $P = 0.22$).

[g] The *A/a* transmission ratios are not different in mice with wide skulls ($df = 5$, $P = 0.79$) but the distortion in the pooled transmission ratios of the selected samples (*Aa/aa* = 91/29) is different from the *A/a* transmission distortion in the unselected sample ($\chi^2 = 8.89$, $df = 1$, $P = 0.003$, $\alpha = 0.05/4 = 0.0125$). There is a higher number of *Aa* among mice with wide skulls.

genetic elements. By performing genome-wide disequilibrium mapping using animals from the extremes of these distributions, the chromosomal regions containing the genes that interact with *Sp*[4] controlling the shape of the face should be identified.

Genetic Models for Waardenburg Syndromes

Currently, *PAX3*, *MITF*, and *EDNRB*, when mutated, are capable of causing Waardenburg syndrome (Foy *et al.*, 1990; Asher *et al.*, 1991; Hughes *et al.*, 1994; Tassabehji *et al.*, 1994; Puffenberger *et al.*, 1994). There are over 50 *PAX3* mutations that cause Waardenburg syndrome type 1 (Farrer *et al.*, 1994; Read, 1995) and all cause dystopia canthorum, a craniofacial anomaly. Only three of these mutations segregating in WS families have penetrance for deafness between 75 and 100% (Baldwin *et al.*, 1992; Morell *et al.*, 1992, 1993). Craniofacial deafness hand Syndrome, *CDHS*, is also caused by a *PAX3* mutation (Asher *et al.*, 1996). In an admittedly small family, this mutation is fully penetrant for both deafness and craniofacial abnormalities. *CDHS* shares many characteristics with WS3, including profound deafness and skeletal anomalies, yet they are clinically distinct (Asher *et al.*, 1996; Goodman *et al.*, 1982; Sommer *et al.*, 1983; Klein, 1983; Sheffer and Zlotogora, 1992). The phenotypic similarities and high levels of penetrance of WS3 and *CDHS* might be explained by the molecular nature of their *PAX3* mutations.

Mutant alleles of *MITF* cosegregate with some instances of Waardenburg syndrome type 2 (WS2). Three *MITF* mutations have been characterized (Tassabehji *et al.*, 1994; Morell *et al.*, unpublished results). As with *PAX3* mutations, the molecular defects caused by *MITF* mutations alone are not sufficient to account for the phenotypic variability observed in WS2 families. The phenotypic variability observed both within and between families with Waardenburg syndromes can be explained by at least three different but not mutually exclusive genetic models: (1) different mutant alleles at a single locus, (2) mutant alleles at more than one locus affecting the same developmental processes, and (3) a single mutant allele at one locus interacting with modifying genes at other loci (Asher and Friedman, 1990).

Identifying Genes Interacting with Pax3

Mouse mutants have been used to help identify the causes of WS variability. Evidence presented here dem-

TABLE 6

Mean Coordinates (X_i, Y_i) for Landmarks (i = 6, 7, and 8) for the Left Side of Mouse Skulls Comparing BC_1 Mice with the 20 Most Extreme Measurements with the Slope (b_i) of the Regression Line Passing through the Landmark (X_i, Y_i), the Standard Deviations ($\hat{s}$), and the t-Tests (t_s) Comparing Individual Means and Slopes

n	Comparison	S	X_6	Y_6	b_6	X_7	Y_7	b_7	X_8	Y_8	b_8
20	N +/+	$\bar{x}$	0.462	0.256	0.060	0.670	0.195	0.073	0.909	0.277	−0.029
		$\hat{s}$	0.039	0.010	0.061	0.049	0.019	0.088	0.042	0.008	0.044
20	N Sp^4/+	$\bar{x}$	0.472	0.281	−0.115	0.704	0.207	−0.060	0.955	0.295	0.007
		$\hat{s}$	0.023	0.020	0.205	0.035	0.010	0.067	0.028	0.011	0.096
20	W +/+	$\bar{x}$	0.398	0.414	−0.183	0.732	0.292	0.181[a]	0.990	0.412	0.344[b]
		$\hat{s}$	0.061	0.035	0.128	0.125	0.033	0.045	0.129	0.053	0.054
20	W Sp^4/+	$\bar{x}$	0.373	0.419	−0.559[c]	0.692	0.294	−0.004	0.983	0.401	−0.127
		$\hat{s}$	0.044	0.042	0.177	0.047	0.027	0.133	0.042	0.030	0.166
N (+/+ vs Sp^4/+)		t_s	0.988	5.000		2.525	2.500		4.075	5.918	
		P_{2n}	0.330	1.3E-5		0.016	0.017		2.3E-4	7.4E-7	
W (+/+ vs Sp^4/+)		t_s	1.486	0.409		1.340	0.210		0.231	0.808	
		P_{2n}	0.145	0.685		0.188	0.835		0.819	0.424	
		t_s			1.721			0.342			2.698
		P_{2n}			0.093			0.734			0.010

Note. n, sample size. S, statistics, including the mean ($\bar{x}$), the standard deviation ($\hat{s}$), and calculated t (t_s). P_{2n}, the probability of observing a value of t_s that large or larger by chance alone with df = 38. For X_i or Y_i of a given group comparison to be considered significant, $P < 0.008$ (0.05/6). For b_i within a given group or between two groups to be considered significant, $P < 0.017$ (0.05/3). b Values and t values meeting this criterion are in boldface. N, the narrowest 20 BC_1 skulls of a particular genotype. W, the widest 20 BC_1 skulls of a particular genotype.

[a] The slope of the regression line passing through landmark 8 is significantly different from zero with t_s = 4.022, df = 18, P = 0.0006.

[b] The slope of the regression line passing through landmark 8 is significantly different from zero with t_s = 6.370, df = 18, $P = 5.33 \times 10^{-6}$.

[c] The slope of the regression line passing through landmark 6 is significantly different from zero with t_s = 3.159, df = 18, P = 0.0054.

onstrates that when Sp^4 (a *Pax3* mutation) is segregating on the highly inbred and coisogenic mouse strain B_6, heterozygotes have white belly spots but rarely exhibit dysmorphic features. On the other hand, when Sp^4 is segregating in a very diverse genetic background, i.e., in an interspecific BC_1 with *Mus musculus* and *Mus spretus* alleles, it is associated with phenotypic variability similar to that observed within large WS families.

Mice with craniofacial abnormalities and very broad interfrontal bones are heterozygous for Sp^4 and likely carry alleles for at least two other loci that interact with *Pax3* to influence skull shape. Wildtype +/+ BC_1 mice do not exhibit craniofacial abnormalities but can have broad interfrontal bones and are likely to carry the same alleles at other loci that interact with a *Pax3* mutant allele producing a very broad interfrontal bone. Because of the sex distribution (Table 5) among mice with extreme skull shapes and because of the sex-associated differences in regression slopes of the F_1, one of these loci is either sex-linked or sex-influenced. This locus appears to help control the posterior shape of the mouse interfrontal bone. A second locus appears to be autosomal and control the anterior shape of the interfrontal bone.

Extensive variability was observed with respect to white belly spots in these BC_1 mice. Approximately 32.1% of the BC_1 Sp^4/+ mice were nonpenetrant for a white belly spot. Sp^4/+ on the inbred C57BL/6J strain are 100% penetrant for a white belly spot. In addition, there is a significant nonrandom association between the sex of the mouse and the presence of a white spot. Male Sp^4/+ mice more frequently have white belly spots than do female Sp^4/+ mice. Thus, both skull shape and the presence of a white belly spot are in some way influenced by the sex of the mouse. Sp^4/+ mice with the narrowest heads and white belly spots are generally males. One simple explanation is the existence of an X-linked allele fixed in the C57BL/6J strain that modifies the effects of Sp^4/+ with respect to the production of a white belly spot and the shape of the mouse skull. Alternatively, these two effects may be controlled by two different X-linked loci. In addition to the influence of sex on the presence of white belly spots, mice with the a/a genotype are more frequently penetrant with respect to the white belly spot. The shape of the face of mice is also related to the *A*-locus. This effect may be directly influenced by the a allele or a gene closely linked to the a allele.

In addition to the phenotypic variability associated with craniofacial morphology and pigmentation, Sp^4 segregating in the BC_1 mice also reduces viability. This effect appears to be enhanced by the *A*-locus genotype as well as the sex of the BC_1 progeny. It has been demonstrated that there is distortion of the 1:1 transmission ratio when B_6 and *M. spretus* mice are used to make an interspecific backcross (Siracusa *et al.*, 1989, 1991). This distortion in transmission ratio involves genes on chromosomes 2 (containing the *A*-locus), 4, and 10 but does not involve chromosome 1 (containing

Pax3). The distortion of transmission ratios reported by Siracusa *et al.* (1989; *Aa/aa* = 77/40) is not different from the distortion reported here (*Aa/aa* = 185/132, contingency $\chi^2 = 1.98$, $df = 1$, $P = 0.16$). In both cases, the distortion of *A/a* transmission ratios is not different when considering males and females separately. Among BC_1 progeny, however, there is a significant deficiency of $Sp^4/+;a/a$ progeny. As chromosome 1 transmission ratio distortion has not been noted previously (Siracusa *et al.*, 1989, 1991), this suggests a unique interaction between Sp^4 and the *a* allele or a gene closely linked to the *A*-locus. This interaction might take place during embryonic development or following birth (Siracusa *et al.*, 1991). An analysis of our breeding data suggests that both are possible. Eighteen +/+ B_6 females produced 35 litters with an average litter size of 6.9 ± 2.3 pups/litter. Fifteen $Sp^4/+$ B_6 females produced 30 litters with an average litter size of 6.7 ± 2.5 pups/litter. These litter sizes do not differ ($t_c = 0.34$, $t_{29} = 2.41$, $P = 0.05$). For 15 $Sp^4/+$ BC_1 females producing 92 litters, the average litter size was 4.1 ± 2.3 pups/litter. BC_1 litters are significantly smaller than B_6 litters by nearly 3 pups/litter ($t_c = 6.13$, $t_{34} = 3.60$, $P = 0.001$). Although BC_1 mice are exceptionally vigorous and mature rapidly and females are very active breeders, their litters are smaller than B_6 litters. In addition, of the 381 pups born to BC_1 females, 28 died between birth and weaning. Thus, both *in utero* and neonatal losses could account for the decreased viability of $Sp^4/+$ progeny. Because allelic variation at the *A*-locus can cause widely disparate phenotypic effects including embryonic lethality, obesity, diabetes, and tumor formation (Bultman *et al.*, 1992), it is possible that the *M. musculus a* allele and Sp^4 might interact directly to lower the viability of $Sp^4/+$ embryos and/or neonates. This could happen through the action of these genes on the neural crest cells.

Genetic modifiers play a major role in the final determination of a phenotype. Coleman (1978) observed that two mouse mutants, *ob* and *db*, on the C57BL/6J genetic background caused obesity but not diabetes. On the C57BL/SK genetic background, these mutations caused both obesity and type II insulin-dependent diabetes. A murine *Apc* (adenomatous polyposis coli) mutant allele is virtually benign on the AKR genetic background but causes intestinal neoplasias on the C57BL/6J genetic background (Dietrich *et al.*, 1993). In a recent finding relevant to the determination of craniofacial and hand phenotypes of humans, Rutland *et al.* (1995) identified two sporadic mutations of fibroblast growth factor receptor 2 (*FGFR2*) in exon 7, T to C at nucleotide 1036 and G to A at nucleotide 1037, Cys342Arg and Cys342Tyr, respectively, that cause Pfeiffer syndrome (craniosynostosis with hand anomalies). In different families, these same two mutations cause Crouzon syndrome (craniosynostosis without hand anomalies). A possible explanation for this phenotypic heterogeneity is the segregation of modifier genes that interact with the *ob*, *db*, *Apc*, and *FGFR2* mutations (Reardon *et al.*, 1994; Rutland *et al.*, 1995). Lander and Schork (1994) reviewed the nature of complex phenotypes and outlined a number of strategies to identify these modifier genes. Pavan *et al.* (1995), using such a strategy, identified six loci that appeared to modify the expression of the *s/s* genotype with respect to white spotting.

We suggest that the phenotypic variability associated with Waardenburg syndrome requires a mutant allele at *PAX3*, *MITF*, or *EDNRB* interacting with other genes. Therefore, to understand the phenotypic variation associated with *PAX3* mutations, the genes interacting with *PAX3* must be identified and cloned and their functions determined. The Sp^4 interspecific backcross mouse model described here offers one opportunity for mapping and eventually cloning these modifier genes.

ACKNOWLEDGMENTS

We thank Darwin Dale, Computer Photografx, Lansing, MI, for the scanning photomacrographs of the mouse skulls and Marlene Cameron for the graphic art. We thank Dr. Dennis Gilliland and Ms. Lei Chen, Statistical Consulting Service, Department of Statistics and Probability, Michigan State University, for their advice. This project was supported in part by grants to J.H.A. and T.B.F. from the Deafness Research Foundation and Grant DC 01160-04 from the National Institute on Deafness and other Communication Disorders, National Institutes of Health. Dr. James H. Asher, Jr., the senior and communicating author on this article, died on May 13, 1996. He was our colleague and friend and will be sorely missed. This paper is dedicated to his memory.

REFERENCES

Aasvod, H. (1962). Waardenburg's syndrome. *Acta Ophthalmol.* 40: 622–628.

Ambani, L. M. (1983). Waardenburg and Hirschsprung Syndromes. *J. Pediatr.* 102: 802.

Anderson, T. W., and Sclove, S. L. (1986). "The Statistical Analysis of Data," 2nd ed., Scientific Press, Palo Alto, CA.

Arias, S. (1971). Genetic heterogeneity in the Waardenburg Syndrome. *Birth Defects Orig. Art. Ser.* 7: 87–101.

Arias, S. (1980). Waardenburg Syndrome—Two distinct types. *Am. J. Med. Genet.* 6: 99–100.

Asher, J. H., Jr., and Friedman, T. B. (1990). Mouse and hamster mutants as models for Waardenburg syndromes in humans. *J. Med. Genet.* 27: 618–626.

Asher, J. H., Jr., Morell, R., and Friedman, T. B. (1991). Waardenburg syndrome (WS): The analysis of a single family with a WSI mutation showing linkage to RFLP markers on Human chromosome 2q. *Am. J. Hum. Genet.* 48: 43–52.

Asher, J. H., Jr., Pierpont, [illegible] and Friedman, T. B. (1993). A Waardenburg syndrome type 2 (WS2) mutation not linked to PAX3. *Am. J. Hum. Genet.* 53(Suppl.): 1685. (Abstract)

Asher, J. H., Jr., Sommer, A., Morell, R., and Friedman, T. B. (1996). Missense mutation in the paired domain of *PAX3* causes Craniofacial-deafness-hand syndrome. *Hum. Mut.* 7: 30–35.

Baldwin, C. T., Hoth, C. F., Amos, J. A., da-Silva, E. O., and Milunsky, A. (1992). An exonic mutation in the HuP2 paired domain gene causes Waardenburg's syndrome. *Nature* 355: 637–638.

Bookstein, F. L. (1991). "Morphometric Tools for Landmark Data: Geometry and Biology," Cambridge Univ. Press, England.

Bultman, S. J., Michaud, E. J., and Woychik, R. P. (1992). Molecular characterization of the mouse agouti locus. *Cell* 71: 1195–1204.

Calinikos, J. (1963). Waardenburg's syndrome. *J. Laryngol. Otol.* 77: 59–62.

Coleman, D. L. (1978). Obese and diabetics: Two mutant genes causing diabetes-obesity syndromes in mice. *Diabetologia* 14: 141–148.

Davis, L. G., Dibner, M. D., and Battey, J. F. (1986). "Methods in Molecular Biology," Elsevier, New York.

Delleman, J. W., and Hageman, M. J. (1978). Ophthalmological findings in 34 patients with Waardenburg syndrome. *J. Pediatr. Ophthalmol. Strabis.* 15: 341–345.

Dickie, M. M. (1964). New splotch alleles in the mouse. *J. Hered.* 55: 97–101.

Dietrich, W. F., Lander, E. S., Smith, J. S., Moser, A. R., Gould, K. A., Luongo, C., Borenstein, N., and Dove, W. (1993). Genetic identification of *Mom-1*, a major modifier locus affecting *Min*-induced intestinal neoplasia in the mouse. *Cell* 75: 631–639.

DiGeorge, A. M., Olmsted, R. W., and Robinson, D. H. (1960). Waardenburg Syndrome. *J. Pediatr.* 57: 649–699.

Divekar, M. V. (1957). Waardenburg's syndrome. *J. All India Ophthalmol. Soc.* 5: 1–5.

Epstein, D. J., Vekemans, M., and Gros, P. (1991). Splotch (Sp^{2H}), a mutation affecting development of the mouse neural tube, shows a deletion within the paired homeodomain of *Pax-3*. *Cell* 67: 767–774.

Farrer, L. A., Grundfast, K. M., Amos, J., Arnos, K. S., Asher, J. H., Jr., Brighton, P., Diehl, S., Fex, J., Foy, C., Friedman, T. B., Greenberg, J., Hoth, C., Marazita, M., Milunsky, A., Morell, R., Nance, W., Newton, V., Ramesar, R., San Augustin, T. B., Skare, J., Stevens, C. A., Wagner, R. G., Wilcox, E. R., Winship, I., and Read, A. P. (1992). Waardenburg syndrome (WS) type I is caused by defects at multiple loci, one of which is near ALPP on chromosome 2: First report of the WS Consortium. *Am. J. Hum. Genet.* 50: 902–913.

Farrer, L. A., Arnos, K. S., Asher, J. H., Jr., Baldwin, C. T., Diehl, S. R., Friedman, T. B., Greenberg, J., Grundfast, K. M., Hoth, C., Lalwani, A. K., Landa, B., Leverton, K., Milunsky, A., Morell, R., Nance, W., Newton, V., Ramesar, R., Rao, V. S., Reynolds, J. E., San Agustin, T. B., Wilcox, E. R., Winship, I., and Read, A. P. (1994). Locus heterogeneity for Waardenburg syndrome is predictive of clinical subtypes. *Am. J. Hum. Genet.* 55: 728–737.

Foy, C., Newton, V., Wellesley, D., Harris, R., and Read, A. P. (1990). Assignment of the locus for Waardenburg syndrome type I to human chromosome 2q37 and possible homology to the splotch mouse. *Am. J. Hum. Genet.* 46: 1017–1023.

Goldberg, M. F. (1966). Waardenburg syndrome with fundus and other anomalies. *Arch. Ophthalmol.* 76: 797–810.

Goodman, R. M., Lewithal, I., Solomon, A., and Klein, D. (1982). Upper limb involvement in the Klein–Waardenburg Syndrome. *Am. J. Med. Genet.* 11: 425–433.

Hageman, M. J., and Delleman, J. W. (1977). Heterogeneity in Waardenburg Syndrome. *Am. J. Hum. Genet.* 29: 468–485.

Hoth, C. F., Milunsky, A., Lipsky, N., Sheffer, R., Clarren, S. K., and Baldwin, C. T. (1993). Mutations in the paired domain of the human *PAX3* gene cause Klein–Waardenburg syndrome (WS-III) as well as Waardenburg syndrome type I (WS-1). *Am. J. Hum. Genet.* 52: 455–462.

Hughes, A. E., Newton, V. E., Liu, X. Z. and Read, A. P. (1994). A gene for Waardenburg syndrome type 2 maps close to the human homologue of the microphthalmia gene at chromosome 3p12–p14.1. *Nature Genet.* 7: 509–512.

Klein, D. (1983). Historical background and evidence for dominant inheritance of the Klein–Waardenburg Syndrome (Type III). *Am. J. Med. Genet.* 14: 231–239.

Lander, E. S., and Schork, N. J. (1994). Genetic dissection of complex traits. *Science* 265: 2037–2040.

Leamy, L. (1974). Heritability of osteometric traits in a random bred population of mice. *J. Hered.* 65: 109–120.

Liu, X., Newton, V. E., and Read, A. P. (1995). Waardenburg syndrome type II: Phenotypic findings and diagnostic criteria. *Am. J. Med. Genet.* 55: 95–100.

Lyon, M., and Searle, A. B. (1989). "Genetic Variants and Strains of the Laboratory Mouse," 2nd ed., Oxford Univ. Press, NY.

Meijer, R., and Walker, J. C. (1964). Waardenburg's syndrome. *Plastic Reconstr. Surg.* 34: 363–367.

Meire, F., Standaert, L., DeLaey, J. J., and Zeng, L. H. (1987). Waardenburg syndrome, Hirschsprung megacolon, and Marcus Gunn Ptosis. *Am. J. Med. Genet.* 27: 683–687.

Morell, R., Friedman, T. B., Moeljopawiro, S., Hartono, Soewito, and Asher, J. H., Jr. (1992). A frameshift mutation in the HuP2 paired domain of the probable human homolog of murine *Pax3* is responsible for Waardenburg syndrome type 1 in an Indonesian family. *Hum. Mol. Genet.* 1: 243–247.

Morell, R., Friedman, T. B., and Asher, J. H., Jr. (1993). A plus-one frameshift mutation in PAX3 alters the entire deduced amino acid sequence of the paired box in a Waardenburg syndrome type 1 (WS1) family. *Hum. Mol. Genet.* 2: 1487–1488.

Nance, W. E., and McConnell, F. E. (1973). Status and prospects of research in hereditary deafness. *Adv. Hum. Genet.* 4: 173–250.

Nance, W. E., and Sweeney, A. (1975). Genetic factors in deafness of early life. *Oto. Clin. N. Am.* 8: 19–48.

Nater, J., and Wasserman, W. (1974). "Applied Linear Statistical Models: Regression, Analysis of Variance and Experimental Design," Richard D. Irwin, Inc., Homewood, IL.

Omenn, G. S., and McKusick, V. A. (1979). The association of Waardenburg syndrome and Hirschsprung megacolon. *Am. J. Med. Genet.* 3: 217–233.

Pantke, O. A., and Cohen, M. M. (1971). The Waardenburg syndrome. *Birth Defects: Orig. Art. Ser.* 7: 147–152.

Partington, M. W. (1964). Waardenburg's syndrome and heterochromia iridis in a deaf school population. *Can. Med. Assoc. J.* 90: 1008–1017.

Pasteris, N. G., Trask, B. J., Sheldon, S., and Gorski, J. L. (1993). Discordant phenotype of two overlapping deletions involving the PAX3 gene in chromosome 2q35. *Hum. Mol. Genet.* 2: 953–959.

Pavan, W. J., Mac, S., Cheng, M., and Tilghman, S. M. (1995). Quantitative trait loci that modify the severity of spotting in *piebald* mice. *Genome Res.* 5: 29–41.

Puffenberger, E. G., Hosoda, K., Washington, S. S., Nakao, K., deWit, D., Yanagisawa, M., and Chakravarti, A. (1994). A missense mutation of the endothelin B receptor gene in multigenic Hirschsprung's disease. *Cell* 79: 1257–1266.

Ray, D. K. (1961). Waardenburg's syndrome. *Br. J. Ophthalmol.* 45: 568–569.

Read, A. P. (1995). Pax genes—*Paired* feet in three camps. *Nature Genet.* 9: 333–334.

Reardon, W., Winter, R. M., Rutland, P., Pulleyn, L. J., Jones, B. M., and Malcolm, S. (1994). Mutations in the fibroblast growth factor 2 gene cause Crouzon syndrome. *Nature Genet.* 8: 98–103.

Reed, W. B., Stone, V. M., Boder, E., and Ziprokowski, L. (1967). Pigmentary disorders in association with congenital deafness. *Arch. Dermatol.* 95: 176–186.

Rugel, S. J., and Keates, E. U. (1965). Waardenburg's syndrome in six generations of one family. *Am. J. Dis. Child.* 109: 579–583.

Rutland, P., Pulleyn, L. J., Reardon, W., Baraitser, M., Hayward, R., Jones, B., Malcolm, S., Winter, R. M., Oldridge, M., Slaney, S. F., Poole, M. D., and Wilki, A. O. M. (1995). Identical mutations in the FGFR2 gene cause both Pfeiffer and Crouzon syndrome phenotypes. *Nature Genet.* 9: 173–176.

Shah, K. N., Dalal, S. J., Desai, M. P., Sheth, P. N., Joshi, N. C., and Ambani, L. M. (1981). White forelock, pigmentary disorder of

irides, and long segment Hirschsprung disease: Possible variant of Waardenburg syndrome. *J. Pediatr.* **99**: 432–435.

Sheffer, R., and Zlotogora, J. (1992). Autosomal dominant inheritance of Klein–Waardenburg syndrome. *Am. J. Med. Genet.* **42**: 320–322.

Siracusa, L. D., Buchberg, A. M., Copeland, N. G., and Jenkins, N. A. (1989). Recombinant inbred strain and interspecific backcross analysis of molecular markers flanking the murine agouti coat color locus. *Genetics* **122**: 669–679.

Siracusa, L. D., Alvord, W. G., Bickmore, W. A., Jenkins, N. A., and Copeland, N. G. (1991). Interspecific backcross mice show sex-specific differences in allelic inheritance. *Genetics* **128**: 813–821.

Snedecor, G. W., and Cochran, W. G. (1967). "Statistical Methods," 6th ed., Iowa State Univ. Press, Ames, IA.

Sommer, A., Young-Wee, T., and Frye, T. (1983). Previously undescribed syndrome of craniofacial, hand anomalies and sensorineural deafness. *Am. J. Med. Genet.* **15**: 71–77.

Stoller, F. M. (1962). A deaf-mute with two congenital syndromes. *Arch. Otolaryngol.* **76**: 42–46.

Tassabehji, M., Read, A. P., Newton, V. E., Harris, R., Balling, R., Gruss, P., and Strachan, T. (1992). Waardenburg's syndrome patients have mutations in the human homologue of the *Pax-3* paired box gene. *Nature* **355**: 635–636.

Tassabehji, M., Newton, V. E., and Read, A. P. (1994). Waardenburg syndrome type 2 caused by mutations in the human microphthalmia (*MITF*) gene. *Nature Genet.* **8**: 251–255.

Vogan, K. J., Epstein, D. J., Trasler, D. G., and Gros, P. (1993). The *Splotch-Delayed* (*Sp*^{d}) mouse mutant carries a point mutation within the paired box of the *Pax-3* gene. *Genomics* **17**: 364–369.

Waardenburg, P. J. (1951). A new syndrome combining developmental anomalies of the eyelids, eyebrows and nose root with pigmentary defects of the iris and head hair and with congenital deafness. *Am. J. Hum. Genet.* **3**: 195–253.

Wang, L., Karmody, C. S., and Pashayan, H. (1981). Waardenburg's syndrome: Variations in expressivity. *Otolaryn. Head Neck Surg.* **89**: 666–670.

040
041 AH2:ZHUMH178XA.91 / 21.5.96 / KKKK / ZNSS / TY: 6

Approx. printed pages: 3½ Hum Hered 178;Morell 1
Note: Underlining of [1], figs. 1 and tabs. 0 will be deleted during pagination

046 *Running title:*
047 Three *PAX3* Mutations and WS1

048 **Short Communication**

049 **Hum Hered**

Three Mutations in the Paired Homeodomain of *PAX3* That Cause Waardenburg Syndrome Type 1

50 *Robert Morell*[a]
51 *Melisa L. Carey*[a]
52 *Anil K. Lalwani*[b]
53 *Thomas B. Friedman*[a,c]
James H. Asher Jr.[a,c]

059 [a] Department of Zoology, Michigan
060 State University, East Lansing,
061 Mich.,
062 [b] Department of Otolaryngology,
063 Head and Neck Surgery,
064 University of California,
065 San Francisco, Calif., and
066 [c] Graduate Program in Genetics,
067 Michigan State University,
068 East Lansing, Mich., USA

071 **Key Words**
072 *PAX3*
073 Waardenburg syndrome
074 WS1

Abstract

Genomic DNA from probands of various Waardenburg syndrome (WS) families were PCR-amplified using primers flanking the 8 exons of *PAX3*. The PCR fragments were screened for sequence variants, and subsequently cycle sequenced. Mutations were detected in exon 6 for 3 probands of WS type 1 families. These mutations all occur in the paired homeodomain DNA-binding motif.

085 KARGER
086
087 E-Mail karger@karger.ch
088 Fax + 41 61 306 12 34
089 http://www.karger.ch

0001–5652/..../....–..../$10.00/0

Robert Morell, PhD
203 Natural Sciences Building
Michigan State University
East Lansing, MI 48824-1115 (USA)

Received:
November 14, 1995
Revision received:
March 25, 1996
Accepted: April 22, 1996

AH2:ZHUM4178XA.92/20.5.96/THBR/ZNSS/TY: 8

Waardenburg syndrome (WS) is an autosomal dominant condition characterized by deafness and various defects of neural-crest-derived tissues [1]. It accounts for over 2% of the congenitally deaf population [2]. At least four types are recognized (types 1, 2, 3 and 4) on the basis of clinical attributes [3]. Mutations in the *PAX3* gene have been demonstrated in individuals with type 1 and type 3 [4–7, 9, 10] and with craniofacial deafness hand syndrome (CDHS) [8]. *PAX3* encodes a transcription factor containing two DNA-binding motifs, a paired domain (exons 2, 3 and 4) and a paired-type homeodomain (exons 5 and 6) [11]. It is expressed in developing neural crest cells and in the brain [12]. Until the availability of sequence information on exons 5–8, mutation screening was confined to exons 1–4; thus, almost all of the WS mutations reported so far have been in the paired domain. WS-associated mutations have been demonstrated recently within the paired-type homeodomain [10]. Here we report three additional mutations in the paired homeodomain of *PAX3*.

Methods for isolation of DNA from blood, PCR primers and cycling parameters for amplifying and sequencing exon 6 of *PAX3*, labelling PCR products by incorporation of ^{33}P α-CTP, and detection of single-strand conformation variants (SSCVs) are described elsewhere [7, 10, 13, 14]. We screened for SSCVs of PCR products for all eight exons of the *PAX3* gene from 34 different individuals (68 chromosomes). These individuals were either probands or obligate mutation carriers from different WS families. SSCVs were detected in exon 6 PCR products amplified from the DNA of probands for 3 WS type 1 families designated: MSU5, MSU7 and MSU9. PCR products from these individuals were gel-purified by electrophoresis through 2% GTG low-melt agarose (FMC), eluted using Wizard PCR prep columns (Promega), and sequenced using the Δ*Taq* cycle sequencing kit (USB).

Two nucleotide substitutions (in MSU5 and MSU7), and one nucleotide insertion resulting in a frameshift (in MSU9) were detected on sequencing gels. For the two substitutions, the sequence change was confirmed by PCR amplification of genomic DNA using allele-specific primers, referred to as amplification refractory mutation system (ARMS) [8]. In MSU5 a substitution 810 C→T would create an Arg271Cys mutation, and is confirmed by substituting TF149 (5'-TCTG-GTTTAGCAACCGCT-3') for E6-5' [10] as the forward primer for PCR amplification of DNA from members of the family (fig. 1A). Allele-specific products (290 bp) were amplified only from DNA of affected members and not from unaffected members. Mutant allele specific PCR products were not detected when genomic DNA from 50 random individuals (100 chromosomes) was amplified using the ARMS primers. In MSU7 an 820 G→A substitution would create a Trp274Trm nonsense mutation, and is confirmed by substituting TF113 (5'-AGCAACCGCCGTGCAA-GATA-3') as the forward primer for PCR amplification. Again, allele-specific products (250 bp) were amplified from DNA of affected members only (fig. 1B). Allele-specific products and control products were resolved on 2% NuSeive 3:1 gels and visualized by ethidium bromide staining.

The 874ins'G' in MSU9 was detected on sequencing gels of PCR fragments as a consistent duplication of bands resulting from the overlap of cycle-sequence products generated from the normal allele and the mutant allele (fig. 1C). The duplicate sequencing bands occurred downstream of the insertion site, while sequencing band patterns upstream of the site were normal. A similar pattern was generated in reactions using a sequencing primer in the reverse direction as well, and was seen only in reactions generated from the DNA of affected individuals. We confirmed that this pattern was due to the insertion of a 'G' in one of the alleles by cloning PCR fragments into the pGEM-T vector (Promega) and sequencing representative clones. Two varieties of clones could be distinguished by both sequencing and by subjecting PCR products generated from cloned DNA as template to SSCV analysis: those comprising the normal exon 6 se-

209
210 AH2:ZH4,84+1178XA.92/20.5.96/THBR/ZHSS/TH: 8

These three mutations are important additions to the literature of *PAX3*. The Arg271Cys mutation in family MSU5 is identical to the one occurring in an apparently unrelated British family [WS.10; A. Read, pers. commun.]. This is the first reported occurrence of a shared mutation among the more than 25 WS mutations described [9, 10]. Haplotype analyses should reveal whether the mutant alleles segregating in families MSU5 and WS.10 have the same origin, or if the nucleotide substitution occurred at least twice in history. This mutation also occurs at the same position as the one described in family NIH8 (Arg271Gly) [10]. The differences in penetrance of deafness between family NIH8 (5/6) and WS.10 plus MSU5 (2/7 and 3/11 respectively) are potentially informative as to the etiology of deafness in WS. MSU7 is segregating for a nonsense (Trp274Trm) mutation. Yet like WS.10, MSU5, and NIH8, all of which have missense mutations in exon 6, the affected individuals in MSU7 have typical WS type 1 features. Three of the four affected individuals in MSU7 display profound sensorineural hearing loss. Another family with typical WS1 features, MSU9, has a frameshift mutation (874ins'G') in exon 6. In MSU9, the frameshift mutation is detected only among the 3 children, each with typical WS type 1 features, but not detected in either parent, who are clinically normal. An earlier study using RFLP markers demonstrated that individual MSU9-1 is the biological father of the three affected children [15]. This confirms the hypothesis that WS1 in this family is the result of a germline mosaicism [15].

Acknowledgements

This work was supported in part by a research grant number R01 DC01160 from the National Institute on Deafness and Other Communication Disorders, National Institutes of Health to JHA and TBF. We would like to thank members of the families for their help and initiative.

References

1 Waardenburg PJ: A new syndrome combining developmental anomalies of the eyelids, eyebrows and nose root with pigmentary defects of the iris and head hair with congenital deafness. Am J Hum Genet 1951;3:195–253.
2 Partington MW: Waardenburg's syndrome and heterochromia iridum in a deaf school population. Canad Med Ass J 1964;90:1008–1017.
3 McKusick VA: Mendelian Inheritance in Man – CD. Baltimore, Johns Hopkins University Press, 1994.
4 Baldwin CT, Hoth CF, Amos JA, da Silva EO, Milunsky A: An exonic mutation in the *HuP2* paired domain gene causes Waardenburg's syndrome. Nature 1992;355:637–638.
5 Tassabehji M, Read AP, Newton VE, Harris R, Balling R, Gruss P, Strachan T: Waardenburg's syndrome patients have mutations in the human homologue of the *PAX-3* paired box gene. Nature 1992;355:635–636.
6 Morell R, Friedman TB, Moeljopawiro S, Hartono, Soewito, Asher JH Jr: A frameshift mutation in the paired domain of HuP2 is responsible for Waardenburg syndrome type 1 in an Indonesian family. Hum Molec Genet 1992;1:243–247.
7 Morell R, Friedman TB, Asher JH Jr: A plus-one frameshift mutation in PAX3 alters the entire deduced amino acid sequence of the paired box in a Waardenburg syndrome type 1 (WS1) family. Hum Molec Genet 1993;2:1487–1488.
8 Asher JH Jr, Sommer A, Morell R, Friedman TB: Missense mutation in the paired domain of *PAX3* causes craniofacial-deafness-hand syndrome. Hum Mutat 1996;7:30–35.
9 Farrer LA, Arnos KS, Asher JH, Baldwin CT, Diehl SR, Friedman TB, Greenberg J, Grundfast K, Hoth C, Lalwani AK, Landa B, Leverton K, Milunsky A, Morell R, Nance WE, Newton V, Ramesar R, Rao VS, Reynolds JE, San Augustin TB, Wilcox ER, Winship I, Read AP: Locus heterogeneity for Waardenburg syndrome is predictive of clinical subtypes. Am J Hum Genet 1994;55:728–737.
10 Lalwani AK, Brister JR, Fex J, Grundfast KM, Ploplis B, San Agustin TB, Wilcox ER: Further elucidation of the genomic structure of *PAX3*, and identification of two different point mutations within the *PAX3* homeobox that cause Waardenburg syndrome type 1 in two families. Am J Hum Genet 1995;56:

AHG:ZHUM4178XA,92/20.5.96/THBR/ZHSS/TY: 6

11 Goulding MD, Chalepakis G, Deutsch U, Erselius JR, Gruss P: *PAX-3*, a novel murine DNA binding protein expressed during early neurogenesis. EMBO J 1991;10: 1135–1147.

12 Stuart ET, Kioussi C, Gruss P: Mammalian PAX genes; in Campbell A, Anderson W, Jones E (eds): Annual Review of Genetics. Palo Alto, Annual Reviews, 1994, vol 28, pp 219–236.

13 Asher JH Jr, Morell R, Friedman TB: Waardenburg syndrome (WS): The analysis of a single family with a WS1 mutation showing linkage to RFLP markers on human chromosome 2q. Am J Hum Genet 1991;48: 43–52.

14 Morell R, Liang Y, Asher JH Jr, Weber JL, Hinnant JT, Winata S, Arhya IN, Friedman TB: Analysis of short tandem repeat (STR) allele frequency distributions in a Balinese population. Hum Molec Genet 1995;4:85–91.

15 Kapur S, Karam S: Germ-line mosaicism in Waardenburg syndrome. Clin Genet 1991;39:194–198.

Fig. 1. A MSU5 pedigree. Numbers below pedigree symbols correspond to the numbers over lanes of the gel. Genomic DNA from each individual was used as a template in PCR reactions containing primers for both exon 2 and the mutant sequence (810 C→T) of exon 6 of *PAX3*. All reactions generated the 535 bp control fragment, the ARMS exon 6 fragment was generated only from DNA of affected individuals. MSU6 pedigree. The left-most lane contains PCR products used in our lab as molecular weight markers. A 535-bp fragment containing exon 2 of *PAX3* is generated from all genomic DNA templates in a PCR reaction while the mutant allele (820 G→A)-specific primers amplify DNA from affected individuals only. C MSU9 pedigree and sequencing gel illustrating the 'G' insertion at nucleotide 874 of *PAX3*. The arrowhead indicates the first occurrence (at nt 874) of the extra band seen in every lane corresponding to DNA from the affected children only. Bands representing sequence 5' to the insertion show the same pattern in all lanes. The same pattern is seen when sequencing reactions are performed in the reverse direction (data not shown).

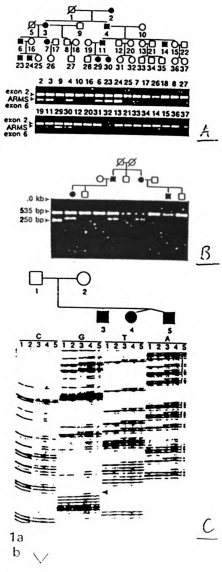

LIST OF REFERENCES

LIST OF REFERENCES

1. Waardenburg, P.J. (1951) A new syndrome combining developmental anomalies of the eyelids, eyebrows and nose root with pigmentary defects of the iris and head hair with congenital deafness. *Am J Hum Genet* **3**, 195-253.

2. Winship, I. and Beighton, P. (1992) Phenotypic discriminants in the Waardenburg syndrome. *Clin Genet* **41**(4), 181-188.

3. Farrer, L.A., Grundfast, K.M., Amos, J., Arnos, K.S., Asher, J.H., Jr., Beighton, P., Diehl, S.R., Fex, J., Read, A.P., et al. (1992) Waardenburg syndrome (WS) type I is caused by defects at multiple loci, one of which is near ALPP on chromosome 2: First report of the WS consortium. *Am J Hum Genet* **50**(5), 902-913.

4. Partington, M.W. (1964) Waardenburg's Syndrome and heterochromia irides in a deaf school population. *Can Med Assoc J* **90**, 1008-1017.

5. Farrer, L.A., Arnos, K.S., Asher, J.H., Jr., Baldwin, C.T., Diehl, S.R., Friedman, T.B., Greenberg, J., Grundfast, K.M., Hoth, C., Lalwani, A.K., et al. (1994) Locus heterogeneity for Waardenburg syndrome is predictive of clinical subtypes. *Am J Hum Genet* **55**(4), 728-737.

6. Arias, S. and Mota, M. (1978) Apparent non-penetrance for dystopia in Waardenburg syndrome type I, with some hints on the diagnosis of dystopia canthorum. *J Genet Hum* **26**(2), 103-131.

7. Arias, S. (1980) Waardenburg syndrome--two distinct types. *Am J Med Genet* **6**(1), 99-100.

8. Arias, S. (1984) Diagnosis and penetrance of dystopia canthorum in Waardenburg syndrome type I (WS1) [letter]. *Am-J-Med-Genet* **17**(4), 863-867.

9. Liu, X.Z., Newton, V.E., and Read, A.P. (1995) Waardenburg syndrome type II: phenotypic findings and diagnostic criteria. *Am J Med Genet* **55**(1), 95-100.

10. Varughese, S., Kumar, A., Rao, S., and Puliyel, J.M. (1988) Type II Waardenburg syndrome. *Indian Pediatr* **25**(4), 384-386.

11. Klein, D. (1983) Historical background and evidence for dominant inheritance of the Klein-Waardenburg syndrome (type III). *Am J Med Genet* **14**(2), 231-239.

12. Goodman, R.M., Lewithal, I., Solomon, A., and Klein, D. (1982) Upper limb involvement in the Klein-Waardenburg syndrome. *Am J Med Genet* **11**(4), 425-433.

13. Klein, D. (1947) Albinisme partiel (leucisme) accompagne de surdimutite, d'osteomyodysplasie, de raideurs articulaires congenitales multiples et d'autres malformations congenitales. *Arch Klaus Stift Vererb Forsch* **22**, 336-342.

14. Klein, D. (1950) Albinisme partiel (leucisme) aves surdimutite, blepharophimosis et dysplasies myo-osteo-articulaires. *Helvet Paediat Acta* **5**, 38-58.

15. Hoth, C.F., Milunsky, A., Lipsky, N., Sheffer, R., Clarren, S.K., and Baldwin, C.T. (1993) Mutations in the paired domain of the human PAX3 gene cause Klein-Waardenburg syndrome (WS-III) as well as Waardenburg syndrome type I (WS-I). *Am-J-Hum-Genet* **52**(3), 455-462.

16. Wilbrandt, H.R. and Ammann, F. (1964) [New observation of the severe form of the Klein-Waardenburg syndrome]. *Arch Julius Klaus Stift Vererbungsforsch Sozialanthropol Rassenhyg* **39**(1-4), 80-92.

17. Sheffer, R. and Zlotogora, J. (1992) Autosomal dominant inheritance of Klein-Waardenburg syndrome. *Am J Med Genet* **42**(3), 320-322.

18. Perrot, H., Ortonne, J.P., and Thivolet, J. (1977) Ultrastructural study of leukodermic skin in Waardenburg-Klein syndrome. *Acta Derm Venereol Stockh* **57**(3), 195-200.

19. Patrizi, A., Colombati, S., and Valenti, L. (1985) [A case of Waardenburg-Klein syndrome]. *G Ital Dermatol Venereol* **120**(4), 277-279.

20. Partsch, C.J. and Schleyer, K.H. (1971) [Chromosome aberrations in the Waardenburg-Klein-Syndrome]. *HNO* **19**(4), 121-123.

21. Ortonne, J.P., Perrot, H., Beyvin, A.J., Revol, L., and Thivolet, J. (1976) [The Waardenburg-Klein syndrome]. *Ann Dermatol Syphiligr Paris* **103**(3), 245-56.

22. Nutman, J., Nissenkorn, I., Varsano, I., Mimouni, M., and Goodman, R.M. (1981) Anal atresia and the Klein-Waardenburg syndrome. *J-Med-Genet* **18**(3), 239-241.

23. Zlotogora, J., Lerer, I., Bar David, S., Ergaz, Z., and Abeliovich, D. (1995) Homozygosity for Waardenburg syndrome. *Am J Hum Genet* **56**(5), 1173-1178.

24. Ariturk, E., Tosyali, N., and Ariturk, N. (1992) A case of Waardenburg syndrome and aganglionosis. *Turk J Pediatr* **34**(2), 111-114.

25. Badner, J.A. and Chakravarti, A. (1990) Waardenburg syndrome and Hirschsprung disease: Evidence for pleiotropic effects of a single dominant gene. *Am J Med Genet* **35**(1), 100-104.

26. de Lumley Woodyear, L., Boulesteix, J., Rutkowski, J., and Umdenstock, R. (1980) Waardenburg syndrome associated with Hirschsprung disease and other abnormalities [letter]. *Pediatrics* **65**(2), 368-369.

27. Omenn, G.S. and McKusick, V.A. (1979) The association of Waardenburg syndrome and Hirschsprung megacolon. *Am J Med Genet* **3**(3), 217-223.

28. Shah, K.N., Dalal, S.J., Desai, M.P., Sheth, P.N., Joshi, N.C., and Ambani, L.M. (1981) White forelock, pigmentary disorder of irides, and long segment Hirschsprung disease: possible variant of Waardenburg syndrome. *J Pediatr* **99**(3), 432-435.

29. Meire, F., Standaert, L., De Laey, J.J., and Zeng, L.H. (1987) Waardenburg syndrome, Hirschsprung megacolon, and Marcus Gunn ptosis. *Am J Med Genet* **27**(3), 683-686.

30. Arias, S. (1971) Genetic heterogeneity in the Waardenburg syndrome. *Birth Defects* **07**(4), 87-101.

31. Hageman, M.J. (1980) Heterogeneity of Waardenburg syndrome in Kenyan Africans. *Metab Pediatr Ophthalmol* **4**(4), 183-184.

32. Darwin, C. (1859)*The Orgin of Species*. 1859, Oxford: Oxford University Press.

33. Brown, K.S., Bergsma, D.R. and Barrow, M.V. (1971) Animal models of Pigment and hearing abnormalities in man. *Birth Defects* **Original Article Series**(VII), 102-109.

34. Fraser, G.R. (1976)*The Causes of Profound Deafness in Childhood.* 1976, Baltimore: Johns Hopkins University Press.

35. Kapur, S. and Karam, S. (1991) Germ-line mosaicism in Waardenburg syndrome. *Clin Genet* **39**(3), 194-198.

36. Mallory, S.B., Wiener, E. and Nordlund, J.J. (1986) Waardenburg's syndrome with Hirschsprungs disease: a neural crest defect. *Pediat Dermat* **3**(2), 119-124.

37. McKusick, V.A. (1973) Congenital deafness and Hirshsprung's disease. *New England Journal of Medicine* **288**, 691.

38. Auerbach, R. (1954) Analysis of the developmental effects of a lethal mutation in the house mouse. *J Exp Zool* **127**, 305-329.

39. Lyon, M.F.a.S., A.G. (1989)*Genetic Variants and Strains of the Laboratory Mouse*. 1989, Oxford: Oxford University Press.

40. Webster, W. (1973) Embryogenesis of the enteric ganglia in normal mice and in mice that develop congenital aganglionic megacolon. *Journal Embryol Exp Morphol* **30**, 573-585.

41. Franz, T. (1992) Neural tube defects without neural crest defects in splotch mice. *Teratology* **46**(6), 599-604.

42. Epstein, D.J., Malo, D., Vekemans, M., and Gros, P. (1991) Molecular characterization of a deletion encompassing the splotch mutation on mouse chromosome 1. *Genomics* **10**(1), 89-93.

43. Epstein, D.J., Vekemans, M., and Gros, P. (1991) Splotch (Sp2H), a mutation affecting development of the mouse neural tube, shows a deletion within the paired homeodomain of Pax-3. *Cell* **67**(4), 767-774.

44. Baker, S.J. and Reddy, E.P. (1995) B cell differentiation: role of E2A and Pax5/BSAP transcription factors. *Oncogene* **11**(3), 413-426.

45. Franz, T. (1993) The Splotch (Sp1H) and Splotch-delayed (Spd) alleles: differential phenotypic effects on neural crest and limb musculature. *Anat Embryol Berl* **187**(4), 371-377.

46. Franz, T., Kothary, R., Surani, M.A., Halata, Z., and Grim, M. (1993) The Splotch mutation interferes with muscle development in the limbs. *AnatEmbryol Berl* **187**(2), 153-160.

47. Franz, T. and Kothary, R. (1993) Characterization of the neural crest defect in Splotch (Sp1H) mutant mice using a lacZ transgene. *Brain Res Dev Brain Res* **72**(1), 99-105.

48. Goulding, M., Sterrer, S., Fleming, J., Balling, R., Nadeau, J., Moore, K.J., Brown, S.D., Steel, K.P., and Gruss, P. (1993) Analysis of the Pax-3 gene in the mouse mutant splotch. *Genomics* **17**(2), 355-363.

49. Moase, C.E. and Trasler, D.G. (1989) Spinal ganglia reduction in the splotch-delayed mouse neural tube defect mutant. *Teratology* **40**(1), 67-75.

50. Moase, C.E. and Trasler, D.G. (1990) Delayed neural crest cell emigration from Sp and Spd mouse neural tube explants. *Teratology* **42**(2), 171-182.

51. Underhill, D.A., Vogan, K.J., and Gros, P. (1995) Analysis of the mouse Splotch-delayed mutation indicates that the Pax-3 paired domain can influence homeodomain DNA-binding activity. *Proc Natl Acad Sci USA* **92**(9), 3692-3696.

52. Vogan, K.J., Epstein, D.J., Trasler, D.G., and Gros, P. (1993) The splotch-delayed (Spd) mouse mutant carries a point mutation within the paired box of the Pax-3 gene. *Genomics* **17**(2), 364-369.

53. Tremblay, P. and Gruss, P. (1994) Pax: genes for mice and men. *Pharmacol Ther* **61**(1-2), 205-226.

54. Asher, J.H., Jr. and Friedman, T.B. (1990) Mouse and hamster mutants as models for Waardenburg syndromes in humans. *J Med Genet* **27**(10), 618-626.

55. Tsukamoto, K., Nakamura, Y., and Niikawa, N. (1994) Isolation of two isoforms of the PAX3 gene transcripts and their tissue-specific alternative expression in human adult tissues. *Hum Genet* **93**(3), 270-274.

56. Ishikiriyama, S., Tonoki, H., Shibuya, Y., Chin, S., Harada, N., Abe, K., and Niikawa, N. (1989) Waardenburg syndrome type I in a child with de novo inversion (2) (q35q37.3). *Am J Med Genet* **33**(4), 505-507.

57. Ishikiriyama, S. (1993) Gene for Waardenburg syndrome type I is located at 2q35, not at 2q37.3. *Am J Med Genet* **46**(5), 608.

58. Foy, C., Newton, V., Wellesley, D., Harris, R., and Read, A.P. (1990) Assignment of the locus for Waardenburg syndrome type I to human chromosome 2q37 and possible homology to the Splotch mouse. *Am J Hum Genet* **46**(6), 1017-1023.

59. Asher, J.J., Morell, R., and Friedman, T.B. (1991) Confirmation of the location of a Waardenburg syndrome type I mutation on human chromosome 2q. Tight linkage to FN1 and ALPP. *Ann N Y Acad Sci* **630**, 295-297.

60. Asher, J.H., Jr., Morell, R., and Friedman, T.B. (1991) Waardenburg syndrome (WS): the analysis of a single family with a WS1 mutation showing linkage to RFLP markers on human chromosome 2q. *Am J Hum Genet* **48**(1), 43-52.

61. Burri, M., Tromvoukis, Y., Bopp, D., Frigerio, G., and Noll, M. (1989) Conservation of the paired domain in metazoans and its structure in three isolated human genes. *EMBO J* **8**(4), 1183-1190.

62. Noll, M. (1993) Evolution and role of Pax genes. *Curr Opin Genet Dev* **3**(4), 595-605.

63. Frigerio, G., Burri, M., Bopp, D., Baumgartner, S., and Noll, M. (1986) Structure of the segmentation gene paired and the Drosophila PRD gene set as part of a gene network. *Cell* **47**(5), 735-746.

64. Bopp, D., Burri, M., Baumgartner, S., Frigerio, G., and Noll, M. (1986) Conservation of a large protein domain in the segmentation gene paired and in functionally related genes of Drosophila. *Cell* **47**(6), 1033-1040.

65. Bopp, D., Jamet, E., Baumgartner, S., Burri, M., and Noll, M. (1989) Isolation of two tissue-specific Drosophila paired box genes, Pox meso and Pox neuro. *EMBO J* **8**(11), 3447-3457.

66. Stapleton, P., Weith, A., Urbanek, P., Kozmik, Z., and Busslinger, M. (1993) Chromosomal localization of seven PAX genes and cloning of a novel family member, PAX-9. *Nature Genet* **3**(4), 292-298.

67. Chalepakis, G. and Gruss, P. (1995) Identification of DNA recognition sequences for the Pax3 paired domain. *Gene* **162**(2), 267-270.

68. Schnittger, S., Rao, V.V., Deutsch, U., Gruss, P., Balling, R., and Hansmann, I. (1992) Pax1, a member of the paired box-containing class of developmental control genes, is mapped to human chromosome 20p11.2 by in situ hybridization (ISH and FISH). *Genomics* **14**(3), 740-744.

69. Wallin, J., Mizutani, Y., Imai, K., Miyashita, N., and Moriwaki, K. (1993) A new Pax gene, Pax-9, maps to mouse chromosome 12. *Mammal Genome* **4**(7), 354-358.

70. Dressler, G.R., Deutsch, U., Chowdhury, K., Nornes, H.O., and Gruss, P. (1990) Pax2, a new murine paired-box-containing gene and its expression in the developing excretory system. *Development* **109**(4), 787-795.

71. Dressler, G.R. and Douglass, E.C. (1992) Pax-2 is a DNA-binding protein expressed in embryonic kidney and Wilms tumor. *Proc Natl Acad Sci USA* **89**(4), 1179-1183.

72. Nornes, H.O., Dressler, G.R., Knapik, E.W., Deutsch, U., and Gruss, P. (1990) Spatially and temporally restricted expression of Pax2 during murine neurogenesis. *Development* **109**(4), 797-809.

73. Czerny, T., Schaffner, G., and Busslinger, M. (1993) DNA sequence recognition by Pax proteins: Bipartite structure of the paired domain and its binding site. *Genes Dev* **7**(10), 2048-2053.

74. Asano, M. and Gruss, P. (1992) Pax-5 is expressed at the midbrain-hindbrain boundary during mouse development. *Mech Dev* **39**(1-2), 29-39.

75. Zannini, M., Francis Lang, H., Plachov, D., and Di Lauro, R. (1992) Pax-8, A paired domain-containing protein, binds to a sequence overlapping the recognition site of a homeodomain and activates transcription from two thyroid-specific promoters. *Mol Cell Biol* **12**(9), 4230-4241.

76. Kozmik, Z., Kurzbauer, R., Doerfler, P., and Busslinger, M. (1993) Alternative splicing of Pax-8 gene transcripts is developmentally regulated and generates isoforms with different transactivation properties. *Mol Cell Biol* **13**(10), 6024-6035.

77. Plachov, D., Chowdhury, K., Walther, C., Simon, D., Guenet, J.L., and Gruss, P. (1990) Pax8, a murine paired box gene expressed in the developing excretory system and thyroid gland. *Development* **110**(2), 643-651.

78. Tamura, T., Izumikawa, Y., Kishino, T., Soejima, H., Jinno, Y., and Niikawa, N. (1994) Assignment of the human PAX4 gene to chromosome band 7q32 by fluorescence in situ hybridization. *Cytogenet Cell Genet* **66**(2), 132-134.

79. Ton, C.C., Miwa, H., and Saunders, G.F. (1992) Small eye (Sey): cloning and characterization of the murine homolog of the human aniridia gene. *Genomics* **13**(2), 251-256.

80. Walther, C. and Gruss, P. (1991) Pax-6, a murine paired box gene, is expressed in the developing CNS. *Development* **113**(4), 1435-1449.

81. Schafer, B.W. and Mattei, M.G. (1993) The human paired domain gene PAX7 (Hup1) maps to chromosome 1p35-1p36.2. *Genomics* **17**(1), 249-251.

82. Schaefer, B.W., Czerny, T., Bernasconi, M., Genini, M., and Busslinger, M. (1994) Molecular cloning and characterization of a human PAX-7 cDNA expressed in normal and neoplastic myocytes. *Nuc Acids Res* **22**(22), 4574-4582.

83. Shapiro, D.N., Sublett, J.E., Li, B., Valentine, M.B., Morris, S.W., and Noll, M. (1993) The gene for PAX7, a member of the paired-box-containing genes, is localized on human chromosome arm 1p36. *Genomics* **17**(3), 767-769.

84. Jostes, B., Walther, C., and Gruss, P. (1990) The murine paired box gene, Pax7, is expressed specifically during the development of the nervous and muscular system. *Mech Dev* **33**(1), 27-37.

85. Chalepakis, G., Goulding, M., Read, A., Strachan, T., and Gruss, P. (1994) Molecular basis of splotch and Waardenburg Pax-3 mutations. *Proc Natl Acad Sci USA* **91**(9), 3685-3689.

86. Read, A.P. and van Heyningen, V. (1994) PAX genes in human developmental anomalies. *Semin Dev Biol* **5**(5), 323-332.

87. Read, A.P. (1995) Pax genes: Paired feet in three camps. *Nat Genet* **9**(4), 333-334.

88. Stoykova, A. and Gruss, P. (1994) Roles of Pax-genes in developing and adult brain as suggested by expression patterns. *J Neurosci* **14**(3 Pt 2), 1395-1412.

89. Strachan, T. and Read, A.P. (1994) PAX genes. *Curr Opin Genet Dev* **4**(3), 427-438.

90. Chalepakis, G., Stoykova, A., Wijnholds, J., Tremblay, P., and Gruss, P. (1993) Pax: gene regulators in the developing nervous system. *J Neurobiol* **24**(10), 1367-1384.

91. Gerard, M., Abitbol, M., Delezoide, A.L., Dufier, J.L., Mallet, J., and Vekemans, M. (1995) PAX-genes expression during human embryonic development, a preliminary report. *C R Acad Sci III* **318**(1), 57-66.

92. Timmons, P.M., Wallin, J., Rigby, P.W., and Balling, R. (1994) Expression and function of Pax 1 during development of the pectoral girdle. *Development* **120**(10), 2773-2785.

93. Wallin, J., Wilting, J., Koseki, H., Fritsch, R., Christ, B., and Balling, R. (1994) The role of Pax-1 in axial skeleton development. *Development* **120**(5), 1109-1121.

94. Grindley, J.C., Davidson, D.R., and Hill, R.E. (1995) The role of Pax-6 in eye and nasal development. *Development* **121**(5), 1433-1442.

95. Hill, R.E., Favor, J., Hogan, B.L., Ton, C.C., Saunders, G.F., Hanson, I.M., Prosser, J., Jordan, T., Hastie, N.D., and van Heyningen, V. (1991) Mouse small eye results from mutations in a paired-like homeobox-containing gene [published erratum appears in Nature 1992 Feb 20;355(6362):750]. *Nature* **354**(6354), 522-525.

96. Quiring, R., Walldorf, U., Kloter, U., and Gehring, W.J. (1994) Homology of the eyeless gene of Drosophila to the Small eye gene in mice and Aniridia in humans [see comments]. *Science* **265**(5173), 785-789.

97. Matsuo, T., Osumi Yamashita, N., Noji, S., Ohuchi, H., Koyama, E., Myokai, F., Matsuo, N., Taniguchi, S., Doi, H., Iseki, S., et al. (1993) A mutation in the Pax-6 gene in rat small eye is associated with impaired migration of midbrain crest cells. *Nat Genet* **3**(4), 299-304.

98. Hanson, I.M., Seawright, A., Hardman, K., Hodgson, S., Zaletayev, D., Fekete, G., and Van Heyningen, V. (1993) PAX6 mutations in aniridia. *Hum Mol Genet* **2**(7), 915-920.

99. Davis, A. and Cowell, J.K. (1993) Mutations in the PAX6 gene in patients with hereditary aniridia. *Hum Mol Genet* **2**(12), 2093-2097.

100. Glaser, T., Walton, D.S., and Maas, R.L. (1992) Genomic structure, evolutionary conservation and aniridia mutations in the human PAX6 gene. *Nature Genet* **2**(3), 232-239.

101. Glaser, T., Jepeal, L., Edwards, J.G., Young, S.R., Favor, J., and Maas, R.L. (1994) PAX6 gene dosage effect in a family with congenital cataracts, aniridia, anophthalmia and central nervous system defects. *Nature Genet* **7**(4), 463-471.

102. Jordan, T., Hanson, I., Zaletayev, D., Hodgson, S., Prosser, J., Seawright, A., Hastie, N., and van Heyningen, V. (1992) The human PAX6 gene is mutated in two patients with aniridia. *Nature Genet* **1**(5), 328-332.

103. DeRespinis, P.A. and Wagner, R.S. (1987) Peters' anomaly in a father and son. *Am-J-Ophthalmol* **104**(5), 545-6.

104. Eiferman, R.A. (1984) Association of Wilms' tumor with Peter's anomaly. *Ann-Ophthalmol* **16**(10), 933-934.

105. Hanson, I.M., Fletcher, J.M., Jordan, T., Brown, A., Taylor, D., Adams, R.J., Punnett, H.H., and van Heyningen, V. (1994) Mutations at the PAX6 locus are found in heterogeneous anterior segment malformations including Peters' anomaly. *Nat-Genet* **6**(2), 168-173.

106. Ivanov, I., Shuper, A., Shohat, M., Snir, M., and Weitz, R. (1995) Aniridia: recent achievements in paediatric practice. *Eur J Pediatr* **154**(10), 795-800.

107. Fantes, J.A., Bickmore, W.A., Fletcher, J.M., Ballesta, F., Hanson, I.M., and van Heyningen, V. (1992) Submicroscopic deletions at the WAGR locus, revealed by nonradioactive in situ hybridization. *Am J Hum Genet* **51**(6), 1286-1294.

108. Schwartz, F., Neve, R., Eisenman, R., Gessler, M., and Bruns, G. (1994) A WAGR region gene between PAX-6 and FSHB expressed in fetal brain. *Hum Genet* **94**(6), 658-664.

109. Mirzayans, F., Pearce, W.G., MacDonald, I.M., and Walter, M.A. (1995) Mutation of the PAX6 gene in patients with autosomal dominant keratitis. *Am J Hum Genet* **57**(3), 539-548.

110. Sanyanusin, P., Schimmenti, L.A., McNoe, L.A., Ward, T.A., Pierpont, M.E., Sullivan, M.J., Dobyns, W.B., and Eccles, M.R. (1995) Mutation of the PAX2 gene in a family with optic nerve colobomas, renal anomalies and vesicoureteral reflux. *Nat Genet* **9**(4), 358-363.

111. Balling, R., Deutsch, U., and Gruss, P. (1988) Undulated, a mutation affecting the development of the mouse skeleton, has a point mutation in the paired box of Pax1. *Cell* **55**(3), 531-535.

112. Balling, R. (1994) The undulated mouse and the development of the vertebral column. Is there a human PAX-1 homologue? *Clin Dysmorphol* **3**(3), 185-191.

113. Chalepakis, G., Fritsch, R., Fickenscher, H., Deutsch, U., Goulding, M., and Gruss, P. (1991) The molecular basis of the undulated/Pax-1 mutation. *Cell* **66**(5), 873-884.

114. Stuart, E.T. and Gruss, P. (1995) PAX genes: what's new in developmental biology and cancer? *Hum Mol Genet*, 1717-1720.

115. Stuart, E.T., Yokota, Y., and Gruss, P. (1995) PAX and HOX in neoplasia. *Adv Genet* **33**, 255-274.

116. Maulbecker, C.C. and Gruss, P. (1993) The oncogenic potential of Pax genes. *EMBO J* **12**(6), 2361-2367.

117. Sharma, P.M., Bowman, M., Yu, B.F., and Sukumar, S. (1994) A rodent model for Wilms tumors: embryonal kidney neoplasms induced by N-nitroso-N'-methylurea. *Proc Natl Acad Sci USA* **91**(21), 9931-9935.

118. Poleev, A., Fickenscher, H., Mundlos, S., Winterpacht, A., Zabel, B., Fidler, A., Gruss, P., and Plachov, D. (1992) PAX8, a human paired box gene: Isolation and expression in developing thyroid, kidney and Wilms' tumors. *Development* **116**(3), 611-623.

119. Poleev, A., Wendler, F., Fickenscher, H., Zannini, M.S., Yaginuma, K., Abbott, C., and Plachov, D. (1995) Distinct functional properties of three human paired-box-protein, PAX8, isoforms generated by alternative splicing in thyroid, kidney and Wilms' tumors. *Eur J Biochem* **228**(3), 899-911.

120. Hazen Martin, D.J., Re, G.G., Garvin, A.J., and Sens, D.A. (1994) Distinctive properties of an anaplastic Wilms' tumor and its associated epithelial cell line. *Am J Pathol* **144**(5), 1023-1034.

121. Eccles, M.R., Yun, K., Reeve, A.E., and Fidler, A.E. (1995) Comparative in situ hybridization analysis of PAX2, PAX8, and WT1 gene transcription in human fetal kidney and Wilms' tumors. *Am J Pathol* **146**(1), 40-45.

122. Tagge, E.P., Hanson, P., Re, G.G., Othersen, H.B., Jr., Smith, C.D., and Garvin, A.J. (1994) Paired box gene expression in Wilms' tumor. *J Pediatr Surg* **29**(2), 134-141.

123. Kozmik, Z., Sure, U., Ruedi, D., Busslinger, M., and Aguzzi, A. (1995) Deregulated expression of PAX5 in medulloblastoma. *Proc Natl Acad Sci USA* **92**(12), 5709-5713.

124. Adams, B., Doerfler, P., Aguzzi, A., Kozmik, Z., Urbanek, P., Maurer Fogy, I., and Busslinger, M. (1992) Pax-5 encodes the transcription factor BSAP and is expressed in B lymphocytes, the developing CNS, and adult testis. *Genes Dev* **6**(9), 1589-1607.

125. Stuart, E.T., Kioussi, C., and Gruss, P. (1994) Mammalian Pax genes. *Annu Rev Genet* **28**, 219-236.

126. Bennicelli, J.L., Fredericks, W.J., Wilson, R.B., Rauscher, F.J.r., and Barr, F.G. (1995) Wild type PAX3 protein and the PAX3-FKHR fusion protein of alveolar rhabdomyosarcoma contain potent, structurally distinct transcriptional activation domains. *Oncogene* **11**(1), 119-130.

127. Biegel, J.A., Nycum, L.M., Valentine, V., Barr, F.G., and Shapiro, D.N. (1995) Detection of the t(2;13)(q35;q14) and PAX3-FKHR fusion in alveolar rhabdomyosarcoma by fluorescence in situ hybridization. *GenesChromosom Cancer* **12**(3), 186-192.

128. Davis, R.J., CM, D.C., Lovell, M.A., Biegel, J.A., and Barr, F.G. (1994) Fusion of PAX7 to FKHR by the variant t(1;13)(p36;q14) translocation in alveolar rhabdomyosarcoma. *Cancer Res* **54**(11), 2869-2872.

129. Pappo, A.S., Shapiro, D.N., Crist, W.M., and Maurer, H.M. (1995) Biology and therapy of pediatric rhabdomyosarcoma. *J Clin Oncol* **13**(8), 2123- 2139.

130. Pappo, A.S. (1994) Rhabdomyosarcoma and other soft tissue sarcomas of childhood. *Curr Opin Oncol* **6**(4), 397-402.

131. Sublett, J.E., Jeon, I.S., and Shapiro, D.N. (1995) The alveolar rhabdomyosarcoma PAX3/FKHR fusion protein is a transcriptional activator. *Oncogene* **11**(3), 545-552.

132. Macina, R.A., Barr, F.G., Galili, N., and Riethman, H.C. (1995) Genomic organization of the human PAX3 gene: DNA sequence analysis of the region disrupted in alveolar rhabdomyosarcoma. *Genomics* **26**(1), 1-8.

133. Barr, F.G., Galili, N., Holick, J., Biegel, J.A., Rovera, G., and Emanuel, B.S. (1993) Rearrangement of the PAX3 paired box gene in the paediatric solid tumour alveolar rhabdomyosarcoma. *Nature Genet* **3**(2), 113-117.

134. Galili, N., Davis, R.J., Fredericks, W.J., Mukhopadhyay, S., Rauscher, F.J., III, Emanuel, B.S., Rovera, G., and Barr, F.G. (1993) Fusion of a fork head domain gene to PAX3 in the solid tumour alveolar rhabdomyosarcoma. *Nature Genet* **5**(3), 230-235.

135. Shapiro, D.N., Sublett, J.E., Li, B., Downing, J.R., and Naeve, C.W. (1993) Fusion of PAX3 to a member of the forkhead family of transcription factors in human alveolar rhabdomyosarcoma. *Cancer Res* **53**(21), 5108-5112.

136. Fredericks, W.J., Galili, N., Mukhopadhyay, S., Rovera, G., Bennicelli, J., Barr, F.G., and Rauscher, F.J., III (1995) The PAX3-FKHR fusion protein created by the t(2;13) translocation in alveolar rhabdomyosarcomas is a more potent transcriptional activator than PAX3. *Mol Cell Biol* **15**(3), 1522-1535.

137. Goulding, M.D., Chalepakis, G., Deutsch, U., Erselius, J.R., and Gruss, P. (1991) Pax-3, a novel murine DNA binding protein expressed during early neurogenesis. *Embo J* **10**(5), 1135-1147.

138. Goulding, M. (1992) Paired box genes in vertebrate neurogenesis. *Semin Neurosci* **4**(5), 327-335.

139. Goulding, M.D., Lumsden, A., and Gruss, P. (1993) Signals from the notochord and floor plate regulate the region-specific expression of two Pax genes in the developing spinal cord. *Development* **117**(3), 1001-1016.

140. Goulding, M. and Paquette, A. (1994) Pax genes and neural tube defects in the mouse. *Ciba Found Symp* **181**, 103-113.

141. Mansouri, A., Stoykova, A., and Gruss, P. (1994) Pax genes in development. *J Cell Sci Suppl* **18**, 35-42.

142. Pruitt, S.C. (1992) Expression of Pax-3- and neuroectoderm-inducing activities during differentiation of P19 embryonal carcinoma cells. *Development* **116**(3), 573-583.

143. Gruss, P.a.W., C (1992) Pax in development. *Cell* **69**, 719-722.

144. Goulding, M., Lumsden, A., and Paquette, A.J. (1994) Regulation of Pax-3 expression in the dermomyotome and its role in muscle development. *Development* **120**(4), 957-971.

145. Bober, E., Franz, T., Arnold, H.H., Gruss, P., and Tremblay, P. (1994) Pax-3 is required for the development of limb muscles: A possible role for the migration of dermomyotomal muscle progenitor cells. *Development* **120**(3), 603-612.

146. Buckingham, M.E. (1994) Muscle: The regulation of myogenesis. *Curr Opin Genet Dev* **4**(5), 745-751.

147. Epstein, J.A., Lam, P., Jepeal, L., Maas, R.L., and Shapiro, D.N. (1995) Pax3 inhibits myogenic differentiation of cultured myoblast cells. *J BiolChem* **270**(20), 11719-11722.

148. Williams, B.A. and Ordahl, C.P. (1994) Pax-3 expression in segmental mesoderm marks early stages in myogenic cell specification. *Development* **120**(4), 785-796.

149. Baldwin, C.T., Hoth, C.F., Macina, R.A., and Milunsky, A. (1995) Mutations in PAX3 that cause Waardenburg syndrome type I: ten new mutations and review of the literature. *Am J Med Genet* **58**(2), 115-122.

150. Baldwin, C.T., Lipsky, N.R., Hoth, C.F., Cohen, T., Mamuya, W., and Milunsky, A. (1994) Mutations in PAX3 associated with Waardenburg syndrome type I. *Hum Mutat* **3**(3), 205-211.

151. Lalwani, A.K., Brister, J.R., Fex, J., Grundfast, K.M., Ploplis, B., San Agustin, T.B., and Wilcox, E.R. (1995) Further elucidation of the genomic structure of PAX3, and identification of two different point mutations within the PAX3 homeobox that cause Waardenburg syndrome type 1 in two families. *Am J Hum Genet* **56**(1), 75-83.

152. Morell, R., Friedman, T.B., Moeljopawiro, S., Hartono, Soewito, and Asher, J.H., Jr. (1992) A frameshift mutation in the HuP2 paired domain of the probable human homolog of murine Pax-3 is responsible for Waardenburg syndrome type 1 in an Indonesian family. *Hum Mol Genet* **1**(4), 243-247.

153. Morell, R., Friedman, T.B., and Asher, J.H., Jr. (1993) A plus-one frameshift mutation in PAX3 alters the entire deduced amino acid sequence of the paired box in a Waardenburg syndrome type 1 (WS1) family. *Hum Mol Genet* **2**(9), 1487-1488.

154. Read, A.P., Foy, C., Newton, V., and Harris, R. (1991) Localization of a gene for Waardenburg syndrome type I. *Ann N Y Acad Sci* **630**, 143-151.

155. Tassabehji, M., Newton, V.E., Liu, X.Z., Brady, A., Donnai, D., Krajewska Walasek, M., Murday, V., Norman, A., Obersztyn, E., Reardon, W., et al. (1995) The mutational spectrum in Waardenburg syndrome. *Hum MolGenet* **4**(11), 2131-2137.

156. Kissinger, C.R., Liu, B.S., Martin Blanco, E., Kornberg, T.B., and Pabo, C.O. (1990) Crystal structure of an engrailed homeodomain-DNA complex at 2.8 A resolution: a framework for understanding homeodomain-DNA interactions. *Cell* **63**(3), 579-590.

157. Xu, W., Rould, M.A., Jun, S., Desplan, C., and Pabo, C.O. (1995) Crystal structure of a paired domain-DNA complex at 2.5 angstrom. *Cell* **80**(4), 639-650.

158. Sommer, A., Young-Wee, T. and Frye, T. (1983) Previously undescribed syndrome of craniofacial, hand anomalies and sensorineural deafness. *Am J Med Genet* **15**, 71-77.

159. Asher, J.H., Jr., Sommer, A., Morell, R. and Friedman, T.B. (1996) Missense mutation in the paired domain of PAX3 causes Craniofacial-deafness-hand syndrome. *Human Mutation* **7**, 30-35.

160. Arias, S. (1993) Mutations of PAX3 unlikely in Waardenburg syndrome type 2 [letter]. *Nat Genet* **5**(1), 8.

161. Hughes, A.E., Newton, V.E., Liu, X.Z., and Read, A.P. (1994) A gene for Waardenburg syndrome type 2 maps close to the human homologue of the microphthalmia gene at chromosome 3p12-p14.1. *Nat Genet* **7**(4), 509-512.

162. Tachibana, M., Perez Jurado, L.A., Nakayama, A., Hodgkinson, C.A., Li, X., Schneider, M., Miki, T., Fex, J., Francke, U., and Arnheiter, H. (1994) Cloning of MITF, the human homolog of the mouse microphthalmia gene and assignment to chromosome 3p14.1-p12.3. *Hum Mol Genet* **3**(4), 553-557.

163. Tassabehji, M., Newton, V.E., and Read, A.P. (1994) Waardenburg syndrome type 2 caused by mutations in the human microphthalmia (MITF) gene. *Nat Genet* **8**(3), 251-255.

164. Burley, S.K., Clark, K.L., Ferre, D.A.A., Kim, J.L., and Nikolov, D.B. (1993) X-ray crystallographic studies of eukaryotic transcription factors. *Cold Spring Harb Symp Quant Biol* **58**, 123-132.

165. Ferre, D.A.A.R., Prendergast, G.C., Ziff, E.B., and Burley, S.K. (1993) Recognition by Max of its cognate DNA through a dimeric b/HLH/Z domain [see comments]. *Nature* **363**(6424), 38-45.

166. Hemesath, T.J., Steingrimsson, E., McGill, G., Hansen, M.J., Vaught, J., Hodgkinson, C.A., Arnheiter, H., Copeland, N.G., Jenkins, N.A., and Fisher, D.E. (1994) Microphthalmia, a critical factor in melanocyte development, defines a discrete transcription factor family. *Genes Dev* **8**(22), 2770-2780.

167. Steingrimsson, E., Moore, K.J., Lamoreux, M.L., Ferre D' Amare, A.R., Burley, S.K., Sanders Zimring, D.C., Skow, L.C., Hodgkinson, C.A., Jenkins, N.A., et al. (1994) Molecular basis of mouse microphthalmia (mi) mutations helps explain their developmental and phenotypic consequences. *Nat Genet* **8**(3), 256-263.

168. Rao, V.V., Loffler, C., and Hansmann, I. (1991) The gene for the novel vasoactive peptide endothelin 3 (EDN3) is localized to human chromosome 20q13.2-qter. *Genomics* **10**(3), 840-841.

169. Attie, T., Till, M., Pelet, A., Amiel, J., Edery, P., Boutrand, L., Munnich, A. and Lyonnet, S. (1995) Mutation of the endothelin-receptor B gene in Waardenburg-Hirschsprung disease. *Human Molecular Genetics* **4**(12), 2407-2409.

170. Puffenberger, E.G., Hosoda, K., Washington, S.S., Nakao, K., deWit, D., Yanagisawa, M., and Chakravart, A. (1994) A missense mutation of the endothelin-B receptor gene in multigenic Hirschsprung's disease. *Cell* **79**(7), 1257-1266.

171. Edery, P., Lyonnet, S., Mulligan, L.M., Pelet, A., Dow, E., Abel, L., Holder, S., Nihoul Fekete, C., Ponder, B.A., and Munnich, A. (1994) Mutations of the RET proto-oncogene in Hirschsprung's disease [see comments]. *Nature* **367**(6461), 378-380.

172. Romeo, G., Ronchetto, P., Luo, Y., Barone, V., Seri, M., Ceccherini, I., Pasini, B., Bocciardi, R., Lerone, M., Kaariainen, H., et al. (1994) Point mutations affecting the tyrosine kinase domain of the RET proto-oncogene in Hirschsprung's disease [see comments]. *Nature* **367**(6461), 377-378.

173. Ceccherini, I., Zhang, A.L., Matera, I., Yang, G., Devoto, M., Romeo, G., and Cass, D.T. (1995) Interstitial deletion of the endothelin-B receptor gene in the spotting lethal (sl) rat. *Hum Mol Genet* **4**(11), 2089-2096.

174. Ceccherini, I., Bocciardi, R., Luo, Y., Pasini, B., Hofstra, R., Takahashi, M., and Romeo, G. (1993) Exon structure and flanking intronic sequences of the human RET proto-oncogene. *Biochem Biophys Res Commun* **196**(3), 1288-1295.

175. Attie, T., Edery, P., Lyonnet, S., Nihoul Fekete, C., and Munnich, A. (1994) [Identification of mutation of RET proto-oncogene in Hirschsprung disease]. *C R Seances Soc Biol Fil* **188**(5-6), 499-504.

176. Attie, T., Pelet, A., Sarda, P., Eng, C., Edery, P., Mulligan, L.M., Ponder, B.A., Munnich, A., and Lyonnet, S. (1994) A 7 bp deletion of the RET proto-oncogene in familial Hirschsprung's disease. *Hum Mol Genet* **3**(8), 1439-1440.

177. Attie, T., Till, M., Pelet, A., Edery, P., Bonnet, J.P., Munnich, A., and Lyonnet, S. (1995) Exclusion of RET and Pax 3 loci in Waardenburg-Hirschsprung disease. *J Med Genet* **32**(4), 312-313.

178. Attie, T., Pelet, A., Edery, P., Eng, C., Mulligan, L.M., Amiel, J., Boutrand, L., Beldjord, C., Nihoul Fekete, C., Munnich, A., et al. (1995) Diversity of RET proto-oncogene mutations in familial and sporadic Hirschsprung disease. *Hum Mol Genet* **4**(8), 1381-3186.

179. Lyonnet, S., Edery, P., Mulligan, L.M., Pelet, A., Dow, E., Abel, L., Holder, S., Nihoul Fekete, C., Ponder, B.A., and Munnich, A. (1994) [Mutations of RET proto-oncogene in Hirschsprung disease]. *C R Acad Sci III* **317**(4), 358-362.

180. Baynash, A.G., Hosoda, K., Giaid, A., Richardson, J.A., Emoto, N., Hammer, R.E., and Yanagisawa, M. (1994) Interaction of endothelin-3 with endothelin-B receptor is essential for development of epidermal melanocytes and enteric neurons. *Cell* **79**(7), 1277-1285.

181. Hosoda, K., Hammer, R.E., Richardson, J.A., Baynash, A.G., Cheung, J.C., Giaid, A., and Yanagisawa, M. (1994) Targeted and natural (piebald-lethal) mutations of endothelin-B receptor gene produce megacolon associated with spotted coat color in mice. *Cell* **79**(7), 1267-1276.

182. Gariepy, C.E., Cass, D.T., and Yanagisawa, M. (1996) Null mutation of endothelin receptor type B gene in spotting lethal rats causes aganglionic megacolon and white coat color. *Proc Natl Acad Sci USA* **93**(2), 867-872.

183. Wilcox, E.R., Rivolta, M.N., Ploplis, B., Potterf, S.B., and Fex, J. (1992) The PAX3 gene is mapped to human chromosome 2 together with a highly informative CA dinucleotide repeat. *Hum Mol Genet* **1**(3), 215.

184. Carezani Gavin, M., Clarren, S.K., and Steege, T. (1992) Waardenburg syndrome associated with meningomyelocele [letter] [see comments]. *Am J Med Genet* **42**(1), 135-136.

185. Calmettes, L., Deodati, F., Bec, P., and Labro, J.B. (1968) [Waardenburg-Klein syndrome with blind lacrimal fistulas]. *Bull Mem Soc Fr Ophtalmol* **81**, 144-155.

186. Char, F. (1971) Cleft lip/palate in the Waardenburg syndrome. *Birth Defects* **7**(7), 258.

187. Hol, F.A., Hamel, B.C., Geurds, M.P., Mullaart, R.A., Barr, F.G., Macina, R.A., and Mariman, E.C. (1995) A frameshift mutation in the gene for PAX3 in a girl with spina bifida and mild signs of Waardenburg syndrome. *J Med Genet* **32**(1), 52-56.

188. Kaplan, P. and de Chaderevian, J.P. (1988) Piebaldism-Waardenburg syndrome: histopathologic evidence for a neural crest syndrome [see comments]. *Am J Med Genet* **31**(3), 679-688.

189. Laor, N. and Korczyn, A.D. (1978) Waardenburg syndrome with a fixed dilated pupil. *Br J Ophthalmol* **62**(7), 491-494.

190. Pierpont, J.W., Doolan, L.D., Amann, K., Snead, G.R., and Erickson, R.P. (1994) A single base pair substitution within the paired box of PAX3 in an individual with Waardenburg syndrome type 1 (WS1). *Hum Mutat* **4**(3), 227-228.

191. Silverman, G.A., Schneider, S.S., Massa, H.F., Flint, A., Lalande, M., Leonard, J.C., Overhauser, J., van den Engh, G., and Trask, B.J. (1995) The 18q- syndrome: analysis of chromosomes by bivariate flow karyotyping and the PCR reveals a successive set of deletion breakpoints within 18q21.2-q22.2. *Am J Hum Genet* **56**(4), 926-937.

192. Strathdee, G., Zackai, E.H., Shapiro, R., Kamholz, J., and Overhauser, J. (1995) Analysis of clinical variation seen in patients with 18q terminal deletions. *Am J Med Genet* **59**(4), 476-483.

193. Begleiter, M.L. and Harris, D.J. (1992) Waardenburg syndrome and meningocele. *Am J Med Genet* **44**(4), 541.

194. Chatkupt, S., Chatkupt, S., and Johnson, W.G. (1993) Waardenburg syndrome and myelomeningocele in a family. *J Med Genet* **30**(1), 83-84.

195. Moline, M.L. and Sandlin, C. (1993) Waardenburg syndrome and meningomyelocele [letter]. *Am J Med Genet* **47**(1), 126.

196. Chatkupt, S., Hol, F.A., Shugart, Y.Y., Geurds, M.P., Stenroos, E.S., Koenigsberger, M.R., Hamel, B.C., Johnson, W.G., and Mariman, E.C. (1995) Absence of linkage between familial neural tube defects and PAX3 gene. *J Med Genet* **32**(3), 200-204.

197. Pierpont, J.W., Storm, A.L., Erickson, R.P., Kohn, B.R., Pettijohn, L., and DePaepe, A. (1995) Lack of linkage of apparently dominant cleft lip (palate) to two candidate chromosomal regions. *J Craniofac Genet DevBiol* **15**(2), 66-71.

198. Kawabata, E., Ohba, N., Nakamura, A., Izumo, S., and Osame, M. (1987) Waardenburg syndrome: a variant with neurological involvement. *Ophthalmic Paediatr Genet* **8**(3), 165-170.

199. Kioussi, C., Gross, M.K., and Gruss, P. (1995) Pax3: a paired domain gene as a regulator in PNS myelination. *Neuron* **15**(3), 553-562.

200. Bankier, A. and Sheffield, L. (1990) Piebaldism, an autosomal dominant trait distinct from Waardenburg syndrome [letter; comment]. *Am J MedGenet* **37**(4), 600-602.

201. Hussels, I.E. (1971) Vitiligo versus Waardenburg syndrome. *Birth Defects* **7**(8), 285.

202. Francois, J. (1979) Albinism. *Ophthalmologica* **178**(1-2), 19-31.

203. Pandya, A., Xia-Juan, X., Landa, B.L., Arnos, K.S., Israel, J., Lloyd, J., James, A.L., Diehl, S.R., Blanton, S.H., and Nance, W.E. (1996) Phenotypic variation in Waardenburg syndrome: mutational heterogeneity, modifier genes or polygenic background? *Hum Mol Genet* **5**(4), 497-502.

204. Reynolds, J.E., Marazita, M.L., Meyer, J.M., Stevens, C.A., Eaves, L.J., Arnos, K.S., Ploughman, L.M., MacLean, C., Nance, W.E., and Diehl, S.R. (1996) Major-locus contributions to variability of the craniofacial feature dystopia canthorum in Waardenburg syndrome. *Am J Hum Genet* **58**(2), 384-392.

205. Reynolds, J.E., Meyer, J.M., Landa, B., Stevens, C.A., Arnos, K.S., Israel, J., Marazita, M.L., Bodurtha, J., Nance, W.E., and Diehl, S.R. (1995) Analysis of variability of clinical manifestations in Waardenburg syndrome. *Am J Med Genet* **57**(4), 540-547.

206. Tassabehji, M., Read, A.P., Newton, V.E., Patton, M., Gruss, P., Harris, R., and Strachan, T. (1993) Mutations in the PAX3 gene causing Waardenburg syndrome type 1 and type 2. *Nat Genet* **3**(1), 26-30.

207. Kirkpatrick, S.J. (1992) Waardenburg syndrome type I in a child with deletion (2) (q35q36. 2). *Am J Med Genet* **44**(5), 699-700.

208. de Kok, Y.J., Merkx, G.F., van der Maarel, S.M., Huber, I., Malcolm, S., Ropers, H.H., and Cremers, F.P. (1995) A duplication/paracentric inversion associated with familial X-linked deafness (DFN3) suggests the presence of a regulatory element more than 400 kb upstream of the POU3F4 gene. *Hum Mol Genet* **4**(11), 2145-2150.

209. Duttlinger, R., Manova, K., Chu, T.Y., Gyssler, C., Zelenetz, A.D., Bachvarova, R.F., and Besmer, P. (1993) W-sash affects positive and negative elements controlling c-kit expression: ectopic c-kit expression at sites of kit-ligand expression affects melanogenesis. *Development* **118**(3), 705-717.

210. Bedell, M.A., Brannan, C.I., Evans, E.P., Copeland, N.G., Jenkins, N.A., and Donovan, P.J. (1995) DNA rearrangements located over 100 kb 5' of the Steel (Sl)-coding region in Steel-panda and Steel-contrasted mice deregulate Sl expression and cause female sterility by disrupting ovarian follicle development. *Genes Dev* **9**(4), 455-470.

211. Fantes, J., Redeker, B., Breen, M., Boyle, S., Brown, J., Fletcher, J., Jones, S., Bickmore, W., Fukushima, Y., Mannens, M., et al. (1995) Aniridia-associated cytogenetic rearrangements suggest that a position effect may cause the mutant phenotype. *Hum Mol Genet* **4**(3), 415-422.

212. Bedell, M.A., Jenkins, N.A., and Copeland, N.G. (1996) Good genes in bad neighbourhoods [news; comment]. *Nat Genet* **12**(3), 229-232.

213. Epstein, J.A., Glaser, T., Cai, J., Jepeal, L., Walton, D.S., and Maas, R.L. (1994) Two independent and interactive DNA-binding subdomains of the Pax6 paired domain are regulated by alternative splicing. *Genes Dev* **8**(17), 2022-2034.

214. Ward, T.A., Nebel, A., Reeve, A.E., and Eccles, M.R. (1994) Alternative messenger RNA forms and open reading frames within an additional conserved region of the human PAX-2 gene. *Cell Growth Differ* **5**(9), 1015-1021.

215. Hodgkinson, C.A., Moore, K.J., Nakayama, A., Steingrisson, E., Copeland, N.G., Jenkins, N.A. adn Arnheiter, H. (1993) Mutations at the mouse microphthalmia locus are associated with defects in a gene encoding a novel basic-helix-loop-helix-zipper protein. *Cell* **74**, 395 404.

216. Grompe, M. (1993) The rapid detection of unknown mutations in nucleic acids. *Nature Genet* **5**(2), 111-117.

217. de Morsier, G. (1956) Etudes sur les dysraphies cranioencephaliques. III. Agenesie du septum lucidum avec malformation du tractus optique: la dysplasie septo-optique. *Schweizer Archiv fur Neurologie und Psychiatrie* **77**, 267.

218. de Morsier, G. (1962) Median Cranioencephalic Dysraphias and Olfactogenital Dysplasia. *World Neurology* **3**, 485-500.

219. Acers, T.E. (1981) Optic nerve hypoplasia: septo-optic-pituitary dysplasia syndrome. *Trans Am Ophthalmol Soc* **79**, 425-457.

220. Aicardi, J. and Goutieres, F. (1981) The syndrome of absence of the septum pellucidum with porencephalies and other developmental defects. *Neuropediatrics* **12**(4), 319-329.

221. Brodsky, M.C. and Glasier, C.M. (1993) Optic nerve hypoplasia. Clinical significance of associated central nervous system abnormalities on magnetic resonance imaging [published erratum appears in Arch Ophthalmol 1993 Apr;111(4):491]. *Arch Ophthalmol* **111**(1), 66-74.

222. Roessmann, U. (1989) Septo-optic dysplasia (SOD) or DeMorsier syndrome. *J-Clin-Neuroophthalmol* **9**(3), 156-159.

223. Stehr, K., Mayer, U., Pfeiffer, R.A., and Reif, R. (1985) Extreme variant of septo-optic dysplasia. *Ophthalmic Paediatr Genet* **5**(3), 159-164.

224. Gendrel, D., Chaussain, J.L., and Job, J.C. (1981) [Congenital hypopituitarism associated with mid-line defects (author's transl)]. *Arch Fr Pediatr* **38**(4), 227-232.

225. Barkovich, A.J., Fram, E.K., and Norman, D. (1989) Septo-optic dysplasia: MR imaging. *Radiology* **171**(1), 189-192.

226. Brook, C.G., Sanders, M.D., and Hoare, R.D. (1972) Septo-optic dysplasia. *Br-Med-J* **3**(830), 811-813.

227. Harris, R.J. and Haas, L. (1972) Septo-optic dysplasia with growth hormone deficiency (De Morsier syndrome). *Arch Dis Child* **47**(256), 973-976.

219. Acers, T.E. (1981) Optic nerve hypoplasia: septo-optic-pituitary dysplasia syndrome. *Trans Am Ophthalmol Soc* **79**, 425-457.

220. Aicardi, J. and Goutieres, F. (1981) The syndrome of absence of the septum pellucidum with porencephalies and other developmental defects. *Neuropediatrics* **12**(4), 319-329.

221. Brodsky, M.C. and Glasier, C.M. (1993) Optic nerve hypoplasia. Clinical significance of associated central nervous system abnormalities on magnetic resonance imaging [published erratum appears in Arch Ophthalmol 1993 Apr;111(4):491]. *Arch Ophthalmol* **111**(1), 66-74.

222. Roessmann, U. (1989) Septo-optic dysplasia (SOD) or DeMorsier syndrome. *J-Clin-Neuroophthalmol* **9**(3), 156-159.

223. Stehr, K., Mayer, U., Pfeiffer, R.A., and Reif, R. (1985) Extreme variant of septo-optic dysplasia. *Ophthalmic Paediatr Genet* **5**(3), 159-164.

224. Gendrel, D., Chaussain, J.L., and Job, J.C. (1981) [Congenital hypopituitarism associated with mid-line defects (author's transl)]. *Arch Fr Pediatr* **38**(4), 227-232.

225. Barkovich, A.J., Fram, E.K., and Norman, D. (1989) Septo-optic dysplasia: MR imaging. *Radiology* **171**(1), 189-192.

226. Brook, C.G., Sanders, M.D., and Hoare, R.D. (1972) Septo-optic dysplasia. *Br-Med-J* **3**(830), 811-813.

227. Harris, R.J. and Haas, L. (1972) Septo-optic dysplasia with growth hormone deficiency (De Morsier syndrome). *Arch Dis Child* **47**(256), 973-976.

228. Hoyt, W.F., Kaplan, S.L., Grumbach, M.M., and Glaser, J.S. (1970) Septo-optic dysplasia and pituitary dwarfism. *Lancet* **1**(652), 893-894.

229. Izenberg, N., Rosenblum, M., and Parks, J.S. (1984) The endocrine spectrum of septo-optic dysplasia. *Clin Pediatr Phila* **23**(11), 632-636.

230. Freude, S., Frisch, H., Wimberger, D., Schober, E., Husler, G., Waldhauser, F., and Aichner, F. (1992) Septo-optic dysplasia and growth hormone deficiency: accelerated pubertal maturation during GH therapy. *Acta Paediatr* **81**(8), 641-645.

231. Chen, H.J., Tsai, J.H., Lai, Y.H., Chen, S.S., and Wang, H.Z. (1985) [Septo-optic dysplasia with pituitary dwarfism--a case report]. *Taiwan I Hsueh Hui Tsa Chih* **84**(9), 1093-1098.

232. Benoit Gonin, J.J., David, M., Feit, J.P., Bourgeois, J., Chopard, A., Kopp, N., and Jeune, M. (1978) [Septo-optic dysplasia with antidiuretic hormone deficiency and central adrenocortical insufficiency. Three cases report in infants (author's transl)]. *Nouv Presse Med* **7**(37), 3327-3331.

233. Arslanian, S.A., Rothfus, W.E., Foley, T.P., Jr., and Becker, D.J. (1984) Hormonal, metabolic, and neuroradiologic abnormalities associated with septo-optic dysplasia. *Acta Endocrinol Copenh* **107**(2), 282-288.

234. Clark, E.A. and Meyer, W.J.d. (1978) Blindness and hypoglycemia: growth hormone deficiency with septo-optic dysplasia. *Tex Med* **74**(2), 47-50.

235. Davis, G.V. and Shock, J.P. (1975) Septo-optic dysplasia associated with see-saw nystagmus. *Arch Ophthalmol* **93**(2), 137-139.

236. Coulter, C.L., Leech, R.W., Schaefer, G.B., Scheithauer, B.W., and Brumback, R.A. (1993) Midline cerebral dysgenesis, dysfunction of the hypothalamic-pituitary axis, and fetal alcohol effects. *Arch Neurol* **50**(7), 771-775.

237. Elster, A.B. and McAnarney, E.R. (1979) Maternal age re septo-optic dysplasia [letter]. *J Pediatr* **94**(1), 162-163.

238. Dominguez, R., Vila Coro, A.A., Slopis, J.M., and Bohan, T.P. (1991) Brain and ocular abnormalities in infants with in utero exposure to cocaine and other street drugs. *Am J Dis Child* **145**, 688-695.

239. Donat, J.F. (1981) Septo-optic dysplasia in an infant of a diabetic mother. *Arch Neurol* **38**(9), 590-591.

240. Landrieu, P. and Evrard, P. (1979) [Septo-optic dysplasia: clinical study and elements of genetic counseling]. *J Genet Hum* **27**(4), 329-341.

241. Benner, J.D., Preslan, M.W., Gratz, E., Joslyn, J., Schwartz, M., and Kelman, S. (1990) Septo-optic dysplasia in two siblings. *Am J Ophthalmol* **109**(6), 632-637.

242. Ellenberger, C., Jr. (1972) Septo-optic dysplasia. *Br Med J* **4**(839), 552.

243. Huseman, C.A., Kelch, R.P., Hopwood, N.J., and Zipf, W.B. (1978) Sexual precocity in association with septo-optic dysplasia and hypothalamic hypopituitarism. *J Pediatr* **92**(5), 748-753.

244. Fitz, C.R. (1983) Holoprosencephaly and related entities. *Neuroradiology* **25**(4), 225-238.

245. Fitz, C.R. (1994) Holoprosencephaly and septo-optic dysplasia. *Neuroimaging Clin N Am* **4**(2), 263-281.

246. Leech, R.W. and Shuman, R.M. (1986) Holoprosencephaly and related midline cerebral anomalies: a review. *J Child Neurol* **1**(1), 3-18.

247. Patel, H., Tze, W.J., Crichton, J.U., McCormick, A.Q., Robinson, G.C., and Dolman, C.L. (1975) Optic nerve hypoplasia with hypopituitarism. Septo-optic dysplasia with hypopituitarism. *Am J Dis Child* **129**(2), 175-180.

248. St. John, J.R.a.R., D.L. (1957) Congenital Absence of the Septum Pellucidum. *Am J Surgery* **94**, 974-980.

249. Williams, J., Brodsky, M.C., Griebel, M., Glasier, C.M., Caldwell, D., and Thomas, P. (1993) Septo-optic dysplasia: the clinical insignificance of an absent septum pellucidum. *Dev Med Child Neurol* **35**(6), 490-501.

250. Pagon, R.A. and Stephan, M.J. (1984) Septo-optic dysplasia with digital anomalies. *J Pediatr* **105**(6), 966-968.

251. LaRoche, G.R. (1984) Septo-optic dysplasia and median cleft face syndrome [letter]. *Am J Dis Child* **138**(8), 795-796.

252. Stewart, C., Castro Magana, M., Sherman, J., Angulo, M., and Collipp, P.J. (1983) Septo-optic dysplasia and median cleft face syndrome in a patient with isolated growth hormone deficiency and hyperprolactinemia. *Am J Dis Child* **137**(5), 484-487.

253. Teng, R.J., Wang, P.J., Wang, T.R., and Shen, Y.Z. (1989) Apert syndrome associated with septo-optic dysplasia. *Pediatr Neurol* **5**(6), 384-388.

254. Michaud, J., Mizrahi, E.M., and Urich, H. (1982) Agenesis of the vermis with fusion of the cerebellar hemispheres, septo-optic dysplasia and associated anomalies. Report of a case. *Acta Neuropathol Berl* **56**(3), 161-166.

255. Kaufman, L.M., Miller, M.T., and Mafee, M.F. (1989) Magnetic resonance imaging of pituitary stalk hypoplasia. A discrete midline anomaly associated with endocrine abnormalities in septo-optic dysplasia. *Arch Ophthalmol* **107**(10), 1485-1489.

256. Byrd, S.E. (1989) Magnetic resonance imaging of supratentorial congenital brain malformations. *J Natl Med Assoc* **81**(8), 873-881.

257. Shapiro, M.B. and Senapathy, P. (1987) RNA splice junctions of different classes of eukaryotes: sequence statistics and functional implications in gene expression. *Nuc Acids Res* **15**(17), 7155-7174.

258. Rogan, P.K. and Schneider, T.D. (1995) Using information content and base frequencies to distinguish mutations from genetic polymorphisms in splice junction recognition sites. *Hum Mutat* **6**(1), 74-76.

259. Declerck, A., Casteels, I., Demaerel, P., and Dralands, L. (1994) Septo-optic dysplasia. *Bull Soc Belge Ophtalmol* **254**, 157-161.

260. Kumura, D., Miller, J.H., and Sinatra, F.R. (1987) Septo-optic dysplasia: recognition of causes of false-positive hepatobiliary scintigraphy in neonatal jaundice. *J Nucl Med* **28**(6), 966-972.

261. Sherlock, D.A. and McNicol, L.R. (1987) Anaesthesia and septo-optic dysplasia. Implications of missed diagnosis in the peri-operative period. *Anaesthesia* **42**(12), 1302-1305.

262. Preston, R.A., Post, J.C., Keats, B.J.B., Aston, C.E., Ferrell, R.E., Priest, J., Nouri, N., Losken, H.W., Morris, C.A., Hurtt, M.R., et al. (1994) A gene for Crouzon craniofacial dysostosis maps to the long arm of chromosome 10. *Nat Genet* **7**(2), 149-153.

263. Bellus, G.A., Hefferon, T.W., Ortiz de Luna, R.I., Hecht, J.T., Horton, W.A., Machado, M., Kaitila, I., McIntosh, I., and Francomano, C.A. (1995) Achondroplasia is defined by recurrent G380R mutations of FGFR3. *Am J Hum Genet* **56**(2), 368-373.

264. Stoilov, I., Kilpatrick, M.W., and Tsipouras, P. (1995) A common FGFR3 gene mutation is present in achondroplasia but not in hypochondroplasia. *Am J Med Genet* **55**(1), 127-133.

265. Rousseau, F., Saugier, P., Le Merrer, M., Munnich, A., Delezoide, A.L., Maroteaux, P., Bonaventure, J., Narcy, F., and Sanak, M. (1995) Stop codon FGFR3 mutations in thanatophoric dwarfism type 1 [letter]. *Nat Genet* **10**(1), 11-12.

266. Tavormina, P.L., Shiang, R., Thompson, L.M., Zhu, Y.Z., Wilkin, D.J., Lachman, R.S., Wilcox, W.R., Rimoin, D.L., Cohn, D.H., and Wasmuth, J.J. (1995) Thanatophoric dysplasia (types I and II) caused by distinct mutations in fibroblast growth factor receptor 3. *Nat Genet* **9**(3), 321-328.

267. Bellus, G.A., McIntosh, I., Smith, E.A., Aylsworth, A.S., Kaitila, I., Horton, W.A., Greenhaw, G.A., Hecht, J.T., and Francomano, C.A. (1995) A recurrent mutation in the tyrosine kinase domain of fibroblast growth factor receptor 3 causes hypochondroplasia. *Nat Genet* **10**(3), 357-359.

268. Park, W.J., Meyers, G.A., Li, X., Theda, C., Day, D., Orlow, S.J., Jones, M.C., and Jabs, E.W. (1995) Novel FGFR2 mutations in Crouzon and Jackson-Weiss syndromes show allelic heterogeneity and phenotypic variability. *Hum Mol Genet* **4**(7), 1229-1233.

269. Ades, L.C., Mulley, J.C., Senga, I.P., Morris, L.L., David, D.J., and Haan, E.A. (1994) Jackson-Weiss syndrome: clinical and radiological findings in a large kindred and exclusion of the gene from 7p21 and 5qter. *Am J Med Genet* **51**(2), 121-130.

270. Schaumann, B. (1979) Comparative dermatoglyphic analysis in two types of acrocephalosyndactyly: Saethre-Chotzen syndrome and Pfeiffer syndrome. *Birth Defects* **15**(6), 661-667.

271. Tsukahara, M., Hagiwara, K., and Kajii, T. (1985) Pfeiffer syndrome or Saethre-Chotzen syndrome? *Jinrui Idengaku Zasshi* **30**(2), 51-56.

272. Pfeiffer, R.A., Rott, H.D., and Angerstein, W. (1990) An autosomal dominant facio-audio symphalangism syndrome with Klippel-Feil anomaly: a new variant of multiple synostoses. *Genet Couns* **1**(2), 133-140.

273. Pfeiffer, R.A., Junemann, G., Polster, J., and Bauer, H. (1973) Epiphyseal dysplasia of the femoral head, severe myopia and perceptive hearing loss in three brothers. *Clin Genet* **4**(2), 141-144.

274. von Lupke, A. (1989) [Evaluation of impulse noise]. *Laryngorhinootologie* **68**(10), 561-562.

275. Pfeiffer, R.A. (1987) New syndrome: mixed hearing loss, mental deficiency, growth retardation, short clubbed digits, and EEG abnormalities in monozygous female twins. *Am J Med Genet* **27**(3), 639-644.

276. Schell, U., Hehr, A., Feldman, G.J., Robin, N.H., Zackai, E.H., de Die Smulders, C., Viskochil, D.H., Stewart, J.M., Wolff, G., Ohashi, H., et al. (1995) Mutations in FGFR1 and FGFR2 cause familial and sporadic Pfeiffer syndrome. *Hum Mol Genet* **4**(3), 323-328.

277. Rutland, P., Pulleyn, L.J., Reardon, W., Baraitser, M., Hayward, R., Jones, B., Malcolm, S., Winter, R.M., Oldridge, M., Slaney, S.F., and et al. (1995) Identical mutations in the FGFR2 gene cause both Pfeiffer and Crouzon syndrome phenotypes [see comments]. *Nat Genet* **9**(2), 173-176.

278. Rohatgi, M. (1991) Cloverleaf skull--a severe form of Crouzon's syndrome: a new concept in aetiology. *Acta Neurochir Wien* **108**(1-2), 45-52.

279. Sirotnak, J., Brodsky, L., and Pizzuto, M. (1995) Airway obstruction in the Crouzon syndrome: case report and review of the literature. *Int J Pediatr Otorhinolaryngol* **31**(2-3), 235-246.

280. Fehlow, P. (1988) [Pseudo-Crouzon syndrome with defective mental development]. *Padiatr Grenzgeb* **27**(4), 327-330.

281. Oldridge, M., Wilkie, A.O., Slaney, S.F., Poole, M.D., Pulleyn, L.J., Rutland, P., Hockley, A.D., Wake, M.J., Goldin, J.H., Winter, R.M., et al. (1995) Mutations in the third immunoglobulin domain of the fibroblast growth factor receptor-2 gene in Crouzon syndrome. *Hum Mol Genet* **4**(6), 1077-1082.

282. Reardon, W., Winter, R.M., Rutland, P., Pulleyn, L.J., Jones, B.M., and Malcolm, S. (1994) Mutations in the fibroblast growth factor receptor 2 gene cause Crouzon syndrome. *Nat Genet* **8**(1), 98-103.

283. Neilson, K.M. and Friesel, R.E. (1995) Constitutive activation of fibroblast growth factor receptor-2 by a point mutation associated with Crouzon syndrome. *J Biol Chem* **270**(44), 26037-26040.

284. Del Gatto, F. and Breathnach, R. (1995) A Crouzon syndrome synonymous mutation activates a 5' splice site within the IIIc exon of the FGFR2 gene. *Genomics* **27**(3), 558-559.

285. Gorry, M.C., Preston, R.A., White, G.J., Zhang, Y., Singhal, V.K., Losken, H.W., Parker, M.G., Nwokoro, N.A., Post, J.C., and Ehrlich, G.D. (1995) Crouzon syndrome: mutations in two spliceoforms of FGFR2 and a common point mutation shared with Jackson-Weiss syndrome. *Hum MolGenet* **4**(8), 1387-1390.

286. Steinberger, D., Mulliken, J.B., and Muller, U. (1995) Predisposition for cysteine substitutions in the immunoglobulin-like chain of FGFR2 in Crouzon syndrome. *Hum Genet* **96**(1), 113-115.

287. Meyers, G.A., Orlow, S.J., Munro, I.R., Przylepa, K.A., and Jabs, E.W. (1995) Fibroblast growth factor receptor 3 (FGFR3) transmembrane mutation in Crouzon syndrome with acanthosis nigricans. *Nat Genet* **11**(4), 462-464.

288. Richtsmeier, J.T. (1987) Comparative study of normal, Crouzon, and Apert craniofacial morphology using finite element scaling analysis. *Am J Phys Anthropol* **74**(4), 473-493.

289. Carter, C.O., Till, K., Fraser, V., and Coffey, R. (1982) A family study of craniosynostosis, with probable recognition of a distinct syndrome. *J Med Genet* **19**(4), 28028-5.

290. de Leon, G.A., de Leon, G., Grover, W.D., Zaeri, N., and Alburger, P.D. (1987) Agenesis of the corpus callosum and limbic malformation in Apert syndrome (type I acrocephalosyndactyly). *Arch Neurol* **44**(9), 979-982.

291. de Leon, G.A., de Leon, G., Grover, W.D., Zaeri, N., and Alburger, P. (1989) Agenesis of the corpus callosum in Apert syndrome? [letter]. *ArchNeurol* **46**(5), 479.

292. Beligere, N., Harris, V., and Pruzansky, S. (1981) Progressive bony dysplasia in Apert syndrome. *Radiology* **139**(3), 593-597.

293. Flerow, W. and Szamak, F. (1979) [The Apert syndrome (acrocephalosyndactylia). A case study]. *Fortschr Med* **97**(10), 438-439.

294. Izumikawa, Y., Naritomi, K., Ikema, S., Goya, Y., Shiroma, N., Yoshida, K., Yara, A., and Hirayama, K. (1988) Apert syndrome with partial polysyndactyly: a proposal on the classification of acrocephalosyndactyly. *Jinrui Idengaku Zasshi* **33**(4), 487-492.

295. Maroteaux, P. and Fonfria, M.C. (1987) Apparent Apert syndrome with polydactyly: rare pleiotropic manifestation or new syndrome? *Am J Med Genet* **28**(1), 153-158.

296. Nicholas, K.C. and Jorgenson, R.J. (1975) Apert syndrome. *Birth Defects* **11**(2), 396.

297. Pyrkosz, A., Grzywna, W., and Grzybowski, A. (1988) [Apert syndrome]. *Pediatr Pol* **63**(9), 590-592.

298. Ruppert, F., Schultz, K., Weisenbach, J., and Bozzay, L. (1974) [Apert's syndrome (acrocephalosyndactylia]. *Orv Hetil* **115**(36), 2127-2130.

299. Solomon, L.M., Medenica, M., Pruzansky, S., and Kreiborg, S. (1973) Apert syndrome and palatal mucopolysaccharides. *Teratology* **8**(3), 287-291.

300. Sow, D., Camara, B., Kuakuvi, N., Traore, A., Diagne, I., Sall, M.G., Moreira, C., and Senghor, G. (1988) [Apert syndrome or type I acrocephalosyndactylia. Apropos of a case]. *Dakar Med* **33**(1-4), 11-13.

301. Szumera, B., Mazurek, A., and Jarczyk, K. (1972) [Wheaton-Apert syndrome]. *Pol Tyg Lek* **27**(6), 231-232.

302. Waterson, J.R., DiPietro, M.A., and Barr, M. (1985) Apert syndrome with frontonasal encephalocele. *Am J Med Genet* **21**(4), 777-783.

303. Phillips, S.G. and Miyamoto, R.T. (1986) Congenital conductive hearing loss in Apert syndrome. *Otolaryngol Head Neck Surg* **95**(4), 429-433.

304. Gould, H.J. and Caldarelli, D.D. (1982) Hearing and otopathology in Apert syndrome. *Arch Otolaryngol* **108**(6), 347-349.

305. Wilkie, A.O., Slaney, S.F., Oldridge, M., Poole, M.D., Ashworth, G.J., Hockley, A.D., Hayward, R.D., David, D.J., Pulleyn, L.J., Rutland, P., et al. (1995) Apert syndrome results from localized mutations of FGFR2 and is allelic with Crouzon syndrome [see comments]. *Nat Genet* **9**(2), 165-172.

306. Borbolla, L. and Menendez, I. (1983) Dermatoglyphics in Saethre-Chotzen syndrome: a family study. *Acta Paediatr Hung* **24**(3), 269-279.

307. Bianchi, E., Arico, M., Podesta, A.F., Grana, M., Fiori, P., and Beluffi, G. (1985) A family with the Saethre-Chotzen syndrome. *Am J Med Genet* **22**(4), 649-658.

308. Gabrielli, O., Moroni, E., Barbato, M., Pierleoni, C., and Felici, L. (1989) [Type-III acrocephalosyndactylia (Saethre-Chotzen syndrome). Description of 2 cases]. *Pathologica* **81**(1073), 295-300.

309. Galluzzi, F., Salti, R., Marianelli, L., and La Cauza, C. (1980) [The Saethre-Chotzen syndrome. Clinical case]. *Minerva Pediatr* **32**(5), 325-328.

310. Jimenez Garcia, M. and Gonzalez Cortes, M.C. (1977) [The Saethre-Chotzen syndrome (acrocephalosyndactylia type III)]. *Bol Med Hosp Infant Mex* **34**(4), 903-908.

311. Kreiborg, S., Pruzansky, S., and Pashayan, H. (1972) The Saethre-Chotzen syndrome. *Teratology* **6**(3), 287-294.

312. Pantke, O.A., Cohen, M.M., Jr., Witkop, C.J., Jr., Feingold, M., Schaumann, B., Pantke, H.C., and Gorlin, R.J. (1975) The Saethre-Chotzen syndrome. *Birth Defects* **11**(2), 190-225.

313. Reardon, W., McManus, S.P., Summers, D., and Winter, R.M. (1993) Cytogenetic evidence that the Saethre-Chotzen gene maps to 7p21.2. *Am J Med Genet* **47**(5), 633-636.

314. Shidayama, R., Hirano, A., Iio, Y., and Fujii, T. (1995) Familial Saethre-Chotzen syndrome with or without polydactyly of the toe. *Ann Plast Surg* **34**(4), 435-440.

315. Friedman, J.M., Hanson, J.W., Graham, C.B., and Smith, D.W. (1977) Saethre-Chotzen syndrome: a broad and variable pattern of skeletal malformations. *J Pediatr* **91**(6), 929-923.

316. Wilkie, A.O., Yang, S.P., Summers, D., Poole, M.D., Reardon, W., and Winter, R.M. (1995) Saethre-Chotzen syndrome associated with balanced translocations involving 7p21: three further families. *J Med Genet* **32**(3), 174-180.

317. Reid, C.S., McMorrow, L.E., McDonald McGinn, D.M., Grace, K.J., Ramos, F.J., Zackai, E.H., Cohen, M.M., Jr., and Jabs, E.W. (1993) Saethre-Chotzen syndrome with familial translocation at chromosome 7p22. *Am J Med Genet* **47**(5), 637-639.

318. Evans, C.A. and Christiansen, R.L. (1976) Cephalic malformations in Saethre-Chotzen syndrome. Acrocephalosyndactyly type III. *Radiology* **121**(2), 399-403.

319. Morell, R., Pierpont, J., Guo, W., Friedman, T.B., Ho, L., Spritz, R.A., Erickson, R.P. and Asher, J.H., Jr. (1996) Possible digenic inheritance of Waardenburg Syndrome type 2 (WS2) and ocular albinism (OA) phenotypes. [*in press*].

320. Morell, R., Carey, M.L., Lalwani, A.K., Friedman, T.B. and Asher, J.H., Jr. (1996) Three mutations in the paired homeodomain of *PAX3* that cause Waardenburg Syndrome type 1. [*in press*].

321. Asher, J.H., Jr., Harrison, R.W., Morell, R., Carey, M.L. and Friedman, T.B. (1996) Effects of PAX3 modifier genes on craniofacial morphology, pigmentation, and viability: a murine model of Waardenburg Syndrome variation. *Genomics* **34**, 285-298.

322. Sadler, T.W. (1990) *Langman's medical embryology, sixth edition*. Williams and Wilkins, Baltimore.

323. Heimer, L. (1983) *The human brain and spinal cord*. Springer-Verlag New York Inc.